

جمهورية العراق

وزارة التعليم العالي و البحث العلمي

جامعة بابل



تشققات انكماش الجفاف في الأعمدة الخرسانية الذاتية الرص المقيدة من النهايات

رسالة

مقدمة إلى كلية الهندسة في جامعة بابل

كجزء من متطلبات نيل درجة الماجستير

في علوم الهندسة المدنية

من قبل

هدى زهير عبد الغني كبه

تشرين الأول - ٢٠٠٦ رمضان - ١٤٢٧

Republic of Iraq



Ministry of Higher Education and

Scientific Research

University of Babylon

***DRYING SHRINKAGE CRACKING OF END RESTRAINED SELF-
COMPACTING CONCRETE MEMBERS***

A Thesis

Submitted to the College of Engineering

of the University of Babylon in partial

Fulfillment of the Requirements

for the Degree of Master

of Science in Civil

Engineering

By

HUDA ZUHEIR A. AL-GANI KUBBA

Supervised by

ASST. PROF. DR. GHALIB M. HABEED

ASST. PROF. MR. SAMIR A. AL-MASHHEDI

October - ٢٠٠٦

Ramadan-١٤٢٨

الإهداء

إلى مصابيح الهدى وسفن النجاة... ألك المصطفى (صلى الله

عليهم أجمعين)

إلى من رضا الله من رضاها... والدي

إلى من قاسمني الصبر... زوجي

إلى فلذة كبدي... عبوسي

إلى فخري وسندي في الحياة... أختي وأخواني

إليهم الهدى عمرة ما وفقني الله إليه .

هدى

بِسْمِ اللَّهِ الرَّحْمَنِ الرَّحِيمِ

وَأَسْأَلُكَ بِرَبِّكَ
وَأَسْأَلُكَ بِرَبِّكَ
وَأَسْأَلُكَ بِرَبِّكَ

رَبِّكَ وَرَبِّكَ
رَبِّكَ وَرَبِّكَ
رَبِّكَ وَرَبِّكَ

صَدَقَ اللَّهُ الْعَظِيمُ

النتيجة

توصف الخرسانة ذاتية الرص على إنها خرسانة لها القابلية على رص نفسها تحت تأثير وزنها دون الحاجة إلى متطلبات الاهتزاز. هذه الدراسة خطت لإنتاج خرسانة ذاتية الرص من المواد المتوفرة محليا طبقا لمتطلبات قابلية التشغيل، ومن ثم دراسة تأثير بعض المواد المألثة مثل الأصباغ (pigments)، الحجر الجيري الناعم (limestone powder) و الميتاكاولين (metakaolin) على التغيرات الحجمية للعتبات الخرسانية الذاتية الرص ومقارنتها مع الخرسانة الاعتيادية. تم استخدام عتبات خرسانية (Beams) مقيدة النهائية لدراسة تشققات الانكماش الحر و المقيد.

هذه الدراسة تهدف لبحث سلوك تشققات الانكماش في الألواح (plates) الخرسانية الذاتية الرص المسلحة و المقيدة عن الحركة من النهايات بحالات تقييد مختلفة. حالات التقييد هي تقييد من النهاية و تقييد من القاعدة. لقد تم خلال البحث قياس قراءات حركة الألواح، المسافة بين التشققات، عرض التشققات و أطوالها.

الفحوصات المختبرية التي استخدمت لإيجاد قابلية التشغيل هي فحص الانسياب و زمن الانسياب ، الصندوق على شكل حرف L، الصندوق على شكل حرف U و القمع على شكل حرف V. تراوحت نتائج الانسياب و زمن الانسياب بين (٦٨٠-٧٥٠) ملم و (٢.٥-٣.٥) ثانية على التوالي، الخلطة الخرسانية ذاتية الرص مع الأصباغ تكون أعلى بالمقارنة مع الخلطات الخرسانية الذاتية مع الحجر الجيري الناعم و الميتاكاولين بمقدار (٣, ٩%) بالنسبة للانسياب و اقل بمقدار (٢٠, ٤٠%) بالنسبة لزمن الانسياب. كما إن نسبة الانسداد للصندوق بشكل حرف L تتراوح بين (٠.٩٥-٠.٩٠) ، تعطي الخرسانة ذاتية الرص مع الميتاكاولين نسبة انسداد اقل بالمقارنة مع الخلطات الخرسانية ذاتية الرص مع الأصباغ و الحجر الجيري الناعم بمقدار (٦, ٣%) على التوالي. إن فرق الارتفاع لمليء الصندوق بشكل حرف U يتراوح بين (٠-٠.٤) ملم. الزمن اللازم لمرور الخرسانة من الصندوق بشكل حرف V يتراوح بين (٦-٨) ثانية، تظهر الخرسانة ذاتية الرص مع الميتاكاولين زمن مرور أعلى بالمقارنة مع الخلطات الخرسانية ذاتية الرص مع الأصباغ و الحجر الجيري الناعم بمقدار (١٣, ٣٣%) على التوالي. بناء على نتائج العمل، من الممكن إنتاج خرسانة مرصوة ذاتيا من المواد المتوفرة محليا و المكونة لهذا النوع من الخرسانة وان الخرسانة المرصوة ذاتيا المنتجة تمتلك قابلية جريان و تشغيل جيدة.

بالنسبة للعتبات كان انكماش الجفاف الحر للخرسانة ذاتية الرص مع الأصباغ أعلى بالمقارنة مع الخرسانة الاعتيادية بمقدار (٢٤ % ليوم واحد و ٥ % لستين يوم) في الشتاء و بمقدار (٥٤ % ليوم واحد و ٦ % لستين يوم) في الصيف. و كان الانكماش الحر للخلطة الخرسانية ذاتية الرص مع الاصباغ أعلى من الخلطات الخرسانية مع الحجر الجيري الناعم و الميتاكاولين بمقدار (٤٣, ٣٣) ليوم واحد و ١١, ١٩ لستين يوم) % على التوالي في الشتاء و بمقدار (٥٥, ٤٥) ليوم واحد و ١٤, ١٠ لستين يوم) % على التوالي في الصيف. في العتبات المقيدة النهائية وقت حدوث التشققات يكون مبكرا عند إضافة الأصباغ و الملدن (SP) إلى الخلطة خلال (٣-١٤ يوم) بينما وقت حدوث التشققات في الخلطة الاعتيادية بدون إضافة (٢٨ يوم).

اعتمادا على نتائج البحث، ظهر إن كل من الألواح المقيدة النهائية من جهتين، ثلاث جهات و أربع جهات تتشقق بشكل مبكر في اليوم الأول بعد الصب. أيضا تم ملاحظة وجود اختلاف في عرض التشققات الموجودة على طول اللوح (plate). في مستوى الحافة المقيدة يوجد عرض معين يتزايد باتجاه مركز اللوح حتى يصل إلى أكبر قيمة له عند مسافة تتراوح بين (٦٠-٢٠%) من طول الشق، والذي فيه يحصل أكبر عرض للشق عادة. و بعد ذلك يأخذ عرض هذا الشق بالتناقص حتى يضمحل ويتلاشى عند طول معين. بينما التشققات التي ظهرت عند الحافات الحرة كانت تمتلك أقصى عرض لها عند مستوى الحافة ثم تقل وتضمحل باتجاه مركز اللوح .

تم تحويل واعتماد معادلات مبسطة لغرض حساب المسافات الدنيا والقصى بين الشقوق وكذلك حساب أقصى عرض لتلك الشقوق في أي موقع على طول اللوح وذلك باستخدام النتائج التي تم استحصالتها من خلال البحث.

ABSTRACT

Self-Compacting Concrete (SCC) describes a concrete with the ability to compact itself by means of its own weight without the requirement of vibration. This study was included of producing SCC from locally available materials according to the requirement of workability measurements, and then studying the effect of some fillers (pigment, limestone powder and metakaolin) on dimensional changes of SCC beams in summer and winter compared with normal concrete. End restrained beams were used to study free and restrained shrinkage cracking.

This study is planned to investigate the cracking behavior of reinforced SCC plates restrained from movement at their ends for different restraint. These restraint were end and base restraints. Plates movement, crack spacing, crack width and crack length were measured.

Workability of SCC is determined by different test methods such as slump flow, T_{50} cm, L-box, U-box and V-funnel tests. The values of slump flow and T_{50} cm range between (680-700 mm) and (2.0-3.0 sec) respectively. The SCC mix containing pigment is higher than those mixes containing limestone powder and metakaolin by (3, 9) % for slump flow and less by (20-25 %) for T_{50} cm respectively. The value of blocking ratios (H_2/H_1) of L-box for SCC mixes are between (0.90-0.95). SCC with metakaolin gave less value of blocking ratio than SCC mixes with pigment and limestone powder by (6, 3) % respectively. The filling height (H_1-H_2) of U-box for SCC mixes is between (0-1.2 mm). The time of concrete flow immediately after mixing in V-funnel is between (6-8 sec). The SCC mix with metakaolin shows higher flow time than SCC mixes with pigment and limestone powder by (33, 13) % respectively. Based on the results of this work, it is possible to produce SCC from locally available materials which

satisfies the requirements of this type of concrete and it can be stated that SCC produced has good flowability and workability.

For beams the free drying shrinkage of SCC mix with pigment is higher than normal concrete mix by (2.4 % for 1-day and 0 % for 28-days) in winter and by (0.4 % for 1-day and 1 % for 28-days) in summer. Free shrinkage of SCC mix with pigment is higher than the SCC mixes with limestone powder and metakaolin by (3.3, 4.3) % for 1-day and (1.1, 1.9) % for 28-days respectively in winter and by (4.0, 0.0) % for 1-day and (1.1, 1.4) % for 28-days respectively in summer. In end restrained beams, the cracking time for SCC mix containing pigment powder and Superplasticizer occurs earlier through (3-4 days), while for normal concrete mix the cracking time is (7-days).

From the results obtained, it was observed that two, three and four end restrained plates cracked early in the first day after casting. It was observed that there is a difference in the crack widths along the plate length. At restrained edge level there is a certain crack width, which increases towards the center of the plate until the level of (2-3 %) of crack length, where the maximum crack width usually occurs. Beyond which the crack width decreases to zero at a certain length. While, cracks which appeared at the free edge have maximum crack width at the edge level and decreases to zero towards the center of the plate.

Simplified formulas were adopted and modified for predicted the minimum and maximum crack spacing and maximum crack width at any position along the plate length.

Acknowledgment

I like to express my sincere appreciation and grateful thanks to my supervisors Asst. Dr. Ghalib M. Habeeb and Asst. Prof. Mr. Samir A. Al-Mashhedi for their valuable advice and aid, criticism and constant encouragement throughout the work of this investigation.

Special thanks to the Mr. Raad and Mr. Mohammed for their assistance and advice.

Great thanks are granted to the staff of civil engineering department especially all the staff of the building materials laboratory for their help throughout the investigation.

I'm really grateful to my family, especially my father, my mother, my husband, my brothers Bahaa and Ali and my sister Noor for their encouragement, interest and support during this study.

Finally, I wish to express my gratitude to all who participate in providing help and assistance to complete this work especially Zainab Hassan, Easam Mohammed and Ahmed Talib.

Huda ٢٠٠٧

Examination Committee Certificate

We certify that we have read the thesis, titled (**Drying Shrinkage Cracking of End Restrained Self-Compacted concrete Members**) and as examining committee, examined the student (**Huda Zuheir A. AL-Gani Kubba**) in its contents and in what is connected with it, and that in our opinion it meets the standards of the thesis for the Degree of Master of Science in Civil Engineering (Construction Materials).

Signature :

Name: Asst. Prof. Dr. Jabbar A. Jabir

(Member)

Date: / / ٢٠٠٧

Signature :

Name: Asst. Prof. Mr. Ali A. Alwash

(Member)

Date: / / ٢٠٠٧

Signature :

Name: Asst. Prof. Dr. Mahdi S. Essa

(Chairman)

Date: / / ٢٠٠٧

Signature :

Name: Asst. Prof. Dr. Ghalib M. Habeeb

(Supervisor)

Date: / / ٢٠٠٧

Signature :

Name: Asst. Prof. Mr. Samir A. Al-Mashhedi

(Supervisor)

Date: / / ٢٠٠٧

Approval of the Civil Engineering Department

Head of the Civil Engineering Department

Signature :

Name: Asst. Prof. Dr. Ammar Y. Ali

Date: / / ٢٠٠٧

Approval of the Deanery of the College of Engineering

Dean of the College of Engineering
Babylon

University of

Signature :

Name: Asst. Prof. Dr. Abd Al-Wahid K. Rajih

Dean of the College of Engineering

University of Babylon

Date: / / ٢٠٠٧

List of Contents

<u>Title</u>	<u>Page</u>
Acknowledgment	I
Abstract	II
List of Contents	IV
List of Tables	X
List of Figures	XII
List of Plates	XVI
Notations	XVII

CHAPTER ONE

INTRODUCTION

1-1- General	1
1-2- Objective of this Work	3
Thesis Layout	4

CHAPTER TWO

REVIEW OF LITERATURES

2-1- Self-Compacting Concrete	6
2-2- Development of Self-Compacting Concrete	6
2-3- Self-Compacting Concrete Achievement	7
2-4- Advanced Materials	9
2-4-1- Cement	10
2-4-2- Aggregate	10
2-4-2-1- Coarse Aggregate	10
2-4-2-2- Fine Aggregate	11
2-4-3- Superplasticizers	11
2-4-4- Supplementary Cementitious Materials or Fillers	12
2-4-4-1- Pigment	13
2-4-4-2- Limestone Powder	13
2-4-4-3- Metakaolin	14
2-5- Mix Design	14

2-6- Mix Design Principles	14
2-7- Adjustment of the Mix	10
2-8- Mix-Design Method	16
2-8-1- Rational Mix-Design Method	16
2-8-2- Common Design Method for SCC	17
2-9- Workability of SCC	19
2-9-1- Rheology of SCC	19
2-10- Properties of Fresh SCC Mixes	20
2-10-1- Filling Ability	21
2-10-2- Passing Ability	21
2-10-3- Segregation Resistance (Stability)	22
2-11- Test Method	22
2-11-1- Slump Flow and T ₅₀ cm Test	23
2-11-2- L-Box Test	24
2-11-3- U-Box Test	24
2-11-4- V-Funnel Test	20
2-12- Conformity Control and Conformity Criteria	26
2-13- Shrinkage Cracking	27
2-13-1- General	27
2-13-2- Shrinkage of SCC	28

2-14- Types of Concrete Shrinkage	29
2-14-1- Plastic Shrinkage	29
2-14-2- Drying Shrinkage	30
2-14-3- Carbonation Shrinkage	31
2-14-4- Autogenous Shrinkage	32
2-15- Factors Affecting Shrinkage of Concrete	32
2-15-1- Cement Type, Composition and Fineness	32
2-15-2- Aggregates	34
2-15-3- Water Content	34
2-15-4- Admixtures	35
2-15-5- Volume-Surface Ratio	37
2-15-6- Relative Humidity and Temperature	38
2-15-7- Curing	38
2-16- Shrinkage Induced Cracking	39
2-17- Plastic Shrinkage Cracking	40
2-18- Restrained Shrinkage Cracking	40
2-18-1- Internal Restraint	42
2-18-2- External Restraint	42
2-18-2-1- End Restrained Shrinkage Cracking	42
2-18-2-2- Base Restrained Shrinkage Cracking	46

۲-۱۹- Factors Influencing Cracking Resistance	۴۸
۲-۱۹-۱- Creep (Relaxation) of Concrete	۴۸
۲-۱۹-۲- Tensile Strain Capacity	۴۹
۲-۱۹-۳- Elastic Tensile Strain Capacity	۴۹
۲-۲۰- Cracking Age	۵۰

CHAPTER THREE

EXPERIMENTAL WORK

۳-۱- Introduction	۵۱
۳-۲- Materials	۵۱
۳-۲-۱- Cement	۵۱
۳-۲-۲- Coarse Aggregate	۵۲
۳-۲-۳- Fine Aggregate	۵۳
۳-۲-۴- Superplasticizer	۵۴
۳-۲-۵- Types of Fillers	۵۴
۳-۲-۵-۱- Pigment	۵۴
۳-۲-۵-۲- Limestone Powder	۵۵
۳-۲-۵-۳- Metakaolin	۵۵
۳-۲-۶- Water	۵۶
۳-۲-۷- Reinforcement	۵۶

3-3- Mix Design	56
3-3-1- Determination of Mix Design Method	56
3-3-2- Mixing Procedure	58
3-4- Testing of Fresh and Hardened Concrete	58
3-4-1- Slump Flow and T ₅₀₀ cm Test	59
3-4-2- L-Box Test	59
3-4-3- U-Box Test	60
3-4-4- V-Funnel Test	60
3-4-5- Compressive Strength Test	61
3-4-6- Flexural Strength Test	61
3-5- Program of the Work	61
3-5-1- Beams	61
3-5-2- Plates	63
3-6- Restraining Reinforced Concrete Slabs	64
3-7- Plate Molds	66
3-8- Casting Procedure of Beams and Plates	69
3-8-1- Mixing and Casting of Beams and Plates	69
3-8-2- Curing	70
3-9- Strain and Crack Width Measurements	70
3-10- Free Volume Change of the Plates	73

3-11- Tensile Strain Capacity Test	70
3-12- Restrained-Shrinkage Test	70

CHAPTER FOUR

RESULTS AND DISCUSSION

4-1- Introduction	77
4-2- Properties of Fresh SCC	77
4-2-1- Slump-Flow and T _{50, cm} Test	77
4-2-2- L-Box Test	79
4-2-3- U-Box Test	79
4-2-4- V-Funnel Test	80
4-3- Free Shrinkage Test for Beams	80
4-4- Restrained Shrinkage Test for Beams	83
4-4-1- Tensile Strain Capacity	83
4-4-2- Elastic Tensile Strain Capacity	84
4-4-3- Creep	84
4-4-4- First Crack Time	84
4-4-5- Crack Location	85
4-4-6- Crack Width	86
4-5- Free Volume Change of plates	88

ξ-٦- Restrained Movement of Plates	٩٢
ξ-٧- Elastic Tensile Strain Capacity of Beams	٩٩
ξ-٨- Cracking of the Plates	٩٩
ξ-٩- Cracking Age and Sequence	١٠٠
ξ-١٠- Crack Spacing	١٠٥
ξ-١١- Crack Length	١١٠
ξ-١٢- Crack Location	١١٢
ξ-١٣- Crack Width	١١٣

CHAPTER FIVE

CONCLUSIONS AND RECOMMENDATIONS

٥-١- Conclusions	١٢٨
------------------	-----

١٣١

٥-٢- Recommendations of this Works

١٣٢

REFERENCES

List of Figures

<u>Title</u>	<u>Page</u>
Figure (۲-۱): Excess Paste Theory	۸
Figure (۲-۲): Concrete Structure	
a) Classical Concrete	
b) Advanced Concrete	۹
Figure (۲-۳): Rational Mix-Design Method	۱۷
Figure (۲-۴): Bingham Rheology Model	۲۰
Figure (۲-۵): L-Box Test	۲۴
Figure (۲-۶): U-Box Test	۲۵
Figure (۲-۷): V-Funnel Test	۲۶
Figure (۲-۸): Effect of Volume to Surface Ratio on the Drying Shrinkage of Concrete	۳۷
Figure (۲-۹): Development of Tensile Stress in Concrete and the Time Required for the First Crack	۴۰
Figure (۲-۱۰): Degree of Tensile Restraint at Center Section	۴۱
Figure (۲-۱۱): Sketch of Strain Distribution in the Concrete Adjacent to a Crack	۴۵
Figure (۳-۱): Ribbon Diagram Mixing Sequence	۵۸
Figure (۳-۲): Schematic Diagram of the End Restrained Beam	۶۲
Figure (۳-۳): Schematic Diagram of Free Slab.	۶۵

Figure (۳-۴): Schematic Diagram of End Restrained Slab	۶۶
Figure (۳-۵): Schematic Diagram of Free SCC Plate	۶۷
Figure (۳-۶): Schematic Diagram of End Restrained SCC Plate	۶۸
Figure (۳-۷): Details of the Reinforced SCC Plate	۶۹
Figure (۳-۸): Stainless Steel Demec Points of Reinforced SCC Free Plate	۷۰
Figure (۴-۱): Free Shrinkage Development With Age for End Restrained Beam in winter	۸۱
Figure (۴-۲): Free Shrinkage Development With Age for End Restrained Beam in Summer	۸۱
Figure (۴-۳): Location of Cracks of Concrete Beam Specimens	۸۰
Figure (۴-۴): Development of Crack Width With Age of Beams for Normal Mix, Plain SCC Mix and Reinforced SCC Mix	۸۷
Figure (۴-۵): Free Shrinkage Development With Age for Plain SCC Free Plate	۸۹
Figure (۴-۶): Free Shrinkage Development in Summer with Age for Beam Model in Different Cast and Measured of SCC (Pigment+SP) and Normal Concrete	۹۰
Figure (۴-۷): Free Shrinkage Development With Age for Reinforced SCC Free Plate	۹۱

Figure (4-8): Shrinkage Strain Development for Reinforced SCC

Free Plate at 0 cm from the Edge 93

Figure (4-9): Shrinkage Strain Development of Two End

Restrained SCC Plate at 0 cm from the Free Edge 94

Figure (4-10): Shrinkage Strain Development of Two End

Restrained SCC Plate at 0 cm from the Restrained

Edge 95

Figure (4-11): Shrinkage Strain Development of Three End

Restrained SCC Plate at 0 cm from the Free Edge 96

Figure (4-12): Shrinkage Strain Development of Three End

Restrained SCC Plate at 0 cm from the Restrained

Edge 97

Figure (4-13): Shrinkage Strain Development of Four End

Restrained SCC Plate at 0 cm from the Restrained

Edge 98

Figure (4-14): Crack Formation Sequence in Two End Restrained

SCC Plate 102

Figure (4-15): Crack Formation Sequence in Three End Restrained

SCC Plate 103

Figure (4-16): Crack Formation Sequence in Four End Restrained

SCC Plate. 104

Figure (4-17): Final Crack Pattern in Two End Restrained of

Reinforced SCC Plate	۱۰۵
Figure (۴-۱۸): Final Crack Pattern in Three End Restrained of	
Reinforced SCC Plate	۱۰۶
Figure (۴-۱۹): Final Crack Pattern in Four End Restrained of	
Reinforced SCC Plate	۱۰۶
Figure (۴-۲۰): Degree of Tensile Restraint at Center Section.	۱۰۹
Figure (۴-۲۱): Relation Between the Maximum Crack Width and	
Maximum Crack Length for Plates	۱۱۰
Figure (۴-۲۲): Position of Maximum Crack Width From the	
Restrained Edge Versus Crack Length for the	
Different Restrained Condition	۱۱۱
Figure (۴-۲۳): Development of Maximum Crack Width With Age of	
Reinforced SCC Plates for Different Restrained Cases	۱۱۳
Figure (۴-۲۴): Variation of Final Crack Width With Distance for	
Two End Restrained SCC Plate	۱۱۵
Figure (۴-۲۵): Variation of Final Crack Width With Distance for	
Three End Restrained SCC Plate	۱۱۷
Figure (۴-۲۶): Variation of Final Crack Width With Distance for	
Four End Restrained SCC Plate	۱۱۹
Figure (۴-۲۷): Comparison Between the Observed and Calculated	
Maximum Crack Width at Different Levels for Two	

End Restrained Reinforced SCC Plate at Free Edge ۱۲۶

Figure (۴-۲۸): Comparison Between the Observed and Calculated
Maximum Crack Width at Different Levels for Three

End Restrained Reinforced SCC Plate at Free Edge ۱۲۶

Figure (۴-۲۹): Comparison Between the Observed and Calculated
Maximum Crack Width at Different Levels for Three

End Restrained Plate at Restrained Edge ۱۲۷

Figure (۴-۳۰): Comparison Between the Observed and Calculated
Maximum Crack Width at Different Levels for

Four End Restrained Plate ۱۲۷

List of Plates

<u>Title</u>	<u>Page</u>
Plate (۳-۱): The Reinforced SCC Plates	۶۴
Plate (۳-۲): The Reinforced Concrete Slabs	۶۵
Plate (۳-۳): Ply Wood Formwork of Plates	۶۹
Plate (۳-۴): The Measurement Devices	۷۱
Plate (۳-۵): Cracks of Two End Restrained SCC Plate at ۶۰ Days Age	۷۲
Plate (۳-۶): Cracks of Three End Restrained SCC Plate at ۶۰ Days Age	۷۲
Plate (۳-۷): Cracks of Four end Restrained SCC Plate at	

60 Days Age	73
Plate (3-8): The Free Movement Plate	74
Plate (3-9): Artificial Gap and Two Demec points on the Sides of the Gap	74

List of Tables

<u>Title</u>	<u>Page</u>
Table (2-1): Materials Used in Normal Concrete and SCC by Absolute Volume.	7
Table (2-2): Mix Proportions of Concrete	18
Table (2-3): Range of Mix Constituents	19
Table (2-4): Test Methods for Evaluating SCC	22
Table (2-5): Acceptance Workability Criteria According to Specification and Guidelines for the Fresh SCC	27
Table (2-6): Suggestions on Suitability of Different Test Methods for SCC	27
Table (3-1): Chemical Composition of Cement	52
Table (3-2): Physical Properties of Cement	52
Table (3-3): Grading of Coarse Aggregate	53

Table (۳-۴): Physical and Chemical Properties of Coarse Aggregate	۵۳
Table (۳-۵): Grading of Fine Aggregate	۵۳
Table (۳-۶): Physical and Chemical Properties of Fine Aggregate	۵۴
Table (۳-۷): Typical Properties of Superplasticizer	۵۴
Table (۳-۸): Chemical Analysis of Pigment	۵۵
Table (۳-۹): Chemical Analysis of Limestone Powder	۵۵
Table (۳-۱۰): Chemical Analysis of Kaolin and Metakaolin	۵۶
Table (۳-۱۱): Mix Proportions in Preliminary Investigations	۵۷
Table (۳-۱۲): Mix Proportions by Weight	۵۸
Table (۴-۱): Properties of Fresh SCC	۷۷
Table (۴-۲): Properties of End Restrained Beams	۸۳
Table (۴-۳): Crack Width of Beam Specimens of Normal and SCC Mixes	۸۷
Table (۴-۴): Cracking Data of Plates	۹۹
Table (۴-۵): Cracking Age of Reinforced SCC Plates	۱۰۰
Table (۴-۶): Maximum Crack Width Calculations for Two End Restrained Plate at Free Edge	۱۲۳
Table (۴-۷): Maximum Crack Width Calculations for Three End Restrained Plate at Free Edge	۱۲۳
Table (۴-۸): Maximum Crack Width Calculations for Three End Restrained Plate at Restrained Edge	۱۲۳
Table (۴-۹): Maximum Crack Width Calculations for Four End	

Restrained Plate at Restrained Edge	١٢٣
Table (٤-١٠): Comparison Between Values of Calculated Maximum Crack Width Using Different Methods for Two End Restrained of the Experimental Reinforced SCC Plate at the Free Edge	١٢٤
Table (٤-١١): Comparison Between Values of Calculated Maximum Crack Width Using Different Methods for Three End Restrained of the Experimental Reinforced SCC Plate at the Free Edge	١٢٤
Table (٤-١٢): Comparison Between Values of Calculated Maximum Crack Width Using Different Methods for Three End Restrained of the Experimental Reinforced SCC Plate at the Retrained Edge	١٢٥
Table (٤-١٣): Comparison Between Values of Calculated Maximum Crack Width Using Different Methods for Four End Restrained of the Experimental Reinforced SCC Plate at the Restrained Edge	١٢٥

Notations

<u>Symbol</u>	<u>Description</u>
Compacting Concrete SCC	Self-
C_a	Constant of total net shrinkage ϵ_{cs} Creep strain after cracking.
C_b	Creep strain before cracking.
d	Bar diameter.

	E_c	Modulus of elasticity of concrete
	e_{sh}	Free shrinkage strain
	e_{shn}	Net shrinkage strain.
	e_{th}	Thermal strain.
	e_{ult}	Elastic tensile strain capacity of concrete.
f_b		Average bond strength between concrete and steel
	f_{tu}	Tensile strength of concrete.
	H	Height of wall
	K	Constant
	R_a	Degree of restraint after cracking
	R_b	Degree of restraint before cracking
	S_{max}	Maximum crack spacing
	S_{min}	Minimum crack spacing
	SP	Superplasticizer
	W_i	Initial crack width.
	W_{max}	Maximum crack width
	W_c	Calculated maximum crack width.
	W_o	Observed crack width (by microscope).
	α_c	Coefficient of expansion of concrete
	ρ	Steel ratio

CERTIFICATE

We certify that the thesis titled “**Drying Shrinkage Cracking of End Restrained Self-Compacting Concrete Members**”, was prepared by “**Huda Zuheir A. Al-Gani Kubba**”, under our Supervision at Babylon University in Fulfillment of Partial Requirements of the Degree of Master of Science in Civil Engineering.

Signature

Name:

Asst. Prof. Dr. Ghalib M. Habeeb

Date: / / ٢٠٠٧

Signature

Name:

Asst. Prof. Mr. Samir A. Al-Mashhedi

Date: / / ٢٠٠٧

CHAPTER ONE

INTRODUCTION

1.1- General

There is no doubt that concrete is one of the most important materials for construction, and its use increases with time. It is used in heavy constructions, such as express highways, bridges, dams as well as other civil engineering uses.

The increase in the complexity of construction, intricate reinforcement details of modern day concrete structures and lack of trained construction workers have demanded a solution to the increasing problems related to uncompact concrete⁽¹⁾.

For this reason and because of many other problems that concrete exhibits, its manufacture has progressed into a highly technical branch of technology and science. Besides cement, aggregate and water, there is a trend to incorporate additional materials in concrete (e.g. admixtures, fibers, fillers and pozzolans) to improve specific features and / or to facilitate placing, conveying, compacting, finishing of concrete operations or to obtain desirable properties⁽¹⁾. In recent years, a lot of study is done on how to improve the performance of concrete, especially on topics regarding how to increase the strength, durability, and flowability of concrete. Self-compacting concrete (SCC) is a new class of a high performance concrete. It was first developed in Japan in order to reach durable concrete structures and to offset a growing shortage of skilled labour.

SCC is described as a concrete with the ability to compact itself only by means of its own weight without the requirement of vibration^(r,ξ). Self-compacting concrete is different than conventional concrete in that it has a lower viscosity and, thus, a greater flow rate when pumped; it also has non segregation, no blocking tendency and appropriate flowability^(σ,ϑ).

The benefits of Self-compacting concrete are^(γ,λ):

1. Self-levelling.
2. Can be placed at a faster rate with no mechanical vibration and less screeding, resulting in savings in placement costs. The extremely fluid and soft consistency allows fast placing of concrete.
3. Improved architectural surface finish with little to no remedial surface work.
4. Improved productivity.
5. Improved consolidation around reinforcement and bond with reinforcement.
6. Shorter construction periods than the normal concrete, due to the fact that no time is wasted with the compaction through vibration.
7. SCC fills all voids and gabs in structural members with high percentage of congested reinforcement.
8. Minimizes movement of ready mixed trucks and pump during placement.
9. Noise reduction.

Placing the concrete without vibration gives a dramatic reduction

in noise. This greatly improves the environment for both employees and neighbours and increasing construction hours in urban areas.

١٠. Improved quality (reduces the need for vibration), durability (lower maintenance in future), reliability of concrete structures, and eliminates some of the potential for human error.

١-٢- Objective of this Work

This work was planned for achieving Self-Compacting Concrete from locally available materials according to the requirement of fresh properties of concrete (workability measurements).

The main aims of this study are as follows:

١. Studying the effect of superplasticizer and fillers (pigment, limestone powder and metakaolin) on free shrinkage of SCC beams (six beams were cast in winter and six beams were cast in summer).
٢. Studying the behavior of free and restrained drying shrinkage of normal concrete beams.
٣. Studying the effect of pigment powder on drying shrinkage of end restrained beams for plain and reinforced SCC (tensile strain capacity, elastic tensile strain capacity, first cracking time and creep).
٤. Studying the effect of pigment powder on reinforced SCC plates (free plate, two end restrained plate, three end restrained plate and four end restrained plate).

- . The main parameter studied was the effect of the end restraint, the base restraint (the roughness or interaction between edge of plate surround slab and the edge of restrained slab) and pigment powder on the cracking behavior of reinforced SCC plates (crack width, crack spacing and crack length).
٦. The compressive strength and flexural strength were tested in this work.

١-٣- Thesis Layout

This thesis consists of five chapters:

Chapter Two “Literatures Review”, introduces a definition of the SCC (Self-Compacting Concrete), SCC achievement, advanced materials used in production of SCC, workability of SCC, conformity control and conformity criteria of SCC, shrinkage cracking, shrinkage of SCC, types of shrinkage and factors influencing it. The end and the base restraints and their effect on cracking behavior of SCC were discussed in this chapter.

Chapter Three describes the experimental work, which consists of three parts. The first part deals with achieving SCC from locally available materials. The second part deals with the effect of some fillers on the dimensional changes of SCC. The third part describes the experimental plate models restrained from movement which was made to investigate the behavior of shrinkage cracking of SCC. Materials, mix design, mixing procedure, casting procedure and procedure of measurements carried out in this study are discussed.

Chapter Four, the analysis and discussion of the experimental work were presented. In this chapter properties of fresh SCC and the effect of fillers on free shrinkage, tensile strain capacity, elastic tensile strain capacity, creep, cracking time, crack width for SCC beams were analyzed and studied. The free and restrained shrinkage of plates, cracking age, crack spacing and a adopted and modified formula for the relationship between maximum crack width and maximum crack spacing were presented in this chapter. The validity of this adopted formula and formulas of previous researchers were examined with reference to the results of the tests performed on the plate models. It was found that there is a good agreement between the present formulas results and experimental plate model measurements.

CHAPTER TWO

REVIEW OF LITERATURES

٢-١- Self-Compacting Concrete

Self-Compacting Concrete (SCC) represents one of the most outstanding advances in concrete technology during the last decade. Due to its specific properties, SCC may contribute to a significant improvement of the quality of concrete structures and open new fields for the application of concrete. Self-Compacting Concrete is not affected by the skills of workers, the shape and

amount of reinforcing bars or the arrangement of the structure. Due to high-fluidity and resistance to segregation it can be pumped longer distances⁽³⁾. In principle, a Self-Compacting Concrete must:

၁. Have a fluidity that can be self-compacted without external energy.
၂. Remain homogeneous in a form during and after the placing process.
၃. Flow easily through congested reinforcement.

The technology of SCC is based on adding or partially replacing Portland cement with amounts of fine materials such as fly ash, blast furnace slag, silica fume and limestone powder. A partial replacement of Portland cement by additives was soon realized to be the best compromise in terms of rheological properties, resistance to segregation, strength level and crack freedom, particularly in mass concrete structures exposed to restrained thermal stresses produced by the heat of hydration of cement⁽¹⁾.

၂-၂- Development of Self-Compacting Concrete

For several years beginning in ၁၉၈၃, the problem of the durability of concrete structures was a major topic in Japan. The creation of durable concrete structures requires an adequate compaction by skilled workers. However, the gradual reduction in the number of skilled workers in Japan's construction industry has led to a similar reduction in the quality of construction work. One solution for achievement of durable concrete structures independent of the quality of construction work is the employment

of Self-Compacting Concrete, which can be compacted into every corner of a formwork, purely by means of its own weight and without the need for vibrating compaction. The concept of Self-Compacting Concrete was proposed in 1986 by Okamura⁽¹¹⁾, but the prototype was first developed in 1988 in Japan by Ozawa⁽¹²⁾ at the University of Tokyo.

2-3- Self-Compacting Concrete Achievement

Two important specific properties to SCC in its plastic state are their flowability and stability. The high flowability of SCC is generally attained by using high range water reducing (HRWR) admixture and not by adding extra mixing water. The stability or resistance to segregation of the plastic concrete mixture is attained by increasing the total quantity of fines in the concrete and / or by using admixtures that modify the viscosity of the mixture. To achieve a balance between flowability and stability, the total content of particles finer than 100 μm has to be high, usually about (0.20 to 0.60) kg/m³⁽¹³⁾. SCC mixture typically have a higher paste volume, less coarse aggregate and higher fine-coarse aggregate ratio than typical concrete mixtures⁽¹³⁾. Table (2-1) shows an example of mix proportion used in SCC as compared to the normal concrete mix (N.C)⁽¹³⁾.

Table (2-1): Materials Used in Normal Concrete and SCC by Absolute

Volume⁽¹³⁾

	C %	W %	A %	F %	F.A %	C.A %
N.C	10	18	2	0	20	40
SCC	10	18	2	8	26	36

Notes:

C: cement W: water A: air F: additions

F.A: fine aggregate C.A: coarse aggregate

The frequency of collision and contact between aggregate particles increase as the relative distance between the particles decreases and the internal stress can increase when concrete is deformed, particularly near obstacles. It's found that the energy required for flowing is consumed by the increased internal stress, resulting in blockage of aggregate particles. Limiting the coarse aggregate content, whose energy consumption is particularly intense, to a level lower than normal is effective in avoiding this kind of blockage⁽¹⁴⁾.

Kennedy⁽¹⁵⁾ proposed the "Excess Paste Theory" which explains the fact that attaining workability is necessary to have not only enough cement paste to cover the surface area of the aggregate, so as to minimize the friction between them, but also more of it to give better flowability. In Figure (3-1), the left side model shows that the aggregates are closely contacted to each other, with voids in between them.

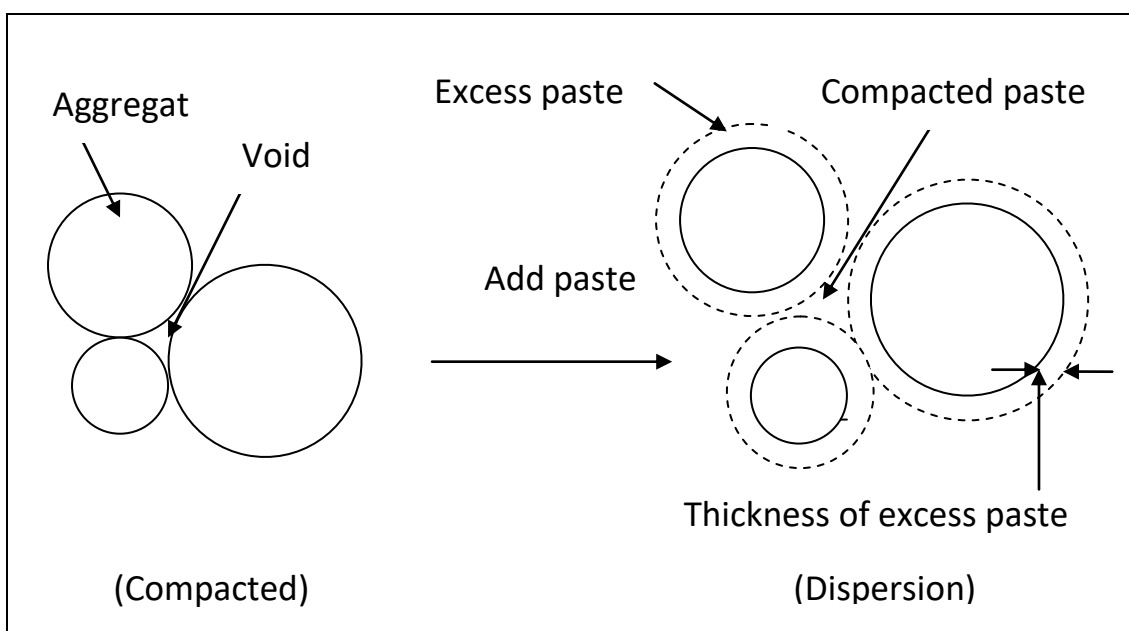


Figure (γ-1): Excess Paste Theory⁽¹⁰⁾

If this model is mixed with cement paste, these closely packed aggregates are then separated by a thin film of cement paste around them, as shown in the model on the right side of the figure. Adding the cement paste will change the interaction between aggregate. This is a sort of dispersion effect, so aggregate are pushed away from each other, which is accompanied with better flowability.

γ-ξ- Advanced Materials

Concrete originally designed as a mixture of aggregate, cement and water developed recently into a composite material containing admixtures and fillers which completely changed the philosophy of its design. In the classical concrete, Figure (γ-α), the grains of coarse aggregate touch and produce a skeleton. The spaces among grains will be filled with the fine aggregate and a high energy was necessary for compaction⁽¹¹⁾. On the other hand, the advanced concrete materials use a "floating" structure. The grains of a coarse aggregate are not in touching, the space among them will fill with fine aggregate, cement paste and fillers Figure (γ-β). The stress will be transferred from one grain to another and will not concentrate on the grain border. The stress will spread over a certain area of fine particles which make the concrete easier for compaction and high strength. The fine material between the grains also improves the workability

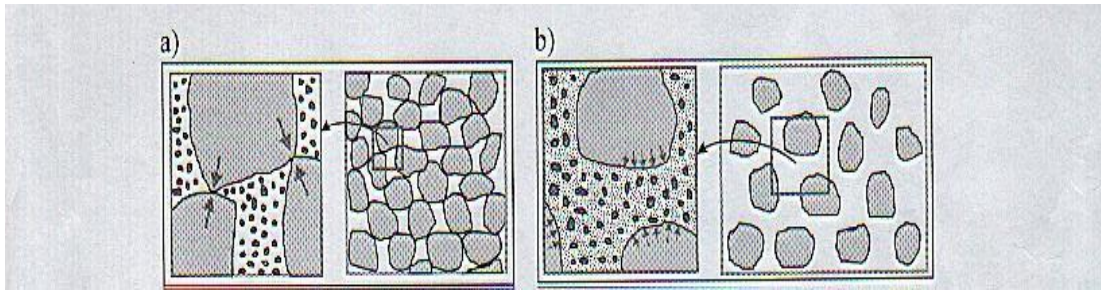


Figure (2-2): Concrete Structure⁽¹⁷⁾ (a) Classical Concrete

(b) Advanced Concrete

2-2-1 - Cement

The first choice to be made when making SCC is definitely that of the cement, even when one or two supplementary cementitious materials are used. Because the performance of cement in terms of rheology and strength becomes critical issue as the target workability and compressive strength increase⁽¹⁸⁾.

There is a wide variety of cements that are used to some extent in the construction and building industries, or to solve special engineering problems⁽¹⁹⁾. The chemical composition of these cements can be quite different, but the greatest amount of concrete used today is made with Portland cements⁽²⁰⁾.

The direct effect of cement on concrete could be simplified by the fact that the cement paste is the effective part in the concrete, and the strength of mortar or concrete depends on the cohesion of the paste, and its adhesion to the aggregate particles⁽²¹⁾.

2-1-2- Aggregate

2-1-2-1- Coarse Aggregate

SCC has been made with both gravels and crushed rock as coarse aggregate. Aggregate blocking must be avoided as SCC flows through the reinforcement and the L-box test is indicative of the passing ability of a SCC mix. The nominal maximum size is generally 20 mm⁽²⁰⁾, however particle size up to 40 mm or more have been used in SCC. Consistency of grading is of vital importance.

Regarding the characteristics of different types of aggregate, crushed aggregates tend to improve the strength because of the interlocking of the angular particles, while rounded aggregates improve the flow because of lower internal friction⁽²¹⁾.

Coarse aggregate makes about (40-50) % by volume of normal concrete according to Table (2-1)⁽¹³⁾, thus the properties of hardened concrete is influenced considerably by the coarse aggregate, while in SCC the coarse aggregate makes up (30-35) % of the concrete volume^(21,22,23), therefore, it has a lower effect on the properties of hardened SCC.

The amount of coarse aggregate is reduced as they take up a lot of energy in moving them. Reduction in the coarse aggregate content is balanced by the increase in paste volume, which has the effect of increasing the aggregate inter-particle distance, thereby reducing the possibility of contact and lowering the aggregate-aggregate friction⁽²⁴⁾.

2-1-2-2- Fine Aggregate

All normal concreting sands are suitable for SCC. Both crushed and rounded sands can be used. The influence of fine aggregate on the fresh properties of the SCC is significantly greater than that of coarse aggregate. The amount of fines less than 0.150 mm size is to be considered as powder and is very important for the rheology of SCC.

The high volume of paste in SCC mixes helps to reduce the internal friction between the sand particles but a good grain size distribution is still very important. The grading of fine aggregate in the mortar should maintain both workability and stability at the same time⁽²⁰⁾.

2-4-3- Superplasticizers

Superplasticizers (high range water reducers) are low molecular-weight, water-soluble polymers designed to achieve high amount of water reduction ($12-30\%$) in concrete mixtures in order to attain a desired slump⁽²¹⁾. These admixtures are used frequently to produce high-strength concrete (> 0 MPa), since workable mixes with water-cement ratios well below 0.4 are possible⁽²²⁾. They also can be used without water reduction to produce concrete with a very high slump, in the range of (100 to 200 mm). At these high slumps, concrete flows like a liquid and can fill forms efficiently, requiring a very little vibration. These highly workable mixtures are called flowing concrete and require slumps to be in excess of 190 mm. The requirements for superplasticizer in Self-compacting concrete are summarized below:

1. High dispersing effect for low water/powder ratio.
2. Maintain of the dispersion effect for at least two hours after mixing.
3. Less sensitivity to temperature changes.

Admixture helps to provide a very good homogeneity and reduces the tendency to segregation. It is a surface-active agent causing dispersion thereby reducing the friction among powder materials. The common superplasticizer used is a new generation type based on polycarboxylated polyether.

2-2-2- Supplementary Cementitious Materials or Fillers

The use of Supplementary Cementitious Materials or Fillers like fly ash, silica fume, metakaolin, and limestone powder have been adopted in prestigious projects, with an aim to achieve higher strengths and better durability⁽²⁴⁾. Special rheological requirements of SCC, both inert and reactive additions are commonly used to improve and maintain the workability as well as to regulate the cement content and so reduce the heat of hydration. There are two types of additions:

1. nearly inert addition as filler aggregate, pigment, and limestone fines.
2. pozzolanic or latent hydraulic addition as fly ash, silica fume, and metakaolin⁽²⁴⁾.

To avoid excessive heat generation, the Portland cement is generally partially replaced by mineral admixtures like limestone filler or fly ash. The nature and the amount of filler added are chosen in order to comply with the strength and durability requirements⁽²⁴⁾. Each filler has its influence on the mix for SCC and must be investigated by different methods (rheology test) and mixing trials.

2-2-2-1- Pigment

The suitability of pigments used in SCC building permitted by BSEN 206-1⁽²⁰⁾ for the coloration of building and filling material to improve the properties of fresh and hardened concrete.

Pigments can be used successfully with SCC, applying the same attention and limitations as in traditional vibrated concrete. However, they can affect fresh properties so they should not be added to an existing SCC without first doing a trial.

Pigments for cement and cement products may be satisfactorily used in the form of water pastes as well as in the more usual milled powder form⁽²¹⁾. Pigments can be added to the mixer, those are powders of fineness similar to, or higher than, that of cement. An improvement in the dispersion of the pigment can be obtained by the use of superplasticizer⁽²²⁾.

2-2-2-2- Limestone Powder

Finely crushed limestone may be used to increase the amount of powder, the fraction less than 0.125mm will be of most benefit. Limestone filler will help to maintain stability in a high workability mix although it will not contribute significantly to the compressive strength development of SCC⁽²³⁾. Limestone filler will also help to control the heat of hydration in mixes that have a high Portland cement content⁽²⁴⁾.

2-2-2-3- Metakaolin

Metakaolin is a highly pozzolanic material produced by calcining China clay at temperature of (700-900) C°. It is permitted by BS 4000 with an appropriate

agreement certificate (BSEN 206-1 and BS 8000)⁽¹¹⁾. The particle size should not be more than 0.125 mm in order to achieve high workability and reactivity when added as a part of cement weight.

2.5- Mix Design

There is no standard method for SCC mix design and many academic institutions, admixture ready-mix, precast and contracting companies have developed their own mix proportioning methods. Mix designs often use volume as a key parameter because of the importance of the need to over fill the voids between the aggregate particles. Some methods try to fit available constituents to an optimized grading envelope⁽¹²⁾. Mix designs of SCC must satisfy the criteria on filling ability, passing ability and segregation resistance. The most common method of mix design is the general method developed by the University of Tokyo and since then, many attempts have been made to modify this method to suit local conditions⁽¹³⁾.

2.6- Mix Design Principles

To achieve the required combination of properties in fresh SCC mixes:

1. The fluidity and viscosity of the paste is adjusted and balanced by careful selection and proportioning of the cement and additions, by limiting the water/powder ratio and then by adding a superplasticizer and (optionally) a viscosity modifying admixture. Correctly controlling these components of SCC, their compatibility

and interaction is a key to achieving good filling ability, passing ability and resistance to segregation^(r°).

٢. The paste is the vehicle for the transport of the aggregate, therefore the volume of the paste must be greater than the void volume in the aggregate so that all individual aggregate particles are fully coated.
٣. The coarse to fine aggregate ratio in the mix is reduced so that individual coarse aggregate particles are fully surrounded by a layer of mortar. This reduces aggregate interlock and bridging when the concrete passes through narrow openings or gabs between reinforcement and increases the passing ability of the SCC^(r°).

٢-٧- Adjustment of the Mix

Laboratory trials should be used to verify properties of the initial mix composition. If necessary, adjustments to the mix composition should then be made. Once, all requirements are fulfilled, the mix should be tested at a full scale at the concrete plant or at site.

In the event that satisfactory performance cannot be obtained, then consideration should be given to fundamental redesign of the mix. Depending on the apparent problem, the following courses of action might be appropriate^(^):

١. using additional or different types of filler, (if available)
٢. modifying the proportions of the sand or the coarse aggregate
٣. using a viscosity modifying agent, if not already included in the mix
٤. adjusting the dosage of the superplasticizer and / or the viscosity modifying agent

- . using alternative types of superplasticizer (and / or Viscosity Modifying Admixture (VMA)), more compatible with local materials
- ٦. adjusting the dosage of admixture to modify the water content, and hence the water-powder ratio^(٣٧).

In SCC mixes, not only the coarse aggregate content might be limited but also the fillers, content of fines (sand and filler) and superplasticizer might be used to prevent segregation and increase flowability^(٣٧).

٢-٨- Mix-Design Method

Some mix design methods developed at academic and other institution are summarized below:

٢-٨-١- Rational Mix-Design Method

Self-Compactability Concrete can be largely affected by the characteristics of materials and the mix proportions. A rational mix-design method for Self-Compacting Concrete using a variety of materials is necessary. Okamura and Ozawa^(٣٨) have proposed a simple mix-proportioning system assuming general supply from ready-mixed concrete plants^(٣٩). The coarse and fine aggregate contents are fixed so that Self-Compactability can be achieved easily by adjusting the water-powder ratio and superplasticizer dosage only.

- ١. The coarse aggregate content in concrete is fixed at ٥٠٪ of the solid volume.
- ٢. The fine aggregate content is fixed at ٤٠٪ of the mortar volume.

- γ. The water-powder ratio in volume is assumed as $\gamma \cdot \eta \cdot \rho$, depending on the properties of the powder.
- ξ. The superplasticizer dosage and the final water-powder ratio are determined so as to ensure Self-compactability.

Ouchi^(ξ) summarized a rational mix-design method, as in Figure (γ-ξ). Only water-powder ratio & S.P./powder are to be adjusted by testing with gravel and sand fixed.

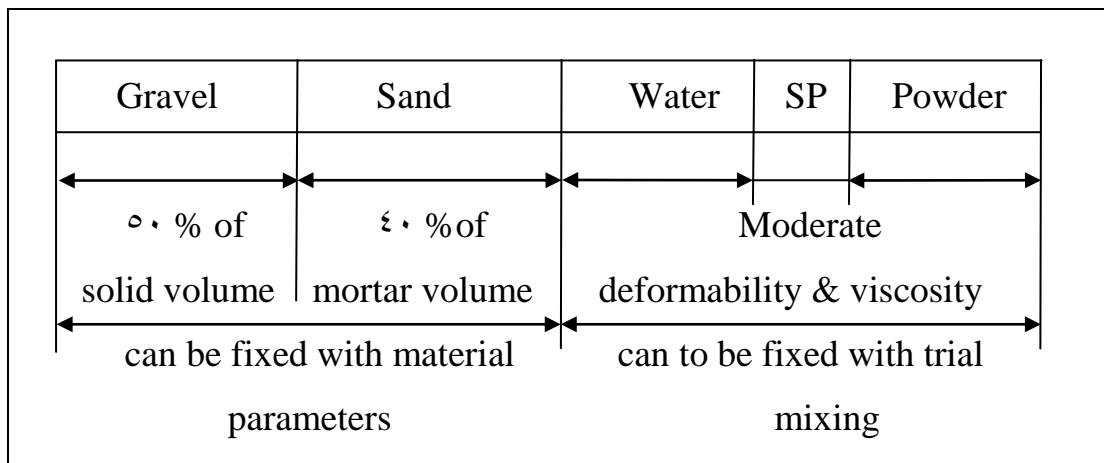


Figure (γ-ξ): Rational Mix-Design Method^(ξ)

In the mix proportioning of conventional concrete, the water-cement ratio is fixed at first from the viewpoint of obtaining the required strength. With Self-Compacting Concrete, however, the water-powder ratio has to be decided taking into account Self-compactability because Self-compactability is very sensitive to this ratio. In most cases, the required strength does not govern the water-cement ratio because the water-powder ratio is small enough for obtaining the required strength for ordinary structures unless most of the powder materials in use are not reactive. The mortar or paste in Self-

Compacting Concrete requires high viscosity as well as high deformability. This can be achieved by the employment of a superplasticizer, which results in a low water-powder ratio for high deformability^(1.2).

2-8-2- Common Design Method for SCC

There is no unique mix design solution for the production of SCC and a wide variety of materials have been used^(1.3). Water-powder ratios are generally less than 0.5 (by weight) and mixes have lower coarse aggregate content and higher paste content than conventional concrete^(1.3). Admixtures and fillers contribute to increase both the workability and segregation resistance^(1.3). Experience in Japan and Europe showed that there are wide variations of materials and proportions that can be used to produce satisfactory SCC, with certain key factors which fall within certain limits. These limits are summarized in Tables (2-2) and (2-3).

Table (2-2): Mix Proportions of Concrete^(2.1)

Materials	Housing		Civil		FSCC
	RH	SCCH	SCCC	RC	
Free water	200	190	192	220	160
Portland cement 42.5	290	280	330	510	280
Limestone powder	---	240	---	---	270
GGBS	---	---	200	---	---
Fiber (Rc 60 130 BN)					30
Total powder content	290	520	530	510	500
Sand (0-5 mm)	840	860	870	600	940
20 mm aggregate (*10 mm)	970	700	700*	930*	710
Viscocrete 2, Kg	---	4.2	0.3	---	4.4
Normal	---			6.4	

superplasticizer					
Water-cement ratio	۰.۶۸	۰.۶۸	۰.۵۸	۰.۴۳	۰.۵۶
Water-powder ratio	۰.۶۸	۰.۳۶	۰.۳۶	۰.۴۳	۰.۲۹

Notations:

SCCH: Self-Compacting Concrete Housing

SCCC: Self-Compacting Concrete Civil Engineering

RH : Reference Housing

RC : Reference Civil Engineering

FSCC: Fiber Self-Compacting Concrete

Table (۲-۳): Range of Mix Constituents^(۲۱,۲۲,۲۳)

Constituents	By volume	By weight (Kg/m ³) of concrete
Coarse aggregate	۳۰-۴۰ % of concrete	۷۵۰-۹۲۰
Fine aggregate	۴۰-۵۰ % of mortar	۷۱۰-۹۰۰
Powder	—	۴۵۰-۶۰۰
Paste	۳۴-۴۰ %	—
Water	۱۵۰-۲۰۰ l/m ³	۱۵۰-۲۰۰

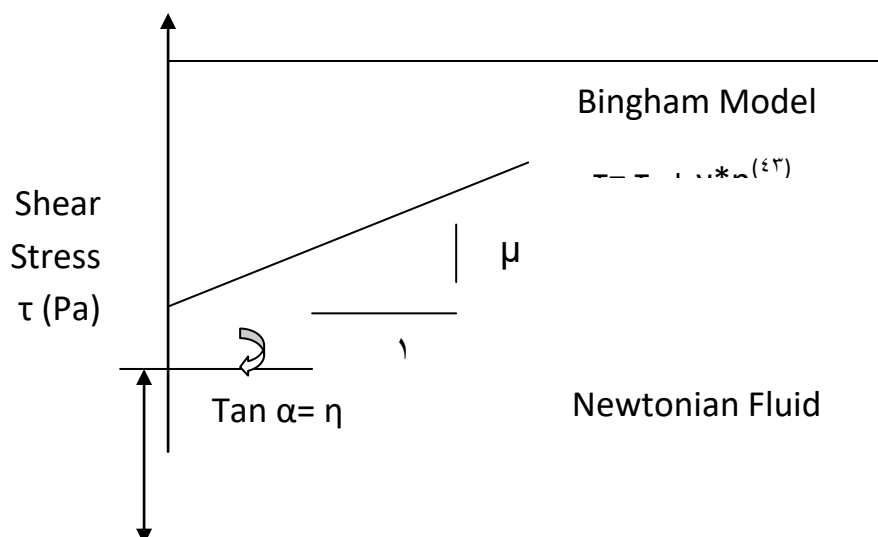
The SCC mixes contain high-volume additions of limestone powder or blast furnace slag to enhance fluidity and cohesiveness and limit heat generation. Such materials are also less reactive than cement and can reduce the problems resulting from loss of fluidity of the rich concrete. The incorporation of one or more powder materials having different morphology and grain-size distribution

can improve particle packing density and reduce interparticle friction and viscosity, hence improving deformability, Self-compactability, and stability.

2-9- Workability of SCC

2-9-1- Rheology of SCC

The science dealing with deformation and flow of materials under stress, and the emphasis on flow means that it is concerned with the relationships between stress, strain rate and time^($\dot{\epsilon}$). Fresh concrete can be described as a particle suspension. Its rheological properties are rather complex because of the large spread of particle sizes and the hydration reactions, which are time dependent^(t). In the fresh state SCC corresponds rheologically to a good approximation to a Bingham solid with the parameters of yield value and viscosity Figure (2-4). The Bingham flow law describes the deformation behavior of a suspension under shear stress. It is composed of a constant factor, the yield value (τ_0) and a variable component that depends on the ratio of the applied shear stress (τ) to the rate of load application ($\dot{\gamma}$) and is described by the viscosity (η). The yield value gives the energy that must be applied externally to make the suspension start to flow. The viscosity describes the resistance to deformation during the flow.



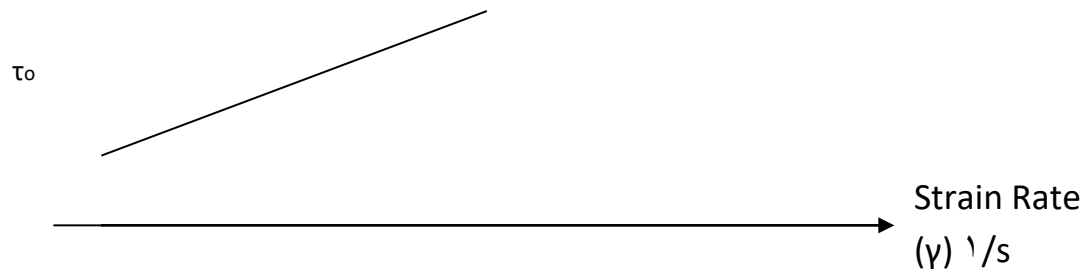


Figure (2-4): Bingham Rheology Model⁽²¹⁾

Once the concrete starts to flow, shear stress increases linearly with increases in strain rate as defined by plastic viscosity (μ). Thus, one target of rheological property of SCC is to reduce the yield stress to as low as possible so as to behave like a Newtonian fluid with zero yield stress. The other target property is an adequate viscosity⁽²¹⁾.

The addition of water reduces both the yield stress and viscosity. However, too much water can reduce the viscosity to such an extent that segregation occurs. Segregation resistance between water and solid particles can be increased by increasing the viscosity of water through the incorporation of viscosity modifying admixtures. The incorporation of superplasticizer reduces the yield stress but causes limited reduction in viscosity^(21, 44).

2-1.1 - Properties of Fresh SCC Mixes

Fresh SCC must possess at required level the following key properties:

1. filling ability
2. passing ability
3. segregation resistance

In order to be able to produce a good SCC, it is necessary to prepare the mixer before the first batch produced. This may be done by mixing a pre-batch of concrete before starting the production of SCC⁽¹⁴⁾.

2-1-1- Filling Ability

It is the ability of SCC to flow into all spaces within the formwork under its own weight. Fluidity or deformability means the ability of the flowing concrete to fill every corner of the moulds, often referred to as filling ability. To enable this to occur, the interparticle friction of the materials must be reduced. This can be achieved in two ways⁽¹⁵⁾:

1. Surface tension can be reduced by the inclusion of superplasticizers.
2. Optimizing the packing of fine particles can be achieved by the introduction of fillers or segregation controlling admixtures.

2-1-2- Passing Ability

Passing ability describes the capacity of the fresh mix to flow through confined spaces and narrow openings such as areas of congested reinforcement without segregation, loss of uniformity or causing blocking. In defining the passing ability, it is necessary to consider the geometry and density of the reinforcement, the flowability/filling ability and the maximum aggregate size⁽¹⁶⁾. To satisfy these requirements, the maximum size aggregate is generally limited to 20 mm. The amount of coarse aggregate is reduced as they take up a lot of energy in moving them. Reduction in coarse aggregate content is balanced by the increase in paste volume, which has the effect of

increasing the aggregate inter-particle distance, thereby reducing the possibility of contact and lowering the aggregate-aggregate friction^(٢٥).

٢-١٠-٣- Segregation Resistance (Stability)

Segregation resistance is the ability of SCC to remain homogenous in composition during transport and placing. Due to the high fluidity of SCC, the risk of segregation and blocking is very high. Preventing segregation is therefore an important feature of the control regime, therefore, needs to be addressed^(١٧):

١. The amount of free water needs to be minimized to avoid bleeding. This can be achieved by the use of superplasticizer to reduce the water demand and well-graded cohesive aggregate to minimize segregation.
٢. The liquid phase needs to be viscous to maintain the coarse particles in suspension, when mobile. The tendency to segregation can be reduced by the use of a sufficient amount of fines (< ٠.١٢٥ mm) or using a Viscosity Modifying Admixture (VMA).

٢-١١- Test Method

Many different test methods have been developed in attempts to characterize the properties of SCC. Table (٢-٤) lists the most common tests grouped according to the property investigate.

Table (٢-٤): Test Methods for Evaluating SCC^(٩,٤٥)

Characteristic	Test Method	Measured Value
----------------	-------------	----------------

Filling ability	Slump flow T ₅₀ · cm V funnel	totals spread flow time flow time
Passing ability	L-box U-box	passing ratio height difference
segregation	V funnel at T ₅₀ minutes	time increase

No single test is capable of assessing all of the key parameters, and combination of tests is required to fully characterize a SCC mix. Similarly no single method has been found which characterizes all the relevant workability aspects so each mix design should be tested by more than one test method for the different workability parameters.

According to Ozawa et al.,⁽⁴⁷⁾ and Victor et al.,⁽⁴⁸⁾ to characterize and quantify the self-compactibility of fresh concrete, a number of tests in Table (2-4) were conducted, including deformability tests using slump flow, flow rate test using a funnel device and self-placing test using a box vessel with reinforcing bars as obstacles to SCC flow. These methods have generally been adopted to quantify the flow properties of Self-Compacting Concrete.

The most important test is:

2-11-1- Slump Flow and T₅₀ · cm Test

The flowing ability of fresh concrete is measured by slump-flow investigated with Abrams cone. The slump-flow test is the most widely used method for evaluating concrete consistency in the laboratory and at job sites. The basic equipment used is the same as for the conventional slump test. With the

slump flow test, the T₅₀ slump flow time was measured. The T₅₀ is the time to reach a spread of 500 mm^(1,2).

The test method differs from the conventional one by the fact that the concrete sample placed into the mold is not rodded and when the slump cone is removed the sample collapses⁽³⁾. The diameter of the spread of the sample is measured, i.e., a horizontal distance is determined as opposed to the vertical distance in the conventional slump test. The slump flow test can give an indication to the consistency, filling ability and workability of SCC. The SCC is assumed of having a good filling ability and consistency if the diameter of the spread reaches values between (700 to 800 mm).

2-11-2- L-Box Test

The L-box test is useful in assessing different parameters such as mobility, filling ability and passing ability. The apparatus consists of a rectangular section box in the shape of an "L", with a vertical and horizontal sections, separated by a movable gate, in front of which vertical length reinforcement bar is fitted⁽⁴⁾ as shown in Figure (2-9). This test, based on Japanese design for under water concrete was described by Petersson⁽⁵⁾.

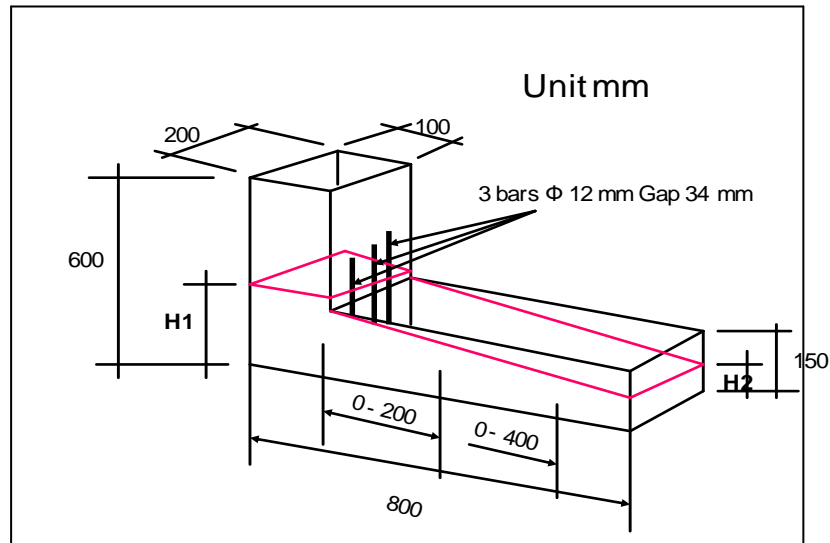


Figure (2-5): L-Box Test ⁽²⁹⁾

The horizontal section of the box can be marked at 200 mm and 400 mm from the gate and the times taken to reach these points are measured. These are known as the T_{200} and T_{400} times which are indication of the filling ability, and the heights H_1 and H_2 of concrete are measured and used to determine the L-box result $(H_2/H_1)^{(T_{200}, T_{400})}$.

2-11-3- U-Box Test

This test was developed by the Technology Center of the Taisei Corporation in Japan ^(23, 29). The test is used to measure the filling ability of Self-Compacting Concrete.

The equipment consists of U-box, as shown in Figure (2-6) ⁽²⁹⁾. The sliding gate is fitted between the two sections. Reinforcing bars with nominal diameter of 12 mm are installed at the gate with center to center spacing of 200

mm. According to ENARC, 200 ± 20 acceptable value of the filling height, $h_1 - h_2$ is normally $(100 - 150)$ mm.

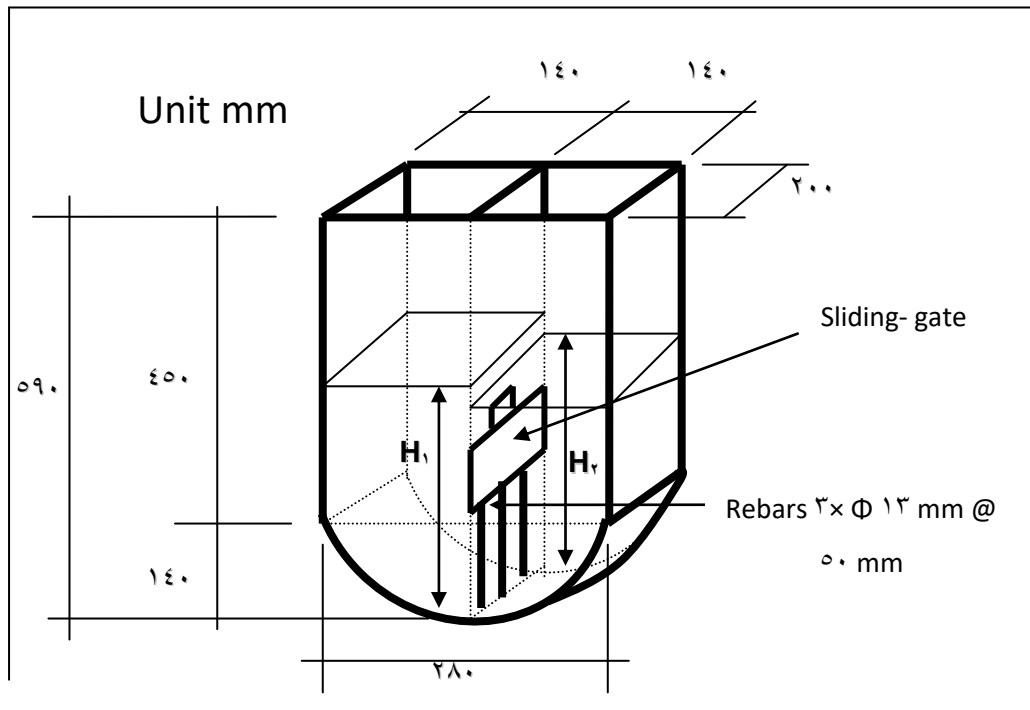


Figure (2-6): U-Box Test⁽²¹⁾

2-11-ξ- V-Funnel Test

Viscosity of the SCC is obtained by using a V-funnel apparatus, which has certain diameter (100mm) as shown in Figure (2-7) for a given amount of concrete to pass through an orifice⁽²⁹⁾. This test was developed in Japan and used by Ozawa et al.,⁽²⁶⁾.

The amount of concrete needed is 12 liters and the maximum aggregate size is 20 mm. The time for the amount of concrete to flow through the orifice is being measured. If the concrete starts to move through the orifice, it means that the stress higher than the yield stress, therefore, this test measures a

value that is related to the viscosity. If the concrete does not move, it shows that the yield stress is greater than the weight of volume used.

High flow time can be associated with low deformability due to high paste viscosity, and with high inter-particle friction^(۲۳). The V-funnel test used to assess the filling ability (flowability) and stability of Self-Compacting Concrete.

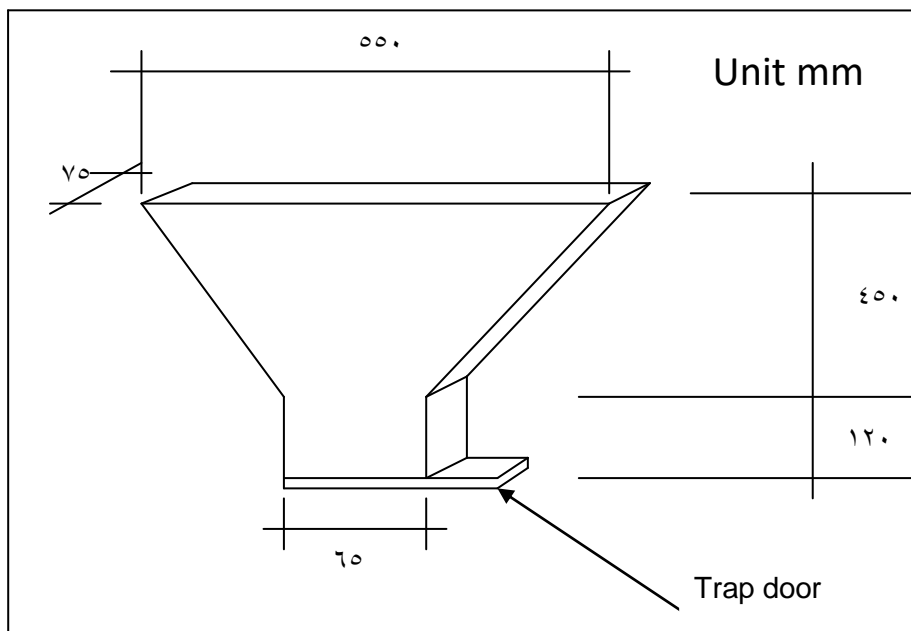


Figure (۲-۷): V-Funnel Test^(۴۹)

۲-۱۲- Conformity Control and Conformity Criteria

In the case of precast and site made concrete where the user and producer are the same party, testing and verification is undertaken as part of the production control at the same rate of testing and using the same criteria as for conformity. In this case, failure to satisfy the criteria does not lead to a declaration of non-conformity but to an internal investigation to assess whether this indication a non-conformity with the requirements of the

hardened concrete. Conformity to the properties of SCC is confirmed if the specified criteria satisfy the limits given in Table (۲-۵)^(۲۳,۵۲). Table (۲-۶) explain the description of suitability of different test methods for SCC^(۵۲).

Table (۲-۵): Acceptance Workability Criteria According to Specification
and Guidelines for the Fresh SCC^(۲۳,۵۲)

Test Methods	Unit	Typical range of volume	
		Minimum	maximum
Slump flow by Abrams cone	mm	۶۵۰	۸۰۰
T۵۰ cm slump flow	sec	۲	۵
V-funnel	sec	۶	۱۲
L-box	h ^۲ /h ^۱	۰.۸	۱.۰
U-box	(h ^۱ -h ^۲)mm	۰	۳۰

Table (۲-۶): Suggestion on Suitability of Different Test Methods for
SCC^(۵۲)

Method	Mobility	Passing ability	Segregation	Viscosity
Slump flow	xx	n.a	x	n.a.
T۵۰ cm	n.a.	n.a.	n.a.	x
L-Box	n.a.	xx	x	x

Notations:

xx : Most suitable

x : Less suitable

n.a : Not applicable

۲-۱۳- Shrinkage Cracking

2-13-1- General

Concrete is a vital component of our infrastructure and society from roads to buildings, and its durability needs to be maintained to insure a proper service life. One aspect of durability under consideration is the materials volume change of concrete, resulting from structural and environmental factors. The volume changes are often attributed to drying of concrete over a long period. Shrinkage is caused by evaporation of water, by hydration of cement, and by carbonation. Shrinkage of concrete occurs in two distinct stages: early and later stages. The early stage includes the first 24 hours of concrete life, whereas the long-term stage refers to the concrete at an age of 24 hours and beyond^(23,24).

2-13-2- Shrinkage of SCC

SCC recipes are often associated with high content of binder, fillers and plasticizing admixtures, which all may contribute to increase drying shrinkage⁽²⁵⁾. Many publications contain very different statements about these materials properties which can be explained with the various influence parameters on shrinkage and creep of concrete. There is a general agreement in existence, however, to the fact that SCC is affected in the same way as normal vibrated concrete by the water cement ratio as well as the kind of specimen curing⁽²⁶⁾.

In direction, the conclusion could be drawn that the shrinkage deformations can achieve clearly higher values in SCC than in comparable normal vibrated concrete. Nevertheless, it should be possible to modify the SCC composition in such a way that smaller shrinkage deformations will be adjusted, similar to these from normal vibrated concrete⁽²⁷⁾.

A large influence on the shrinkage deformations seems to result from the aggregate combination, especially the relation of coarse to fine aggregate as well as fineness and content of ultra fines. So the shrinkage can be reduced by using a higher content of coarse aggregates. However, a minimum paste volume must be presented in order to ensure an optimal Self-compacting of SCC without segregation. Furthermore, a denser microstructure of the cement paste can be achieved by addition of fillers with fineness larger than that of cement fineness, whereby the shrinkage dimension is positively affected (increased)⁽⁶⁹⁾.

In the majority of the publications it is shown that the drying shrinkage of SCC is (10 to 20) % higher than that of conventional concrete. Remarkable is the substantially steeper rise of the deformations particularly for young concrete aged up to 28 days, which decreases again with an increasing age. Special attention should be given to the early age shrinkage of SCC that is substantially stronger pronounced opposite to conventional concrete, which can be related to the increased fine grain portion. These deformations can be limited by appropriate subsequent curing methods⁽⁶⁷⁾.

Increased shrinkage may result in more cracks in restrained concrete elements, which can accelerate the deterioration of both the concrete and the reinforcement. It is important to consider that the risk of cracking is not solely linked to the shrinkage. Cracks develop when the shrinkage leads to stress equals to the tensile strength of the concrete. This stress is dependent on the product of shrinkage, modulus of elasticity and creep/relaxation provided that the structure is 100 % restrained⁽⁶⁸⁾.

Sonebi et. al.,⁽⁶¹⁾ studied the drying shrinkage of different types of concrete. The dimensions of prisms used to measure the drying shrinkage were

(100x100x400 mm). A demec gauge was used to measure the drying shrinkage on two parallel sides. The drying shrinkage of SCC at 7-days was slightly higher than that of the reference mix but at 28-days and later, the reference mixes exhibited greater shrinkage than SCC mixes. The drying shrinkage of the reference mixes was higher than those of the SCC at 100-days by (30 %) for Reference Housing and (30%) for Reference civil engineering. This is considered to be due to the effect of the volume of paste and water-powder ratio. Similarly, the drying shrinkage of Fiber Self-Compacting Concrete at 120-days was about 47 % lower than that of Reference civil engineering (490 Mm/m versus 720 Mm/m).

2-1-4- Types of Concrete Shrinkage

2-1-4-1- Plastic Shrinkage

Plastic shrinkage is due to moisture loss from the concrete before the concrete sets. When water evaporates from the surface of freshly placed concrete faster than it is replaced by bleed water, the surface concrete shrinks. The magnitude of plastic shrinkage is affected by the amount of water lost from surface of concrete, which is influenced by many factors related to the concrete properties or the ambient conditions such as, concrete temperature, ambient temperature, relative humidity and wind velocity⁽⁶⁸⁾.

2-1-4-2- Drying Shrinkage

Drying shrinkage refers to the reduction in concrete volume resulting from a loss of water from the concrete stored in unsaturated air. Drying shrinkage magnitudes are highly dependent on the amount of water lost and the rate of evaporation.

According to Power and Brownyard⁽²⁹⁾ there are three types of water occurring in cement paste which are:

1. Non-evaporable water {fixed water}
2. Gel water {free water}
3. Capillary water {free water}

The non-evaporable water has entered into chemical combination with the cement and can be removed only by the application of considerable heat. The gel is composed of colloidal matter, which comprises an appreciable proportion of pores. These with the capillary pores are initially filled with water. The presence of these two types of water largely determines drying shrinkage. Capillary water is easily to evaporate but its effect on shrinkage is limited by the paste structure, while gel water is difficult to evaporate. The evaporation takes many years and it is the principle cause of drying shrinkage.

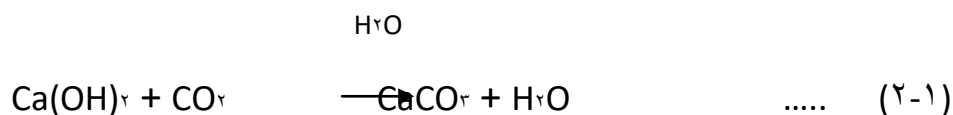
Neville⁽³⁰⁾ discussed the loss of water in concrete associated with drying shrinkage. The change in volume of the concrete is not equal to the volume of the water lost. The loss of free water occurs first, this causes little or no shrinkage. As the drying of the concrete continues, the adsorbed water is removed. This adsorbed water is held by hydrostatic tension in small capillaries ($< 0.1 \mu\text{m}$). The loss of this water produces tensile stresses which causes the concrete to shrink. The shrinkage due to this water loss is significantly greater than that associated with the volume of free water lost.

Reversible drying shrinkage is the part of the drying shrinkage of the concrete that is reproducible during wetting and drying cycles⁽³¹⁾. Irreversible drying shrinkage is the part of the total drying shrinkage during the first drying cycle that cannot be reproduced during subsequent wetting and drying cycles. The authors state that the irreversible shrinkage is probably due to the

development of the chemical bonds within the calcium silicate hydrate structure as a consequence of drying of the concrete.

2-1 ε-3- Carbonation Shrinkage

Carbonation occurs when cement paste in the hardened concrete (hydrated lime) reacts with moisture and carbon dioxide in the air, in accordance with equation (2-1) (Mehta and Monteiro)⁽¹⁾. This results in a slight shrinkage and a reduction in the pH of the concrete. Lowering the pH can be detrimental to concrete, primarily corrosion of steel reinforcement. The corrosive rust can cause expansion cracking and spalling of the concrete⁽¹⁾.



The amount of carbonation is dependent on the concrete density and quality but is usually limited to 5 cm of depth on the exposed surface. The actual rate of carbonation depends on the permeability of concrete, moisture and the CO₂ content and relative humidity of the ambient medium, therefore concrete with high water-cement ratio and inadequately cured will be more prone to carbonation.

2-1 ε-4- Autogenous Shrinkage

Autogenous shrinkage is defined as a concrete volume change occurring without moisture transfer to the environment. It is associated with the loss of water from the capillary pores due to the hydration of the cement⁽¹⁾. It is merely a result of the internal chemical reactions of the cement components.

Autogenous shrinkage tends to increase at higher temperatures, with a higher cement content, cements which have higher C_rA and C₃AF contents and possibly with a finer cement⁽¹³⁾. This type is considered small for the usual concrete mixes. For practical purposes, the typical value is normally taken equal to 1.5×10^{-4} at the age of one month and 1.0×10^{-4} at five years⁽¹⁴⁾. Tazawa and Miyazawa⁽¹⁵⁾ stated that, the autogenous shrinkage increases with decreasing water/cement ratio. It is slightly reduced by superplasticizers. It is usually a concern in high performance, or a high strength concrete (> 40 MPa) where the water to cement ratio (w/c) is under approximately 0.42: indeed, in this case the cement does not have enough water for hydration⁽¹⁶⁾.

2-1-0- Factors Affecting Shrinkage of Concrete

Delarrard et al.,⁽¹⁷⁾ discussed some of the factors that affect the magnitude of drying shrinkage in concrete. These factors include the aggregate used, the water-cement ratio, the relative humidity, and the member size.

2-1-0-1- Cement Type, Composition and Fineness

In general the increase of cement content increases the shrinkage and therefore the cracking tendency, but at the same time the increase in cement content increases the strength of concrete and the tensile strain capacity⁽¹⁸⁾.

Troxell et. al.⁽¹⁹⁾ concluded that shrinkage of low heat cement (type IV) is greater than that of (type I). This is believed to be due to high (C₃S) content in (type IV) cement, which exhibits high shrinkage. Shrinkage of high alumina cement is of the same magnitude as Portland cement, but it takes place more rapidly⁽²⁰⁾.

C₃S has a relatively low shrinkage because of C₃S produces a high percentage of Ca(OH)₂ with a low surface area where the shrinkage is proportional to the surface area ($\gamma C_3S + 1H \rightarrow C_3S \cdot H_2 + \gamma Ca(OH)_2$). C₂S has a high shrinkage because that C₂S has a low percentage of Ca(OH)₂ ($\gamma C_2S + \xi H \rightarrow C_2S \cdot H_2 + Ca(OH)_2$). C₄A has a very high shrinkage for producing a family of non-stable compounds and with time these compounds loose water. For C₃A there is not enough information about its influence on shrinkage.

ACI Committee 224R⁽¹⁷⁾, showed that the shrinkage is lower with higher C₃A/F, lower Alkali content (Na₂O and K₂O) and lower C₃A/SO₃ ratio. According to Lerch⁽¹⁸⁾ the addition of gypsum decreases the shrinkage of drying cement pastes, because it will alter the rate and products of hydration, thus changing the structure of the hardened paste. It was indicated that for cements of high C₃A content or high alkalis, the concentration on drying can be decreased as much as 30-60 % by the use of larger addition of gypsum than are permitted by current specification.

Carlson⁽¹⁹⁾ pointed out that fineness of cement has probably two opposing influences on shrinkage of concrete. Finer cement hydrates more extensively and thus produces a denser gel, which has a lesser shrinkage. On the other hand, the gel of the finer cement is stronger and therefore it has a higher effect against restraint of aggregate and this increases the shrinkage.

2-10-2- Aggregates

The aggregate appears clearly to have a great influence on the shrinkage of concrete. It occupies about (60-70 %) of total concrete volume and restrains

the shrinkage of cement paste. Carlson et al.,⁽¹⁰⁾ reported that the aggregate dilutes and reinforces the cement paste against contraction, thus, its magnitude to (1/8 to 1/6) its original value depending on the type and amount of aggregate used.

ACI Committee 224⁽¹¹⁾, explained that the ability of aggregate to restrain shrinkage of cement paste depends on the compressibility (higher stiffness or modulus of elasticity), the shrinkage of aggregate, the extensibility of cement paste and the bond between the cement paste and the aggregate. Smaller aggregate experience more uniform shrinkage. The type of aggregate, rather than the aggregate size, has an enhanced effect on the concrete shrinkage. Aggregate that shrinks considerably has a low rigidity compared to the tensile stresses developed by the shrinkage of the cement paste. These types of aggregate may have a large water absorption value which will result in a concrete with higher shrinkage⁽¹¹⁾. Types of aggregate such as quartz, feldspar, limestone and dolomite with a high modulus of elasticity produce a concrete with less shrinkage⁽¹¹⁾.

2-10-3- Water Content

Water content is the most important factor affecting the shrinkage of paste and concrete. The drying shrinkage is the main shrinkage, which is related to the water content because the later determines the amount of evaporation of water from the cement paste and the rate at which water can move towards the surface of the specimen⁽¹²⁾. Brooks⁽¹²⁾ demonstrated that shrinkage of hydrated cement paste is directly proportional to the water-cement ratio between the values of about 0.2 to 0.6. At higher water-cement ratios, the additional water is removed upon drying without resulting in shrinkage.

Carlson et al.⁽¹⁰⁾ reported that the shrinkage decreases about (30) percent when water content is reduced to (10) percent. A similar trend was given by the ACI Committee 224⁽¹¹⁾, for (10) percent reduction of water content, the one year drying shrinkage was lowered by about (10) percent.

2-10-ξ- Admixtures

Chemical admixtures have varying effects on the drying shrinkage of concrete. Informations on the effect of water reducing admixture on shrinkage is conflicting. Long-term shrinkage may be less, depending on the degree to which the water content of the concrete is reduced⁽¹²⁾. In other hand it is reported that superplasticizers increase the shrinkage by (10~20) percent, whereas, retarders may allow more shrinkage to be accommodated in the form of plastic shrinkage and probably increase the extensibility of concrete and therefore reduce cracking. Air entraining agents increase the amount of air in concrete and will increase shrinkage⁽¹³⁾.

Al-Nassar⁽¹⁴⁾ studied the effect of some admixture on dimensional changes and cracking of concrete. Four types of chemical admixtures were used: superplasticizer, plasticizer, water proofing and modified sodium lignosulphonate local plasticizer known commercially as (BVD). He found that the development of shrinkage is affected by the type and amount of admixture.

Shah et al.,⁽¹⁵⁾ used three different organic admixtures as shrinkage-reducing agents. They concluded that the addition of these admixtures significantly reduce the free shrinkage of concrete. The increasing amount of admixtures causes greater reduction of free shrinkage.

Silica fume increases the long-term shrinkage, fly ash and ground granulated blastfurnace slag increase shrinkage⁽³³⁾.

A study of four commercially available superplasticizers were used with type I Portland cement concrete mixes by Whiting⁽³⁴⁾. They represented both melamine and naphthalene formaldehyde condensation products. Hardened concrete specimens were prepared and tested for drying shrinkage. Whiting found that high range water reducers were capable of lowering the net water content of concrete mixtures from (10 to 20) % when they used in dosages recommended by the manufacturers. It was found that the drying shrinkage was slightly reduced in the attempt to lower the net water content of the concrete mixtures.

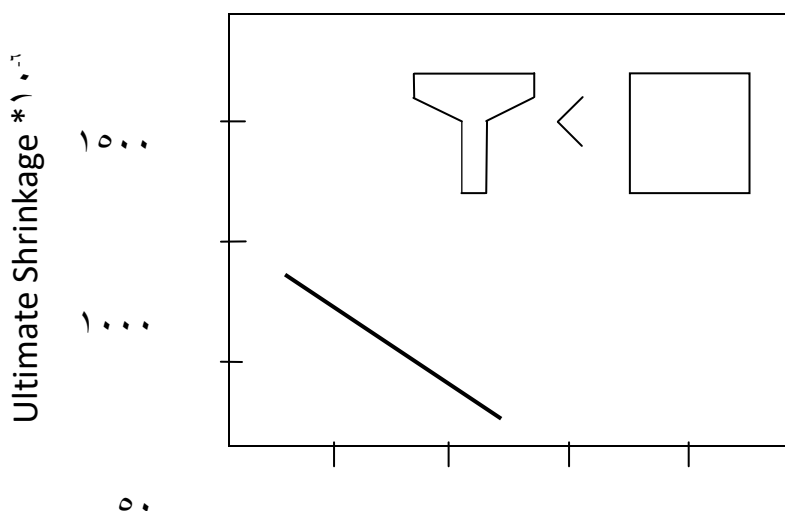
Lane⁽³⁵⁾ studied the shrinkage of Self-Consolidating Concrete. The mixtures contained type II Portland cement and class F fly ash was added 20 percent of the total cementitious material. Several admixtures were included in the mixture such as (HRWRA) complying with the requirements of ASTM C 494-92⁽³⁶⁾, Type F. The dimensions of prisms used to measure the drying shrinkage were (70x70x280 mm). The results showed that the shrinkage values varied from 82×10^{-6} to 89×10^{-6} at 28-days, which were higher than that required 80×10^{-6} , (which is the maximum limit for satisfactory performance in bridge deck concrete)⁽³⁷⁾.

Johansen and Hammer⁽³⁸⁾ studied the drying shrinkage of "Norwegian Self-Compacting Concrete" with an open grain size distribution between (0.150 and 2.0 mm) and with a natural filler (<0.150 mm), straight grain size distribution and dense grain size distribution between (2 and 8 mm) [the reduce amount of filler in straight and dense grain size due to loss fine sand, was compensated by increased amount of limestone filler (0.150 mm)], and studied drying

shrinkage of SCC with different silica fume (SF) contents (ξ, γ, 10 %). Drying shrinkage was tested as the length change of (100*100*50 mm) beams, with w/c ratio equal to 0.6. The grain size distribution, however, showed apparently a large influence, i.e. the dense distribution has a significantly lower shrinkage. The concrete with the highest content of limestone filler (dense) had a lowest shrinkage and evaporation. The result indicates that the silica fume contents (ξ and 10) % does not influence significantly the drying shrinkage. However, a comparison with the investigation results of concrete without silica fume indicates that the addition of silica fume increases drying shrinkage at first (γ to γ) weeks of drying period.

2-10-5- Volume-Surface Ratio

The duration of shrinkage is dependent on the concrete size and shape since they control the rate of moisture loss. The size and shape are often considered together as the volume to surface area ratio. Large specimens will shrink for longer periods but the ultimate magnitude may be lower. A high volume to surface ratio will usually result in a reduction of drying shrinkage magnitudes, as shown in Figure (2-8).



0 5 10 15 20 25

Volume to Surface Ratio (mm)

Figure (2-1): Effect of Volume to Surface Ratio on the Drying

Shrinkage of Concrete⁽²⁾

Mindess and Young⁽²⁾ also show the example of a T-beam compared to a solid beam with the different volume to surface ratios. If the two beams have equal widths and heights, the T-beam will dry more rapidly and will exhibit slightly more ultimate shrinkage since it has the lower volume to surface ratio. The faster drying is attributed to the shorter diffusion path for water to travel to reach an equivalent relative humidity through the cross-section.

2-10-6- Relative Humidity and Temperature

The reduction in the shrinkage is proportional to the increase of relative humidity because of the reduction of water evaporation from the surface of concrete. Troxell et al.,⁽²⁾ demonstrated that the drying shrinkage of concrete in an atmosphere of 70 percent relative humidity is about one-third lower than in 90 percent relative humidity. Neville⁽²⁾ states that the magnitude of shrinkage is independent on the rate of drying except that transferring specimens directly from water to a very low humidity can lead to fracture.

2-15-7- Curing

Neville⁽³⁷⁾ reported that well cured concrete shrinks more rapidly and therefore the relief of shrinkage stress by creep is smaller where the concrete also is being stronger and having an inherent low creep capacity. These factors may balance the higher tensile strength of well-cured concrete and may lead to cracking. In another report by Neville prolonged moist curing delays the initiate of shrinkage but the curing effect on the shrinkage magnitude is small, though rather complex. As far as neat cement paste is considered, the greater the quantity of hydrated cement the smaller is the volume of unhydrated cement particles, which restrain the shrinkage. Thus prolonged curing could expect to lead to greater shrinkage. But the hydrated cement baste contains less water and becomes stronger with age and is able attain a larger fraction of its shrinkage tendency with out cracking. However, in concrete, if cracking takes place e.g. around aggregate particles, the overall shrinkage, measured on concrete specimens, apparently decreases. In general the length of the curing period is not an important factor in shrinkage⁽³⁷⁾.

2-16- Shrinkage Induced Cracking

Concrete is always under some degree of restraint, either externally (by the foundation or by another part of the structure) or internally (by reinforcing steel embedded in concrete and the rigidity of the concrete aggregate) in structures during its contraction due to exposure to the environment of temperature and humidity variation conditions. So, the tendency of the concrete to contract upon drying and the restraint which resists action will develop tensile stresses within the concrete. These stresses increase with time, but the rate of this increase will decrease due to the decreased shrinkage rate and due to the relaxation of

stresses in concrete. Relaxation takes place and may prevent the development of cracking when the shrinkage develops slowly. If the tensile stress produced by the restrained shrinkage and reduced by the relaxation exceeds the tensile strength of concrete, which is a function of time, the cracking will occur as shown in Figure (۲-۹)^(۲۸,۲۹).

The magnitude of tensile stress developed during drying of the concrete is influenced by a combination of factors such as:

۱. The amount of shrinkage.
۲. The degree of restraint.
۳. The modulus of elasticity of the concrete.
۴. The creep or relaxation of the concrete.

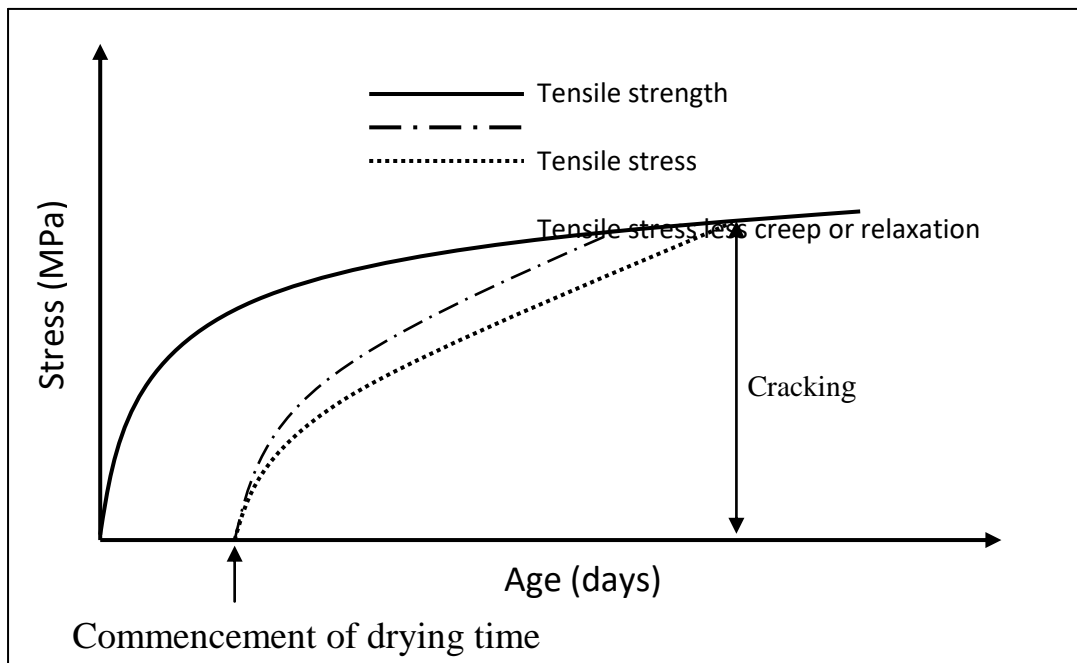


Figure (۲-۹): Development of Tensile Stress in Concrete and the Time

Required for the First Crack^(2.8, 2.9)

2-1.7- Plastic Shrinkage Cracking

Plastic shrinkage cracks are the most dangerous cracks. These cracks are often fairly wide at the surface^(2.8). They occur when concrete is still in the plastic state and subjected to the fast loss of large amount of water per unit area. The width of plastic shrinkage cracks may reach 1 mm, therefore, can result in serious problems.

Plastic shrinkage cracking is sometimes confused with another type of cracking called plastic settlement cracking. The plastic settlement cracking occurs on the surface of fresh concrete and caused by differential settlement of fresh concrete due to some obstructions to settlement, such as large particles of aggregate or reinforcing bars^(2.9).

2-1.8- Restrained Shrinkage Cracking

Restraint acts to hinder the change in dimensions due to volume change, thus producing elastic strain within the concrete member^(2.8). Normally, restraint conditions that will induce compressive stresses in concrete are not considered in design because of the ability of concrete to withstand compression. On the other hand, restraint conditions that induce tensile stresses are of main concern because of the low tensile strength of concrete. Figure (2-10) shows the distribution of restrained movement expressed as degree of restraint (K_R) at the center lines of concrete walls restrained completely at the base with different values of L/H ratios.

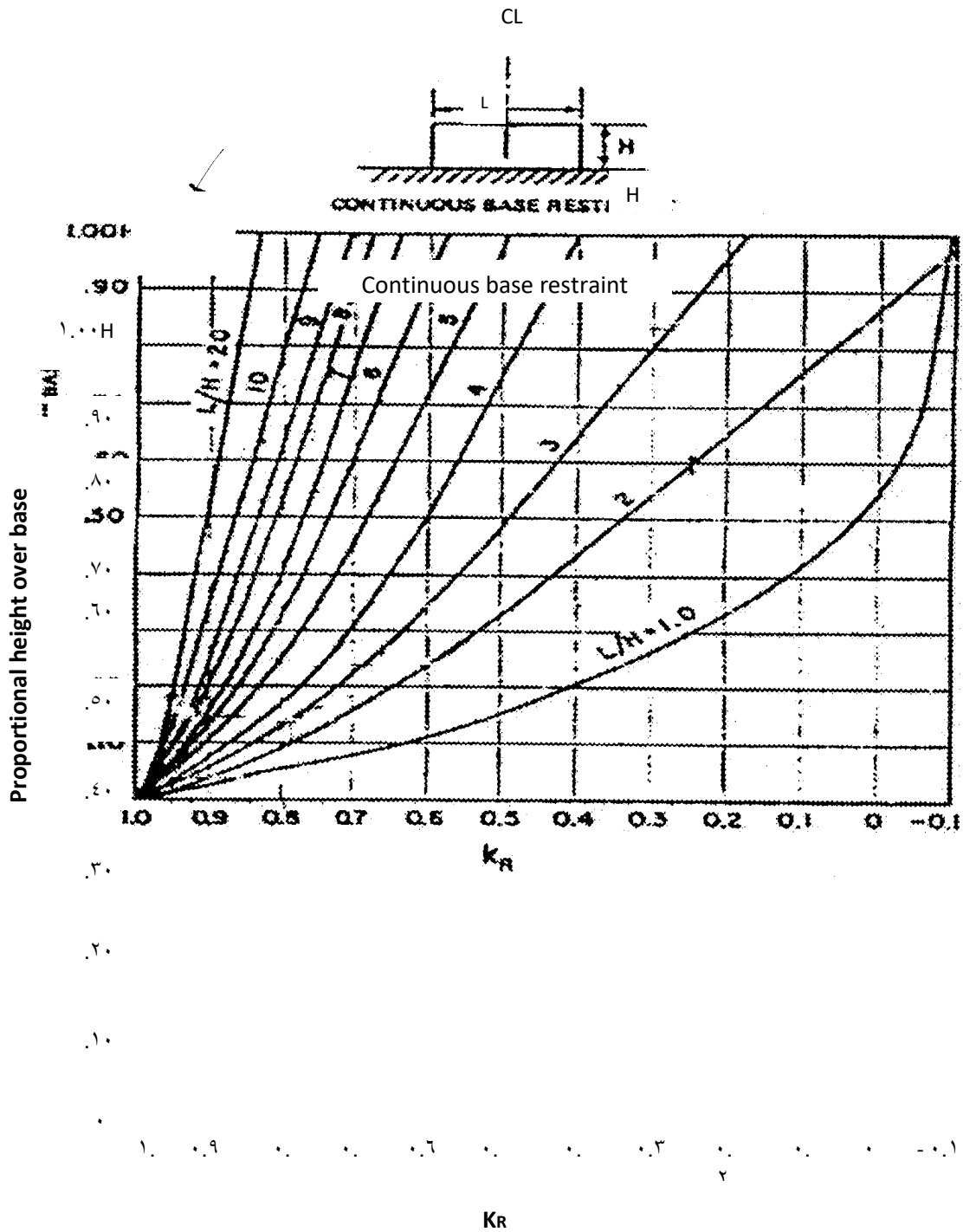


Figure (2-10): Degree of Tensile Restraint at Center Section^(A)

The degree of restraint depends largely on relative dimensions, strength, creep or relaxation, modulus of elasticity of concrete and the restraining

object. The induced stresses in concrete due to the restraint tend to increase in-direct proportion to the decrease in stiffness of the restraining part. The possible restraints of concrete members are internal restraint, external end-restraint, and base-restraint.

2-1.8-1- Internal Restraint

The source of internal restraint is steel reinforcement, aggregate, and occurs as a consequence of potential non-uniform volume change through a member cross-section, as in the case of mass concrete subject to shrinkage that will be non-uniform along its section. Moisture loss takes place at the surface so that a moisture gradient is established in the concrete section, which is subjected to differential shrinkage. This shrinkage is compensated by strain due to internal stresses, tensile near the surface and compressive in the core⁽¹³⁾. Internal restraint occurs for example, with slabs, walls, or masses with interior temperatures greater than surface temperatures⁽¹³⁾.

2-1.8-2- External Restraint

2-1.8-2-1- End Restrained Shrinkage Cracking

Since the restraining edges only at the member ends, the restraint in such members will be uniform, accordingly, a uniform state of tensile strain will develop in the member as it shrinks or contracts. The member cracking will be to propagate at the weakest section existing at any position within the member length⁽¹³⁾.

In fact, crack location depends mainly on the position of the weakest concrete section. Al-Rawi⁽¹⁹⁾ used concrete beams reinforced with deformed bars and welded wire mesh. He found that using the deformed bar reinforcement can control both the minimum crack spacing and the maximum crack width. He found also a formula for the minimum crack spacing, (based on experimentally measured bond slip distance), using a new model which was believed to resemble field conditions:

$$S_{min} = 1.4 K \times d / \rho \quad \dots\dots\dots (2-2)$$

S_{min} : the minimum crack spacing (mm).

K : constant depending on the type of reinforcement which may be taken as (1.4) for indented deformed bars and (1.7) for ribbed deformed bars.

d : diameter of bars (mm)

ρ : steel ratio

The width of crack at the onset of cracking (W_i) is:

$$W_i = \frac{1}{3} S_{max} \times \epsilon_{ult} \quad \dots\dots\dots (2-3)$$

The final maximum crack width W_{max} is:

$$W_{max} = S_{max} [e_{shr} - (\text{creep} + \text{loss of restraint}) - (\epsilon_{ult} + \text{creep})] / 3 \quad \dots\dots\dots (2-4)$$

S_{max} : maximum crack spacing (mm), $S_{max} = 3 \times S_{min}$

e_{shr} : final shrinkage strain (10⁻⁶)

ϵ_{ult} : elastic tensile strain capacity of concrete (10⁻⁶)

creep₁: creep prior to cracking (ϵ^{-1})

creep₂: creep after cracking (ϵ^{-1})

Kadhum⁽¹³⁾ studied the behavior of drying shrinkage cracking of reinforced concrete slabs for different restraint cases (crack width, crack length and crack spacing). The selected dimensions were fixed for the four slabs as (2200 × 2200 × 100 mm). Ratio of steel reinforcement (ρ) was kept at (0.42%) for the four slabs. Restraint cases were varied as (free slab, two end restrained, three end restrained and four end restrained) to investigate their effect on shrinkage. He found that the slabs which were cracked first are the four, three and two end restrained respectively, which means that the cracking age increases if restraint decreases.

Kadhum⁽¹³⁾ suggested two formulae to calculate crack width for restrained slabs at any level by using the strain distribution in the concrete and steel adjacent to a crack, as suggested by Al-Rawi⁽¹⁴⁾ as shown in Figure (3-11).

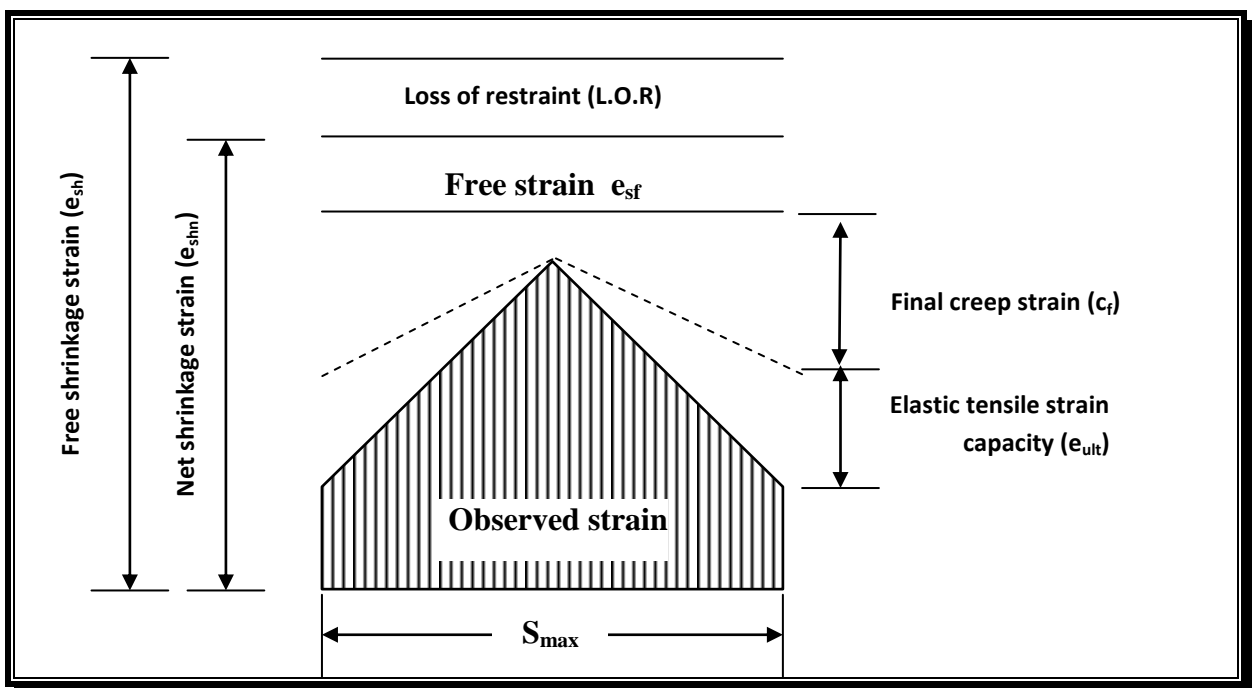


Figure (٢-١١): Sketch of Strain Distribution in the Concrete Adjacent to a Crack^(Aξ)

For two and three end restrained slabs from free edge the maximum crack width can be calculated from the following equation:

$$W_{c_{max}} = S_{max} \left[-10.06 \times e_{shn} + 26.92 \times C_f - 50.22 \times \frac{e_{ult}}{2} \right] \dots\dots\dots (٢-٥)$$

For three and four end restrained slabs from restrained edge the maximum crack width can be calculated from the following equation:

$$W_{c_{max}} = S_{max} \left[0.83 (R_b - 0.7 R_a) e_{shn} + 3.9 \times C_f - 23.46 \times \frac{e_{ult}}{2} \right] \dots\dots\dots (٢-٦)$$

S_{max} : Maximum crack spacing, (mm), $S_{max} = \gamma \times S_{min}$

For two and three end restrained slabs from free edge:

$$S_{min} = 0.85K \frac{d}{(\rho + \rho_R)} \dots\dots\dots (٢-٧)$$

For three end restrained from restrained edge:

$$S_{min} = 0.85K \frac{d}{(\rho + K_{R1})} \dots\dots\dots (٢-٨)$$

For four end restrained slab:

$$S_{min} = 0.85K \frac{d}{(\rho + 0.8 K_{R2})} \dots\dots\dots (٢-٩)$$

e_{sh} : Shrinkage strain plus strain due to decrease in temperature (\cdot^{-1}).

e_{ult} : Elastic tensile strain capacity (\cdot^{-1}).

e_{shn} : Net shrinkage stain, ($e_{shn} = e_{sh} - L.O.R$) (\cdot^{-1}).

L.O.R.: Loss of restraint due to ends contraction before cracking (ϵ_s^{-1}).

C_f : Final creep strain, ($C_f = K \times e_{sh}$) (ϵ_s^{-1}).

R_a : Degree of restraint after cracking

R_b : Degree of restraint before cracking (at slab center)

Evans and Hughes⁽¹⁰⁾ derived the equation:

$$S_{min} = \frac{1}{\xi} \cdot d/\rho \times f_{tu}/f_b \quad (\text{For rounded bars}) \quad \dots\dots\dots (\gamma-11)$$

d: bar diameter (mm).

ρ : steel ratio.

f_{tu} : tensile strength of concrete (MPa).

f_b : average bond strength between steel and concrete (MPa).

Evans and Hughes⁽¹⁰⁾ assumed that the f_{tu}/f_b ratio can be taken as 0.75, 0.8, and 1.0 for ribbed, indented and plain round bars respectively. They expressed the maximum crack width as the product of maximum crack spacing by the average free shrinkage strain minus the average residual surface strain between cracks (taken as half the elastic tensile strain capacity of concrete):

$$W_{max} = S_{max} (e_{sh} - e_{ult}/\gamma) \quad \dots\dots\dots (\gamma-11)$$

The width of crack due to drying shrinkage and heat of hydration in restrained slabs and walls may be obtained by B.S. 5337⁽¹¹⁾.

$$W_{max} = S_{max} [\epsilon_{cs} + \epsilon_{te} - (\epsilon_s \times \epsilon_s^{-1})] \quad \dots\dots\dots (\gamma-12)$$

ϵ_{cs} : shrinkage strain

ϵ_{te} : total thermal contraction after peak temperature due to heat of hydration

The value of W_{max} can be calculated as suggested by B.S. 5323⁽¹⁶⁾ [taking into consideration the cooling to ambient from the peak hydration and the seasonal variation]:

$$W_{max} = S_{max} \alpha / \gamma (T_1 + T_2) \dots\dots\dots (\gamma-13)$$

T_1 : fall in temperature between hydration peak and ambient

T_2 : fall in temperature due to seasonal variations.

α : coefficient of thermal expansion of concrete

2-18-2-2- Base Restrained Shrinkage Cracking

Walls cast on a continuous base are examples of the base restrained members. The restraint in the walls is not uniform throughout the wall, but varies from point to point within the wall. This variation depends on several factors, these factors include the walls (length/height ratio), the position of the roughness of the contact surface between the wall and base, and amount and distribution of reinforcement.

Al-Rawi and Kheder⁽¹⁷⁾ investigated the combining effects of the base restraint and the reinforcing steel in distribution volume change cracking. They suggested the following semi empirical equation for prediction of minimum crack spacing (S_{min} (mm)) in base restrained concrete members:

$$S_{min} = [K_1 \times d \times H] / [\rho \times H + K_1 \times d] \dots\dots\dots (\gamma-14)$$

K_1 : equals to (0.07, 0.14 and 0.20) for deformed, indented and plain rod bar, respectively

d: bar diameter which its unit is (mm)

ρ : steel reinforcement ratio

H: wall height, which its unit is (mm)

In the same investigation, the following semi empirical equation was given for predicting the crack width:

$$W_{max} = S_{min} [K (R_b - \rho \cdot R_a) \times e_{ult} / \gamma] \quad \dots\dots\dots (\gamma - 1 \circ)$$

K: equals to $(\rho \cdot c_{\text{cr}})$, assuming the sum of creep strain before cracking C_b and the average value of the creep strain after cracking C_a to be c_{cr} (constant) of the total net shrinkage where c_{cr} is equal to $(\rho \cdot \xi \cdot \rho)$ and $(\rho \cdot \gamma \circ)$ for reinforced and plain concrete walls, respectively.

R_a and R_b : degree of restraint after cracking and before cracking respectively. In addition, a reduction factor of $(\gamma \cdot \%)$ in the degree of restraint in the wall after cracking, due to the slippage between the wall and the base was assumed.

The B.S. $\rho \gamma \gamma^{(\wedge \wedge)}$ gives the following equation for the predication of maximum crack width:

$$W_{max} = S_{max} [e_{th} / \gamma + e_{sh} - e_{ult} / \gamma] \quad \dots\dots\dots (\gamma - 1 \uparrow)$$

Using the equation above, results in a uniform predicated crack width along the wall height. Harrison^(\wedge \wedge) modified this equation by introducing the effect of the degree of restraint before cracking at the wall center line.

Thus, equation above will become:

$$W_{max} = S_{max} [\rho \cdot R_b (e_{th} + e_{sh}) - e_{ult} / \gamma] \quad \dots\dots\dots (\gamma - 1 \uparrow)$$

R_b: is the degree of restraint before cracking

Since R_b is the maximum at the wall base, and decreases toward the wall top, therefore, according to Harrison's formula the crack width will be the maximum at the base and minimum at the wall top. Harrison considered the creep to be about 0.1% of the total volume change (e_{th}+e_{sh}).

ACI Committee 209⁽¹⁾ presented an expression for crack width taking the effect of variation in restraint in the wall before cracking only into consideration:

$$W_{\max} = 1.9 S_{ave} (R_b \times \alpha_c T_e - f_{ct} / E_c) \dots\dots\dots (2-18)$$

S_{ave} : average crack spacing (mm).

α_c : coefficient of thermal expansion of concrete.

T_e : effective temperature change including an equivalent temperature change to compensate for drying shrinkage

f_{ct} : tensile strength of concrete (MPa).

E_c : modulus of elasticity of concrete (MPa).

R_b : the degree of restraint before cracking

The committee suggested that the lower half of the wall, (near the base) requires maximum reinforcement and the upper half of the wall, requires minimum reinforcement.

2-19- Factors Influencing Cracking Resistance

2-19-1- Creep (Relaxation) of Concrete

Creep is defined as the gradual increase in deformation (strain) with time for a constant applied stress, also taking into account other time dependent deformations not associated with the applied stress, i.e. shrinkage, swelling and thermal deformation^(r°).

Creep in compression reduces the prestressing forces in prestressed concrete elements and causes a slow transfer of load from the concrete onto the reinforcement. Creep in tension can be beneficial in that it in part relieves the stresses induced by other restrained movements, e.g. drying shrinkage and thermal effects. However, if the restraints are such that a stressed concrete specimen is subjected to a constant strain (such as the case of restrained shrinkage movement), creep will be expressed as a progressive decrease in stress with time known as "relaxation"^(r°).

Creep takes place in the cement paste and it is influenced by its porosity which is directly related to its water/cement ratio. During hydration, the porosity of the cement paste reduces, and so for a given concrete, creep reduces as the strength increases. The type of cement is important if the age of loading is fixed. Cements that hydrate more rapidly will have a higher strength at the age of loading, a lower stress/strength ratio and a lower creep^(r°). As the aggregates restrain the creep of the cement paste, the higher the volume of the aggregate and the higher the E-value of the aggregate, the lower the creep will be. Due to the higher volume of cement paste, the creep coefficient for SCC may be expected to be higher than for normal concrete of equal strength.

2-19-2- Tensile Strain Capacity

Cracking of concrete depends partly upon the maximum strain that concrete can sustain in tension before cracking occurs. The maximum strain is termed the "tensile strain capacity". The tensile strain capacity includes both the elastic strain capacity and the creep strain. It develops during tensile strain built up by restrained shrinkage, which is time dependent. Hughes and Ghunaim⁽¹⁹⁾ reported that tensile strain capacity increases with the increase of concrete age. Hoobs⁽²⁰⁾ concluded that the strain capacity will be improved with age and strength of concrete. The values of tensile strain capacity are about (100-200) microstrain⁽²¹⁾.

2-19-3- Elastic Tensile Strain Capacity

The elastic tensile strain capacity is the amount of strain that is instantly relieved due to the elastic recovery of restrained concrete upon cracking. It is defined by Al-Rawi⁽²²⁾ as the observed free contraction of concrete at the onset of cracking. Elastic tensile strain capacity does not include creep strain, which was lost during tension built up, before the occurrence of cracking. It is considered as a basic concrete property that may be used for calculation of shrinkage crack width⁽²³⁾. From the researchs it was found that the elastic tensile strain capacity for 7- days was 98, and 99 and for 28-days 130, and 140 by^(24,25) respectively.

2-20- Cracking Age

It is the time required for the shrinkage induced strains to build up and exceed the tensile strain capacity of concrete. The age of the first crack and the cracking sequence is dependent on the some factors that influence the cracking tendency of concrete (i.e., degree of restraint, shrinkage, creep,

tensile strain capacity etc.). Thus, cracking age, as stated by Al Rawi^(V9) could be used as an index to assess the possibility of cracking of various mixes. He also reported that the cracking time depends on both shrinkage and tensile strain capacity. It increases with a decrease in water/cement ratio, an increase in a normal curing time and the use of smaller size and amount of the crushed coarse aggregate.

CHAPTER THREE

EXPERIMENTAL WORK

3-1 - Introduction

This chapter describes the experimental work, which consists of three parts. The first part deals with the experimental work, which is necessary for achieving Self-Compacting Concrete from locally available materials according to the requirement of fresh properties of concrete (workability measurement).

The second part deals with the effect of some fillers such as (Pigment, Limestone powder and Metakaolin) on the dimensional changes of Self-Compacting Concrete in two seasons (Summer and Winter) and also studies the dimensional changes of normal concrete. For free and end-restrained drying shrinkage, end restrained beams were used to determine free shrinkage, first cracking time, crack width, tensile strain capacity, elastic tensile strain capacity and creep prior to cracking.

The third part has been carried out to study the shrinkage cracking behavior (crack width, crack length, crack spacing) of reinforced Self-Compacting Concrete plates restrained from movement at their ends for different restrained cases.

٣-٢- Materials

٣-٢-١- Cement

The cement used in this study is ordinary Portland cement manufactured by the New Cement Plant of Kufa. The cement was properly stored in the laboratory. This cement complied with the Iraqi specification No.٥/١٩٨٤^(٩٢). Tables (٣-١) and (٣-٢) show the chemical and physical properties of this cement respectively. The test was made in the environmental laboratory of Babylon University.

Table (٣-١): Chemical Composition of Cement

Oxide	%	I.O.S. ٥:١٩٨٤ ^(٩٢) Limits
CaO	٦٠.٧٩	—
SiO _٢	٢٠.٧٥	—
Fe _٢ O _٣	٣.٠٠	—
Al _٢ O _٣	٦.٢٠	—
MgO	٤.١١	< ٥.٠
SO _٣	٢.٣٢	< ٢.٨
L.O.I	٢.٠٠	< ٤.٠
L.S.F	٠.٨٨	٠.٦٦-١.٠٢
Compound Composition	%	I.O.S. ٥:١٩٨٤ ^(٩٢) Limits
C _٣ S	٣٧.٢٦	----
C _٢ S	٣١.٣٩	----
C _٣ A	١١.٣٥	----
C _٤ AF	٩.١٢	----

Table (٣-٢): Physical Properties of Cement

Physical Properties	Test Results	I.O.S. ٥:١٩٨٤ ^(٩٣) Limits
Fineness, Blaine, cm ² /gm	٣١٢٤	> ٢٣٠٠
Setting Time:		
Initial hrs: min.	١:٤٥	> ٠٠:٤٥
Final hrs: min	٣:٤٦	< ١٠:٠٠
Compressive Strength MPa		
٣-days	٢٠	> ١٥
٧-days	٢٧	> ٢٣
٢٨-days	٣٣	

٣-٢-٢- Coarse Aggregate

The coarse aggregate was AL-Nibae gravel of maximum size ١٩ mm is used. The gravel used conforms to the Iraqi specification (I.O.S.) No.٤٥/١٩٨٤^(٩٣). Table (٣-٣) shows the grading of the coarse aggregate. Table (٣-٤) shows the physical and chemical properties of the coarse aggregate.

Table (٣-٣): Grading of Coarse Aggregate

Sieve Size (mm)	Passing %	I.O.S. ٤٥:١٩٨٤ Limits ^(٩٣)
٣٧.٥	١٠٠	١٠٠
١٩	١٠٠	٩٥-١٠٠
٩.٥	٦٥	٥٠-٨٥
٤.٧٥	٦	٠-١٠

Table (٣-٤): Physical and Chemical Properties of Coarse Aggregate

Physical Properties	Test Results	I.O.S. ٤٥:١٩٨٤ Limits ^(٩٣)
---------------------	--------------	---------------------------------------

Specific gravity (S.G)	۲.۶۴	—
Absorption %	۰.۷	—
Sulfate content (SO _r)%	۰.۰۸	≤ ۰.۱
Clay %	۰.۶	≤ ۱.۰

۳-۲-۳- Fine Aggregate

Natural sand from AL-Akaidur region was used. Table (۳-۵) shows the grading of the fine aggregate and the limits of the Iraqi specification NO. ۴۵/۱۹۸۴^(۹۳). Table (۳-۶) shows the physical and chemical properties of fine aggregate.

Table (۳-۵): Grading of Fine Aggregate

Sieve Size (mm)	Passing %	I.O.S. ۴۵:۱۹۸۴ Limits ^(۹۳) Zone (۳)
۵	۱۰۰	۹۰-۱۰۰
۲.۳۶	۹۴	۸۵-۱۰۰
۱.۱۸	۸۴	۷۵-۱۰۰
۰.۶۰	۶۶	۶۰-۷۹
۰.۳۰	۳۷	۱۲-۴۰
۰.۱۵	۳	۰-۱۰

Table (۳-۶): Physical and Chemical Properties of Fine Aggregate

Physical Properties	Test Results	I.O.S. ۴۵:۱۹۸۴ Limits ^(۹۳)
Specific gravity (S.G)	۲.۶۵	—
Absorption %	۱.۶	—
Sulfate content (SO _r)%	۰.۴۳۲	≤ ۰.۵
Clay %	۲.۳	≤ ۳.۰

3-2-ε- Superplasticizer

For the production of Self-Compacting Concrete, superplasticizer (high range water reducing agent) called as URA-PLAST SF is used. The normal dosage for the Ura-plast is between 1-0 liters per 100 Kg of cement. According to ASTM C494-92⁽⁷⁶⁾, this SP is classified as type G, it has a retarding effect on the SCC. The typical properties are shown in Table (3-ν).

Table (3-ν): Typical Properties of Superplasticizer⁽⁹⁴⁾

Subsidiary effect	Hardening retarder
Form	Viscous liquid
Colour	Dark brown
Relative density	1.1 @ 20°C
Viscosity	128 ± 30 CPS @ 20°C
pH	6.6

Types of Fillers

3-2-ο-1- Pigment

This material is brought from local market, and then it is used in the concrete mixes after passing sieve size 0.075mm (No. 200) sieve. The chemical composition of the pigment is shown in Table (3-λ). The test was made in the chemical laboratory of Old Cement Plant of Kufa.

Table (3-λ): Chemical Analysis of Pigment

Oxide	%
-------	---

CaO	٦٦.٧٤
Al ₂ O ₃	٠.٨٤
Fe ₂ O ₃	٠.٦٤
SiO ₂	١.٨٤
MgO	٠.٦٥
L.O.I	٢٦.٨٠
SO ₃	٠.٣٤

٣-٢-٥-٢- Limestone Powder

Finely crushed limestone which has been brought from local market is used. The chemical composition of this limestone is shown in Table (٣-٩). It is passing sieve size ٠.٠٧٥mm (No. ٤٠٠) sieve. The test was made in the environmental laboratory of Babylon University.

Table (٣-٩): Chemical Analysis of Limestone Powder

Oxide	%
CaO	٥٢.٧٦
Al ₂ O ₃	٠.٧٠
Fe ₂ O ₃	٠.١٧
SiO ₂	١.٤٠
MgO	٠.١٠
Na ₂ O+K ₂ O	—
L.O.I	٤٠.٦٠
SO ₃	٢.٩١

٣-٢-٥-٣- Metakaolin

Metakaolin is a highly pozzolanic material produced by calcining China clay using an oven at temperature of (700-900) C° for 1.0 hour⁽³⁰⁾. Then, the sample is left to cool. The particle passing sieve size 0.075mm (No. 200) sieve. The chemical composition of kaolin and metakaolin is shown in Table (3-10). The test was made in the environmental laboratory of Babylon University.

Table (3-10): Chemical Analysis of Kaolin and Metakaolin

Oxide	Kaolin %	Metakaolin %
CaO	10.00	6.14
Al ₂ O ₃	13.83	12.74
Fe ₂ O ₃	1.12	3.02
SiO ₂	52.27	68.84
MgO	6.00	6.16
L.O.I	14.06	1.40
SO ₃	1.32	0.86

3-2-6- Water

Tap water is used throughout this work for both mixing and curing concrete.

3-2-7- Reinforcement

Deformed steel bars of 10 mm diameter were used.

3-3- Mix Design

3-3-1- Determination of Mix Design Method

Mix design of SCC must satisfy the criteria of filling ability, passing ability and segregation resistance. The concrete is designed according to the Japanese mix design system, (fine aggregate content 40.0% of mortar volume, coarse aggregate 30.0% of concrete volume)^(21,22,23), as shown in Table (3-2). Superplasticizer type (G) is added to attain the retarding effect. Three types of filler are added to the concrete mixes to improve the quality of binding phase and the aggregate matrix bond.

Many trial mixes were done in the construction materials laboratory to find a suitable mix that satisfy the requirements of Self-Compacting Concrete in the fresh state as well as at hardened. Table (3-11) shows the mix proportion details of fresh and hardened concrete properties in preliminary investigations.

Table (3-11): Mix Proportions in Preliminary Investigations

Mix proportions	Test series	1	2	3	4	5	6	7
	Units							
Cement	(Kg/m ³)	300	320	280	378	320	320	400
Filler (pigment)	(Kg/m ³)	264	160	240	160	160	160	80
Sand	(Kg/m ³)	729	912	860	800	912	912	912
Gravel	(Kg/m ³)	700	760	700	780	760	760	760
Water	(Kg/m ³)	231	197	210	290	366	269	240
W/p	---	0.41	0.41	0.4	0.00	0.7	0.06	0.00
SP	(L/m ³)	3	4.1	4.2	8	8	8	8
U-box (H ¹ -H ²)	cm	6	4	---	---	3	2	0
L-box (H ² /H ¹)	%	---	---	17	---	93	86	90
V-funnel	sec	---	---	---	---	7	7	6
Compressive strength								

3-days	MPa					10	19	21
7-days	MPa					17	21	20
28-days	MPa					18	37	39

Table (3-12) shows the mix proportions by weight used for normal concrete and Self-Compacting Concrete in this work.

Table (3-12): Mix Proportions by Weight

Materials	Normal concrete mix	Self-Compacting concrete mix
Cement (Kg/m ³)	400	400
Filler (Kg/m ³)	—	80
Sand (Kg/m ³)	912	912
Gravel (Kg/m ³)	760	760
Water (l/m ³)	240	240
SP (l/m ³)	—	8
W/P	0.50	0.50
W/C	0.60	0.60

3-3-2- Mixing Procedure

Mixing procedure is important to obtain the required workability and homogeneity of the concrete mix. Concrete is mixed in tilting laboratory mixer. The sequence of mixing is shown in Figure (3-1).

Sand + $\frac{1}{3}$ of water	Mixing 1 minute
Cement + filler + $\frac{1}{3}$ of (water + SP)	Mixing 1.0 minute
$\frac{1}{3}$ coarse aggregate + $\frac{1}{3}$ of (water + SP)	Mixing 1.0 minute
$\frac{1}{3}$ coarse aggregate + $\frac{1}{3}$ SP	Mixing 1 minute

Figure (3-1): Ribbon Diagram Mixing Sequence

3-2- Testing of Fresh and Hardened Concrete

The test methods used for the assessment of fresh properties of SCC are Slump flow, L-box, U-box and V-funnel.

3-2-1- Slump Flow and T₅₀₀ cm Test:

The slump flow test is used to determine filling ability and consistency of SCC. The procedure described below has been used:

1. The flow table is surely made horizontal and a concentric diameter of 500 mm is marked on it.
2. The surface of the cone and the table are cleaned with water then dried with a cloth so that they are moist, but without free water.
3. The slump cone is placed centrally on the table.
4. The slump cone is filled with about 7 liters of concrete.

- o. The slump cone is lifted vertically and allow the concrete to flow out freely.
- ٦. Start the stop watch and record the time taken for concrete to reach the ٥٠٠ mm spread circle, (this is $T_{٥٠٠}$ cm).
- ٧. The final diameter (D-final) of concrete is measured by measuring two perpendicular diameters. The value (٦٥٠-٨٠٠) mm, is the best indicator of flow.

٣-٤-٢- L-Box Test

L-box test is used to measure filling ability, passing ability and segregation of the Self-Compacting Concrete. The procedure described below has been used:

- ١. The vertical part of the box is filled with ١٢.٧ liters of concrete and left to stay for one minute in order to allow any segregation to occur.
- ٢. The sliding gate is opened and the concrete flows out of the vertical part into the horizontal part through the reinforcement bars.
- ٣. After the sliding gate is opened and when the concrete has stopped, the height of the concrete at the beginning (H_1) and end of the box (H_2) is measured and used to determine the L-box result (H_2/H_1), which is acceptable when ranges from ٠.٨ to ١.٠.

٣-٤-٣- U-Box Test

U-box test is used to measure the filling ability of SCC. The procedure of the test is as follows:

- ١. The apparatus is leveled on the firm ground and the sliding door is checked to make sure that it can be opened and closed freely.

٢. The inside surface of U-box are moistened, and then any surplus water is removed.
٣. The left chamber of the U-box is completely filled with about ٢٠ liters of SCC, while the sliding door between the two chambers is closed.
٤. The concrete is left to stay for ١ minute.
٥. The door is then opened and the concrete flows through the rebars into the right chamber.
٦. After the concrete has come to rest. The height of the concrete in the chamber is measured in two places and the mean (h_1) is calculated. The height in the right chamber (h_2) is measured also.
٧. The filling height (h_1-h_2) is calculated. The filling height is considered as acceptable value for SCC when it ranges from ٠ to ٣٠ mm. The "filling height" close to zero, the better the flow and passing ability of the concrete.

٣-٤-٤- V-Funnel Test

V-funnel test is used to determine flowability and stability of SCC. The procedure of the test is as follows:

١. About ١٢ liters of concrete are needed to perform the test.
٢. The V-funnel is sited on firm ground.
٣. The inside surfaces of the funnel are moistened
٤. The bottom gate is kept open to allow any surplus water to drain.
٥. The container is placed under the funnel opening.
٦. The concrete (without compaction) is poured into the funnel with the gate blocking the bottom opening.

4. Within 10 sec after the funnel is completely filled, the bottom gate is opened and the time for the concrete to flow out of the funnel (flow time) is measured. The flow time (1-12) sec is the best indication of flow ability and stability of SCC.

3-4-5- Compressive Strength Test

For the hardened SCC, the compressive strength test was carried out according to BS. 1881: part 116:1983⁽¹⁰⁾, using a machine of 2000 kN maximum capacity. Three cubes (100 mm) were tested at (7, 28-days) for the determination of compressive strength. All specimens were cured in water until testing age. The load was applied and increased gradually at a constant rate.

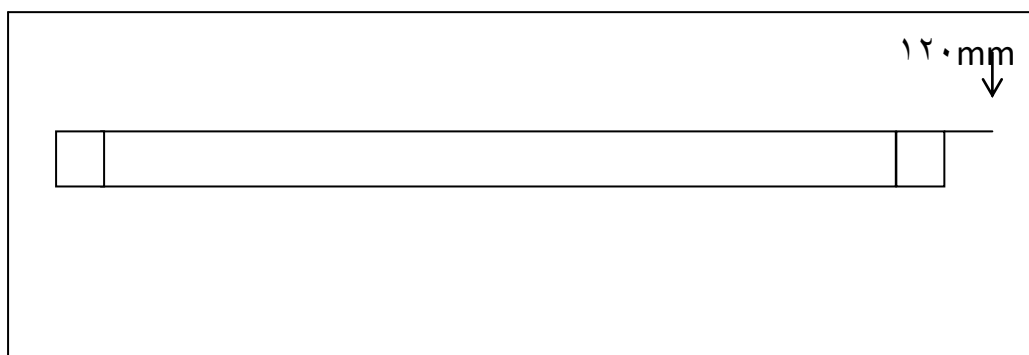
3-4-6- Flexural Strength Test

Concrete prisms of dimensions (100*100*400) mm with a span of 300 mm were cast. The prisms were demolded and cured in a similar manner as the cubes. Modulus of rupture test according to BS1881:118:1983⁽¹¹⁾ were performed using two-point load.

3-5- Program of the Work

3-5-1- Beams

In this work, end restrained beams with the dimensions (130x120x3000) mm (height, width, length) respectively shown in Figure (3-2) were used to study free and end-restrained shrinkage for normal concrete and Self-Compacting Concrete.



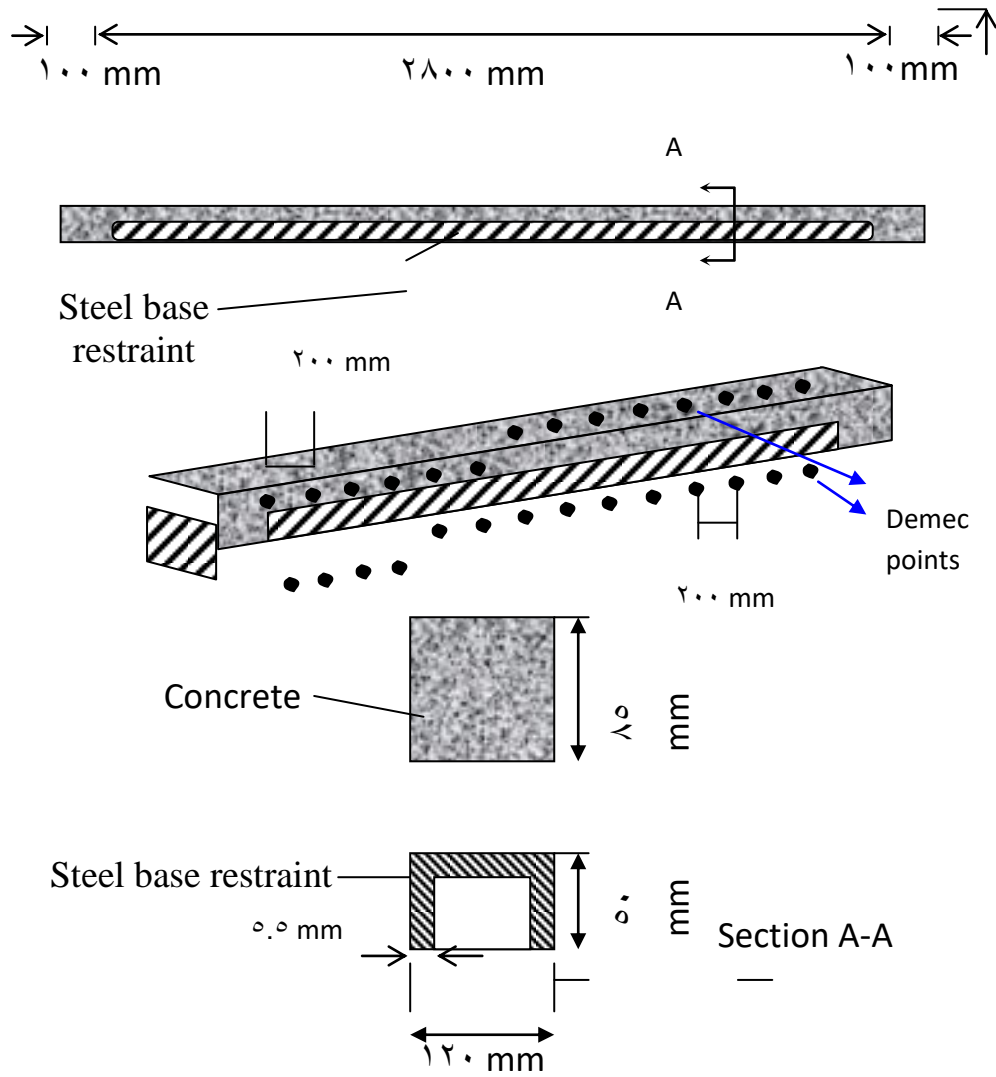


Figure (3-2): Schematic Diagram of the End Restrained Beam

The end-restrained beams used in this study were as follows:

1. Eight beams were cast in winter from first of December to first of February. Two beams were cast for normal concrete (without filler and superplasticizer), and six beams were cast for Self-Compacting Concrete [for each filler (pigment, limestone powder and metakaolin)] to study the free shrinkage of these beams, and also to determine the filler of the higher effect on free shrinkage.

- ϒ. Eight beams as above were cast in summer from first of March to first of May.
- ϓ. After decision, that the pigment filler has caused the relatively high free shrinkage than normal concrete and the others fillers, six end-restraint beams were cast to find out first cracking time, crack width, tensile strain capacity, elastic tensile strain capacity and creep prior to cracking (in Summer in the same period of the beams cast for free shrinkage). Two end-restrained beams was cast for normal concrete, and the other four end-restrained beams were cast for Self-Compacting Concrete (pigment and superplasticizer) two with reinforcement and the others without reinforcement.
- ϔ. Self-Compacting Concrete plates containing (pigment and superplasticizer) were cast in Summer at first of July to the first of September, to study the behavior of drying shrinkage cracks. Two beams were cast to determine the free shrinkage (first day movement) for plates, and also two end-restrained beams were cast to determine elastic tensile strain capacity for plates.

These beams were cleaned and rigidly tightened. Polyethylene sheets were put over the steel base of beam and sides and oiled to minimize the base and the side friction.

ϒ-ϔ-ϒ- Plates

The study of cracking characteristics of plates was based on four reduced scale reinforced SCC plates cast in laboratory. The selected dimensions were varied for the four plates as (220.*220.*80mm), (260.*220.*80mm),

(260.*240.*80mm) and (260.*260.*80mm) (length*width*thickness respectively).

The plates were all cast in the same period to prevent or minimize the variation in the exposure conditions. Ratio of steel reinforcement (ρ) was kept constant at (0.07%) for the four plates. Two types of restraint were provided to investigate their effect on shrinkage when exposed to drying. The first type of restraint was end restraint (two end restrained, three end restrained and four end restrained). The end restraint was provided by reinforced concrete slabs which were cast in laboratory by Kadhum^(A) from first of October to the first of December (2003). The second type of restraint was the base restraint. It was provided by roughness between the plate cast and the side of the slab restraint. Crack spacing, crack length and crack width measurements were carried out for each plate for a period of 60 days. Plate (3-1) shows these plates.



Plate (3-1): The Reinforced SCC Plates

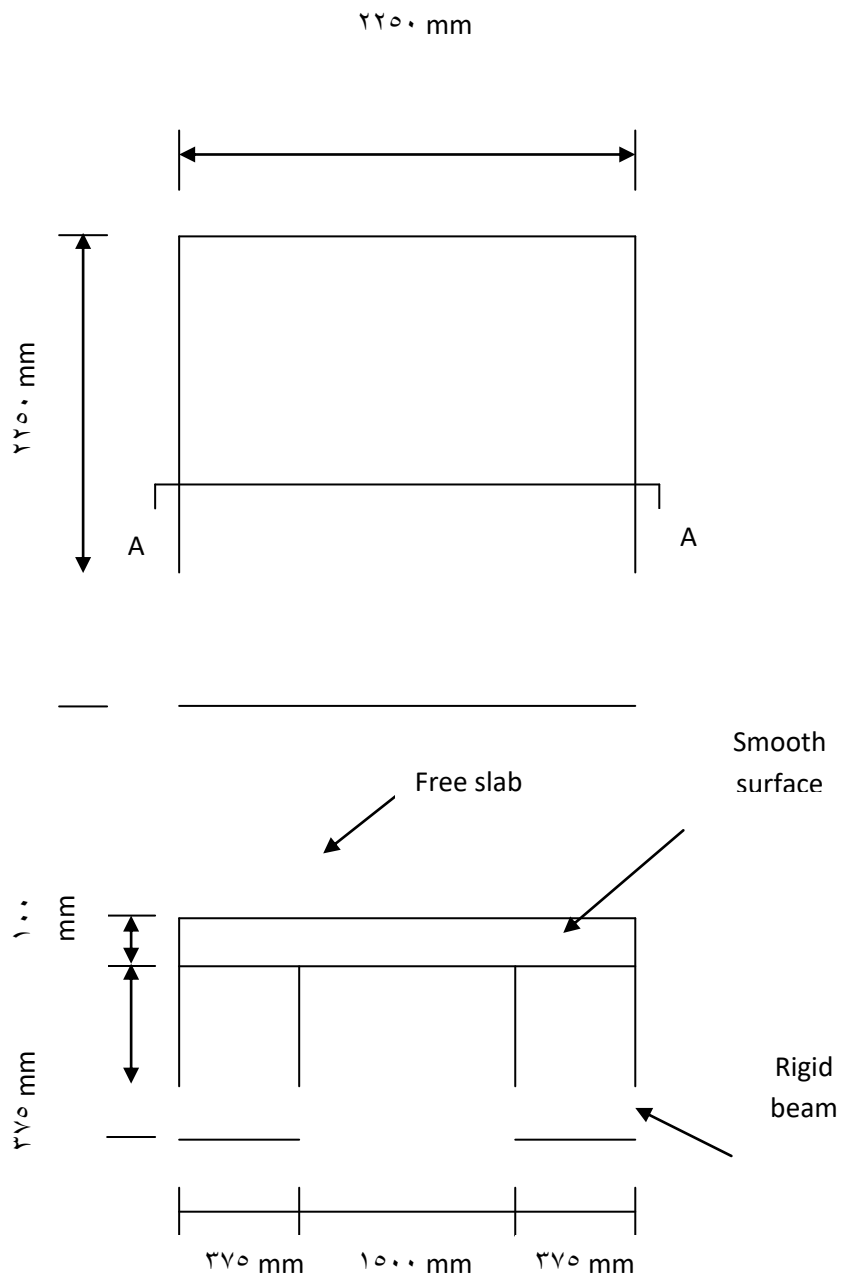
3-6- Restrained Reinforced Concrete Slabs

An existence reinforced concrete slab (cast in laboratory by Kadhum^(A3) from the first of October to the first of December (2003)) was used as a base in order to provide different restrained conditions from the ends to the new plates. These slabs were with different dimensions (220*220*100mm), (260*220*100mm), (260*240*100mm) and (260*260*100mm) (length ×width× thickness respectively) for free slab, two end restrained, three end restrained and four end restrained slabs. Plate (3-2) shows these slabs.

Figure (3-3) and (3-4) show the free and end restrained slab respectively. These slabs were cleaned and a layer of polythene sheets was put over them to minimize the friction between the reinforced Self-Compacting Concrete plate and slabs.

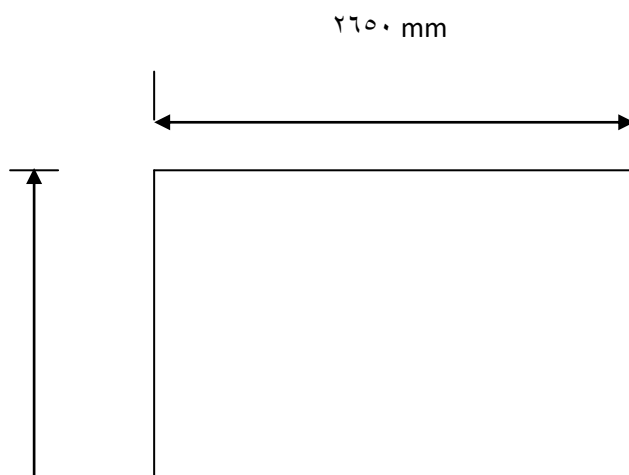


Plate (3-2): The Reinforced Concrete Slabs^(A3)



Section (A-A)

Figure (3-3): Schematic Diagram of Free Slab^(A3)



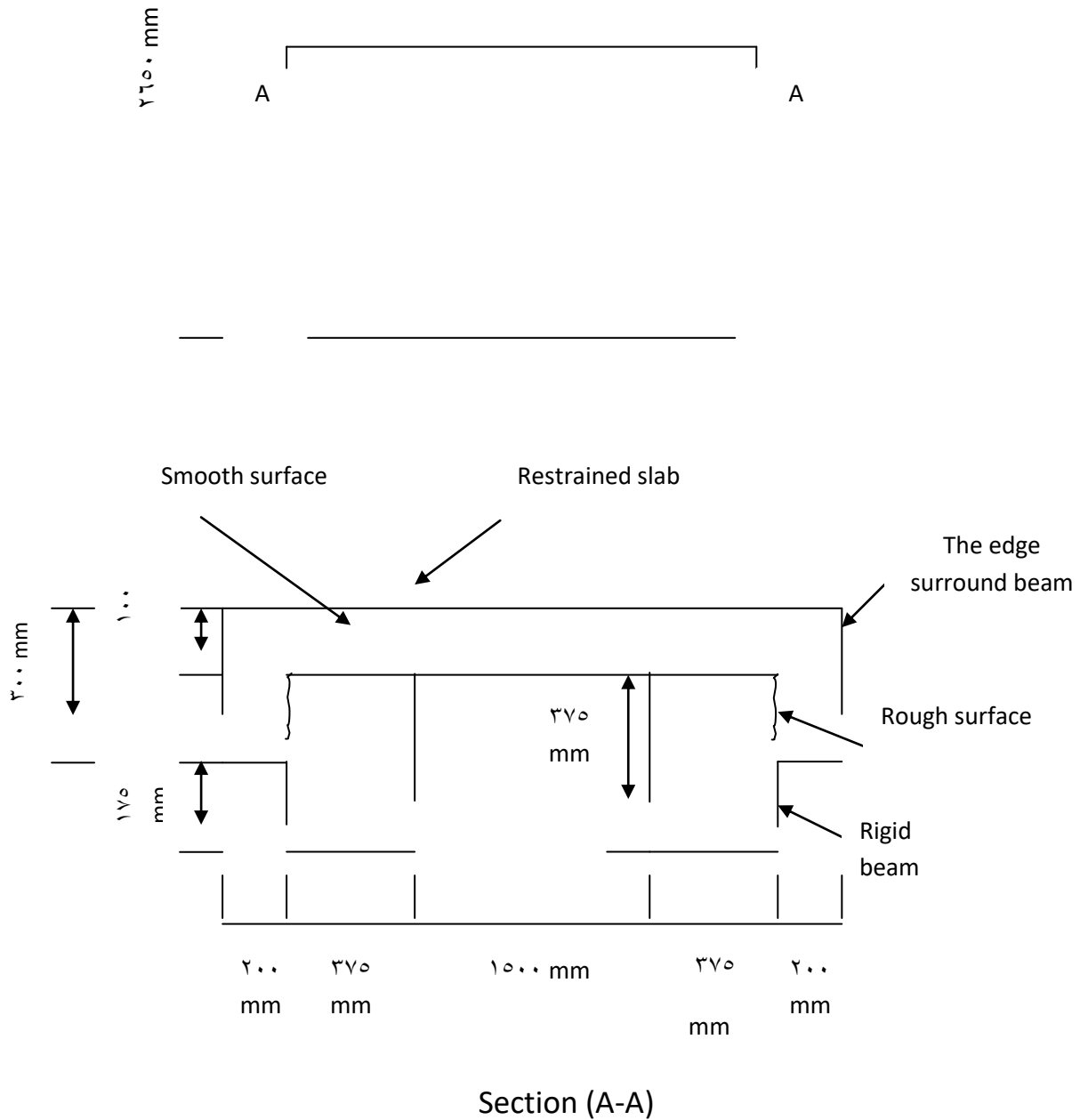
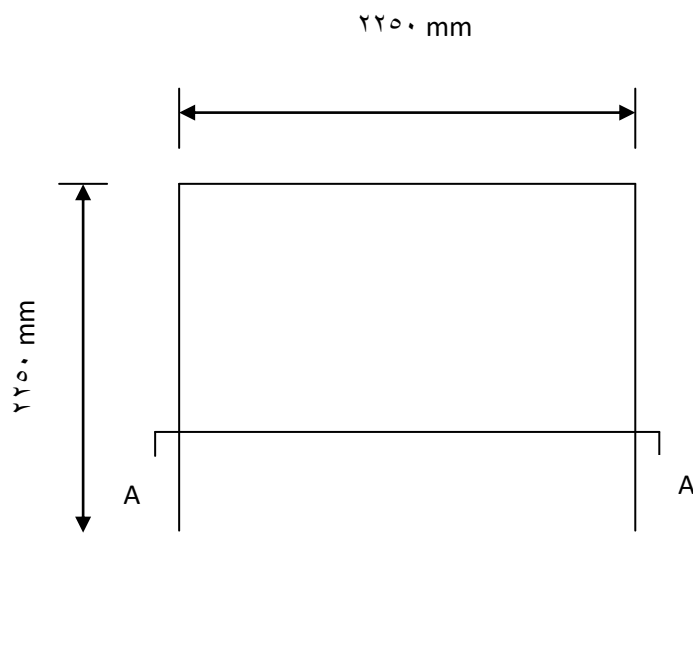


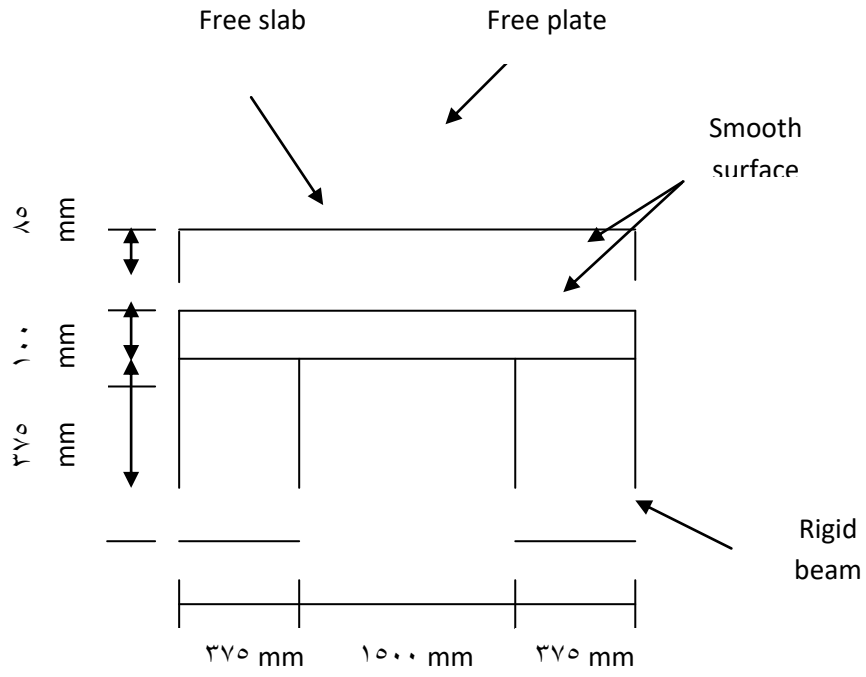
Figure (3-4): Schematic Diagram of End Restrained Slab^(A3).

3-7- Plate molds

Four plate molds were cast on the above slabs. These plates were cast with different restrained conditions (two end, three end and four end restrained),

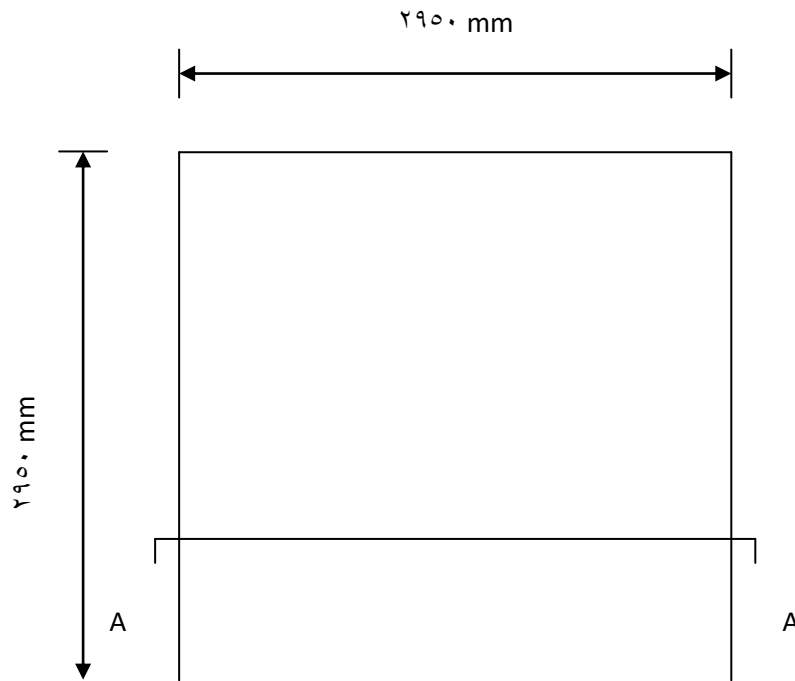
and another plate was cast without any restraint (free plate). The edges surrounded slabs which attain the action of restraint are of cross-section (260x100 mm) and c/c span of 2800 mm as shown in Figure (3-6). The mix proportions of SCC were (400 : 912 : 760 : 80 : 8) (cement : sand : gravel : filler (pigment) : superplasticiser) respectively with an effective water/powder ratio of 0.50 and slump flow of SCC is (700 mm). The 7 and 28 days compressive strength of this mix were 20 MPa and 39 MPa respectively, whereas the flexural strength was 3.2 MPa and 3.6 MPa. Figure (3-5) and (3-6) show free and end restrained plate respectively. The reinforcement used is deformed steel bars with 10 mm diameter, and the steel ratio adopted in this work is (0.07%) which is the minimum ratio allowed for shrinkage according to ACI Code 318⁽⁹⁸⁾. In order to get a constant cover, small pieces of steel as chairs of 2.0 cm height were placed under the plate reinforcement. Figure (3-7) shows the details of reinforcement for free plate and restrained plate.





Section (A-A)

Figure (3-5): Schematic Diagram of Free SCC Plate



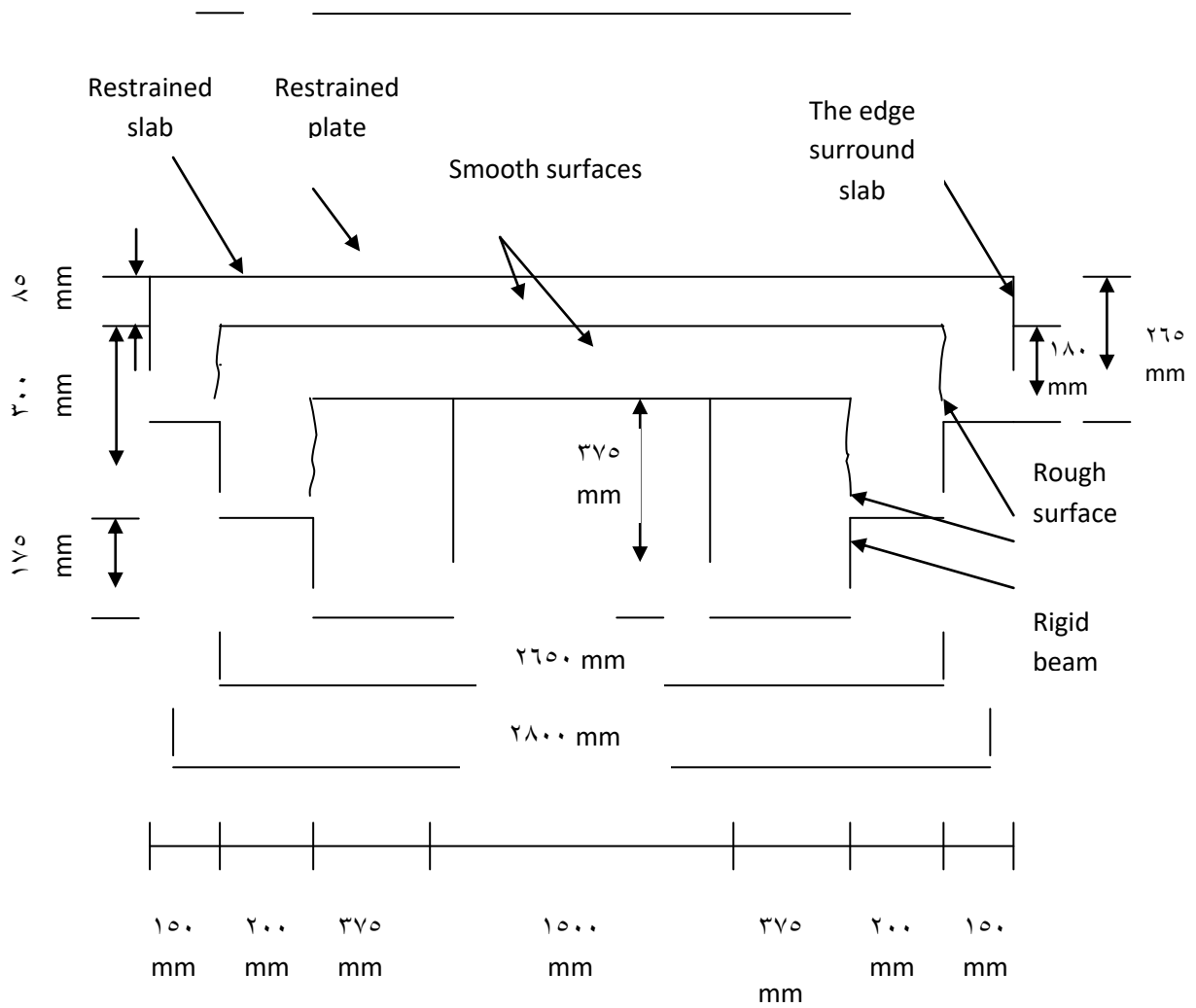
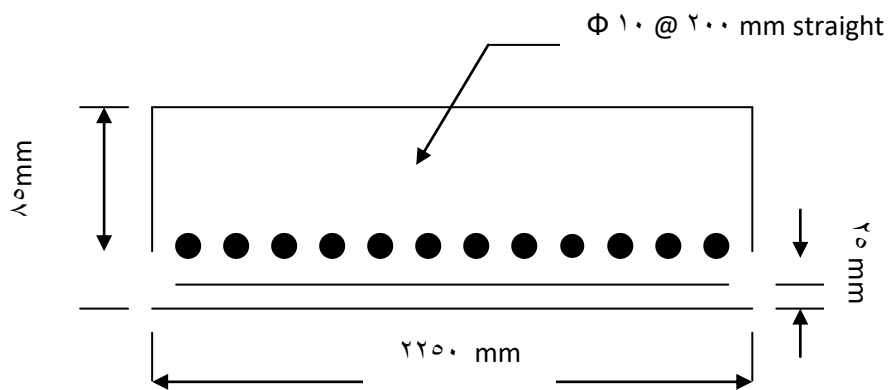
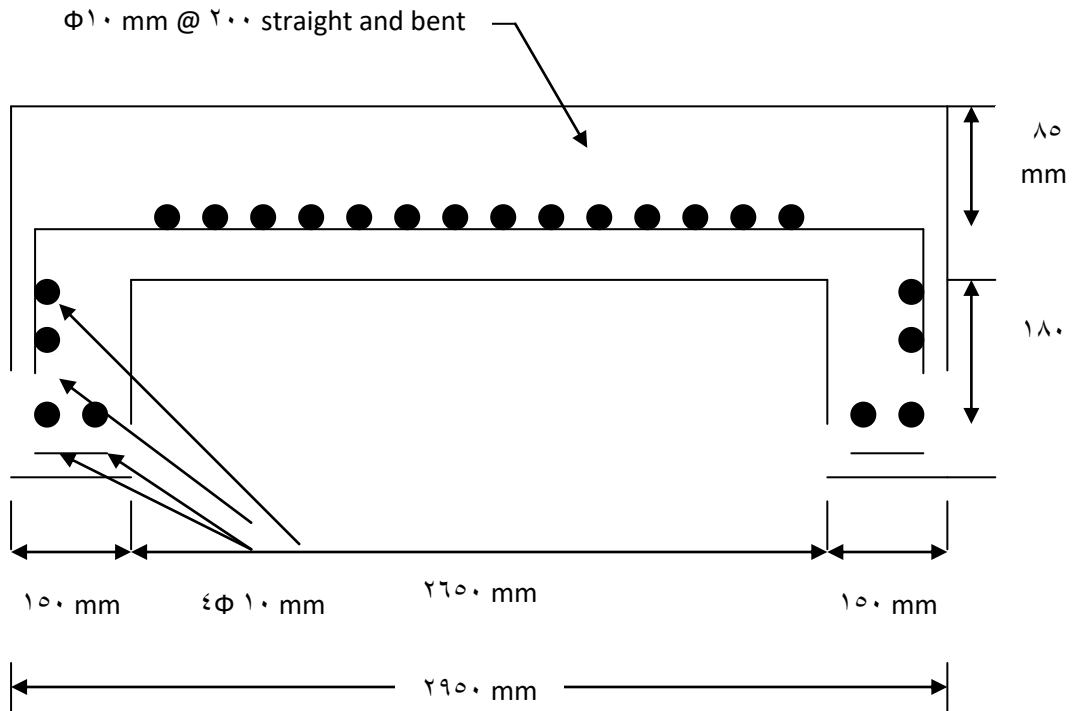


Figure (3-6): Schematic Diagram of End Restrained SCC Plate



a- Free Plate



b- Restrained Plate

Figure (3-7): Details of the Reinforced SCC Plate.

3-8- Casting Procedure of the Beams and Plates

3-8-1- Mixing and Casting of Beams and Plates

For beams and plates, the concrete was mixed in tilting mixer. The interior surface of the mixer was cleaned and moistened before placing the materials. The SCC beams and plates were mixed using the same procedure shown in Figure (3-1). The SCC plates were cast into the plywood formwork as shown in plate (3-3).



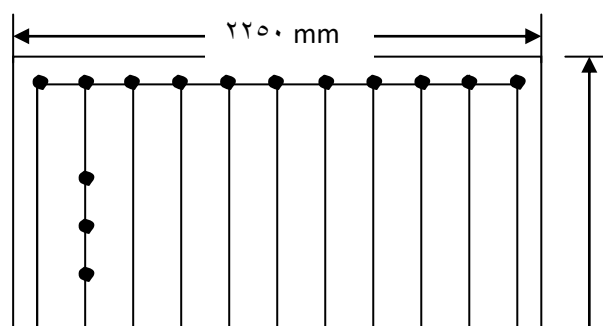
Plate (3-3): Ply Wood Formwork of Plate

3-8-2- Curing

To prevent plastic shrinkage cracking due to rapid evaporation from the upper surface of the beams and plates, Wetted Hessian sheets and polythene sheets were used to cover the upper surface of the beams and plates after 30 minute from the casting. The beams and plates were cured by covered them with Hessian and polythene sheets and wetted once every day for first 7-days, then air dried in uncontrolled laboratory conditions until age of 28-days.

3-9- Strain and Crack Width Measurements

Surface strain measurements were carried out by using stainless steel demec points inserted on 3 rows on the plates. The rows were at 50 mm, 100 mm from all edges and at the center as shown in Figure (3-4). The spacing between demec points in the same row was 200 mm apart. The demec points were positioned in the beams and plates after 24 hours from casting.



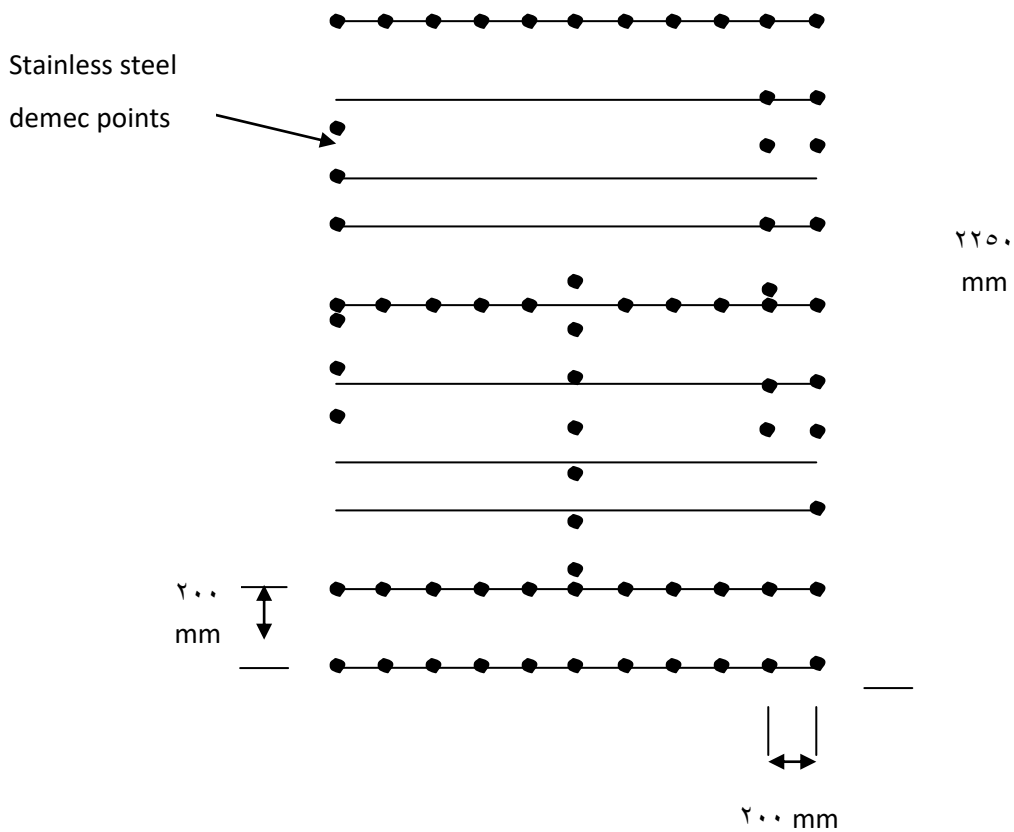


Figure (3-8): Stainless Steel Demec Points of Reinforced SCC Free Plate

An extensometer, with an accuracy of (0.002 mm/division) was used to measure the strain in panels of the plate. The panel represents the distance between any two consecutive demec points in the same row so, panel length = 200 mm. The measurement devices are shown in Plate (3-9).

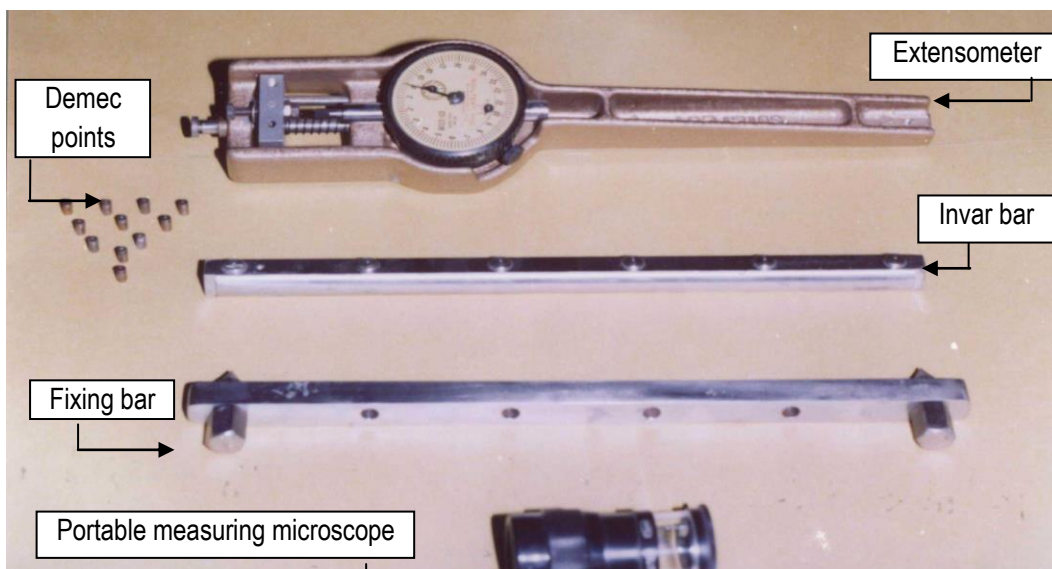
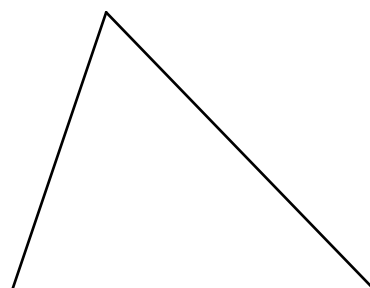


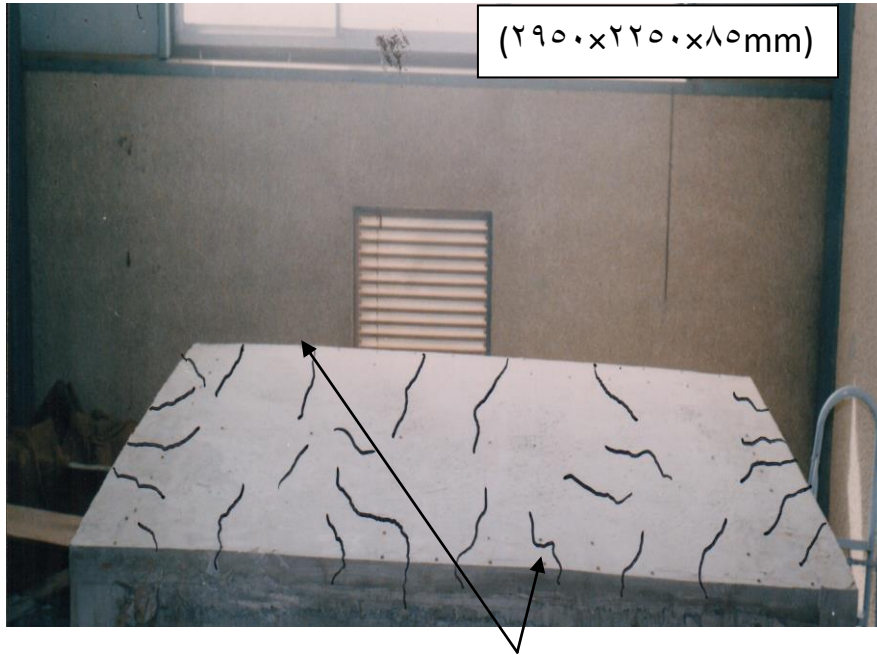
Plate (૩-૬): The Measurement Devices

The measurements were taken in the first three days after casting and continued until no appreciable changes in demec readings were obtained (at about ૧૦ days), and a stable cracking pattern had been formed. Crack widths have also been measured at many locations from the edges, the spacing between these locations was ૫૦૦ mm apart.

The measurement was carried out by using a portable microscope. The crack pattern in the (two, three and four) end restrained of the reinforced Self-Compacting Concrete plates are shown in plates (૩-૦, ૩-૧ and ૩-૨) respectively.

Restrained
edge

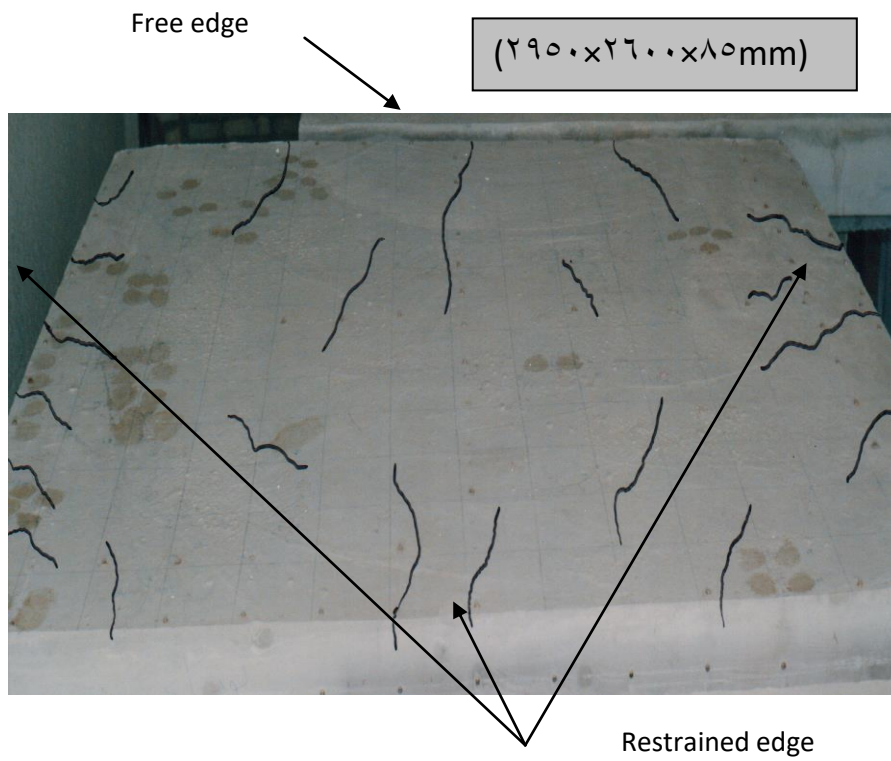




Free edge

Plate (3-5): The Cracks of Two End Restrained SCC Plate at 70 Days

Age



Free edge

(290. x 260. x 80mm)

Restrained edge

Plate (۳-۶): The Cracks of Three End Restrained SCC Plate at ۶۰ Days

Age

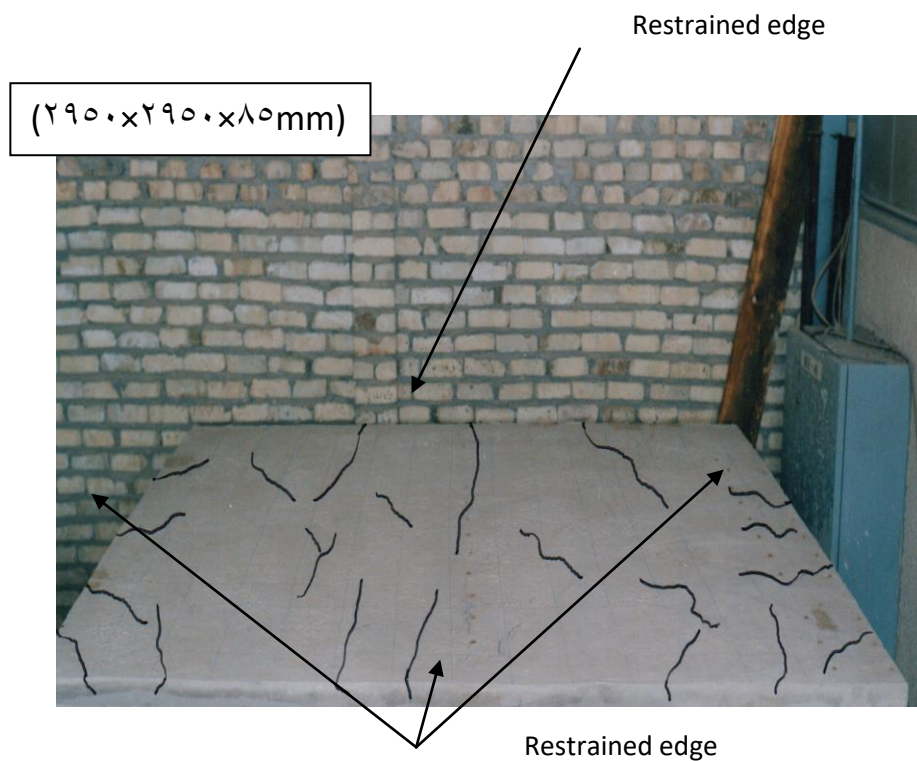


Plate (۳-۷): The Cracks of Four End Restrained SCC Plate at ۶۰ Days

Age

۳-۱۰- Free Volume Change of the Plates

In order to obtain an idea about the free volume change of the plates. Plate with dimensions of (۱۰۰۰*۱۰۰۰*۸۰ mm) was cast, and was exposed to the same conditions of restrained plates. There was no connection between the plate and slab. The friction, in the plane of contact between the plate and the

slab was minimized by applying two layers of greased polythene sheets, and this plate was left free to shrink and move. The movements were measured by demec points and an extensometer. Plate (3-8) shows the free movement plate.

The first day movement of the plate was obtained by the use of 3.0 meter end restrained beams as shown in Figure (3-2), in which an artificial crack (gap) was made in the mid-span of the web by using a 1.5 mm steel diaphragm. This beam was subjected to exposure conditions similar to those of the plates. The increase in gap width after one day would represent the first day shrinkage⁽³⁻⁹⁾, see plate (3-9). A portable microscope was used to measure subsequent free shrinkage movements after the first day.

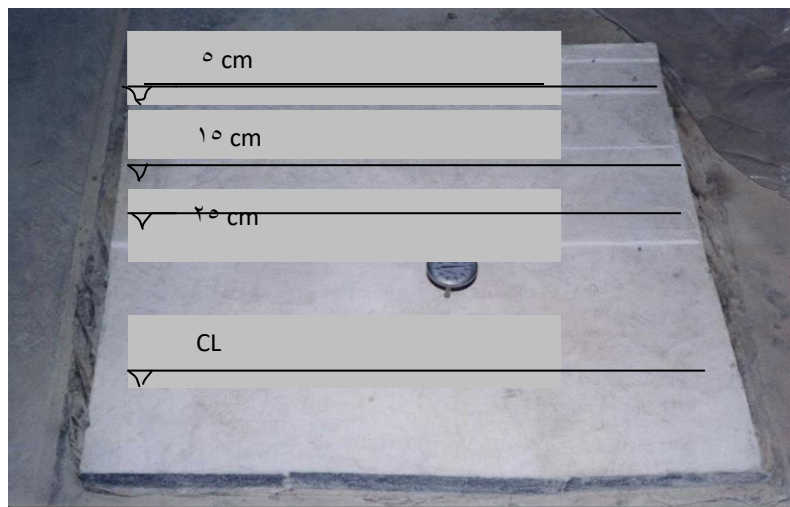


Plate (3-8): The Free Movement Plate

The first day thermal strain of the plate, due to loss of its heat of hydration to the surrounding atmosphere from its peak temperature to the temperature when the first strain reading of the plate was taken, was measured by embedded thermometer in the concrete plate to determine temperature drop, then the thermal strain by adopting a coefficient thermal expansion of $10.1 \times 10^{-6} / C^{\circ(AV)}$ for concrete.

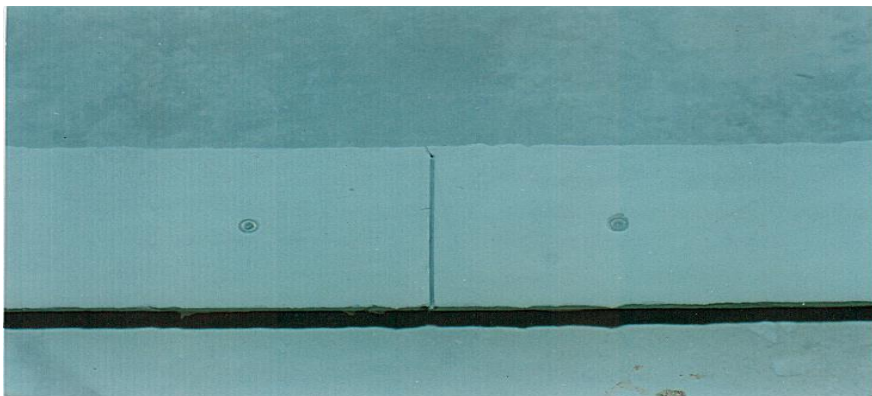


Plate (3-9): The Artificial Gap and Two Demec points on the Sides of the Gap.

3-11 - Tensile Strain Capacity Test

The elastic strain capacity is the amount of strain that is instantly relieved due to the elastic recovery of restrained concrete upon cracking. It is defined as the observed free contraction of concrete at the onset of cracking^(V9). Elastic tensile strain capacity of concrete was measured by using the same end restrained beam. Plain beams were cast and allowed to shrink. After the first crack occurred, the amount of strain which was relieved as a result of elastic recovery of restrained concrete was measured between fixed points together with crack width measurement by a microscope. This crack opening was assumed to represent elastic tensile strain capacity of concrete.

3-12- Restrained-Shrinkage Test

Concrete beams were tested for restrained shrinkage. The shrinkage cracking model was based on the model devised by Hassan⁽⁹⁾ shown in Figure (3-2). The beams were left in the molds (to achieve a restraint by the mold). For each filler, four end restrained beams with artificial crack (opening) in the web were used to determine free shrinkage, two were cast in winter and the others were cast in summer. Another six of end restrained beams were cast for the restrained shrinkage test for normal concrete and Self-compacting concrete (pigment and SP) with and without reinforcement. The depth of the beam was about 100 mm. The ends of the beam provide end restraint to the web, so that transverse cracks across the web can be formed as a result of stresses induced when the concrete shrinks.

The contraction at the surface of the dried concrete web was measured by taking readings at demec points, using mechanical dial gauge with (20 cm) gauge length and an accuracy of (0.002 mm/division). The demec points were fixed along the center of the web at (20 cm) distance using an adhesive epoxy resin.

After the occurrence of cracking, the measurement was repeated to record the recovery free contraction of concrete (the elastic tensile strain capacity) at the onset of cracking. Further demec points were fixed at the beam side in order to measure the amount of loss of restraint, which is due to shortening of the steel mold prior to cracking as shown in Figure (3-2). The free shrinkage of concrete was determined by fixing demec points at both sides of the gap for beams with artificial crack (opening) in the web and by daily measuring the

widening of the artificial crack in the middle of the beam. Readings were taken from the next day after leaving the molds in the laboratory, till little or no movement could be recorded.

Creep strain was calculated by subtraction the tensile strain capacity from the elastic tensile strain capacity.

CHAPTER FOUR

RESULTS AND DISCUSSION

ξ-1 - Introduction

In this chapter, the results obtained from the experimental work are analyzed and studied. These results include the following characteristics of the concrete.

ξ-2 - Properties of Fresh SCC

Workability tests are conducted on the fresh concrete immediately after mixing, including Slump flow, T₅₀₀ cm, L-box, U-box and V-funnel tests.

ξ-γ-λ - Slump-Flow and T₅₀ cm Test

The flowing ability of the fresh concrete is measured by slump-flow investigated with Abrams cone. The results of slump-flow and T₅₀ cm range between (780-700) mm and between (2.0-3.0) sec. respectively. These results are shown in Table (ξ-λ).

Table (ξ-λ): Properties of Fresh SCC

Workability tests	Type of filler			Limitation
	Pigment	Limestone Powder	Metakaolin	
Slump-flow	700	730	780	700-800 mm
T ₅₀ cm	2.0	3.0	3.0	2-0 sec
L-box	0.90	0.93	0.90	0.80-1.00
U-box	0	0.1	0.4	0-3 cm
V-funnel	6	7	8	6-12 sec

These results show that the SCC mix used is complying with the requirements found in the literature^(22,23,24). Its found from results that the SCC which is used has a good consistency, flowing ability and workability in its fresh state. This can be attributed to the high content of fine materials which reduce the voids in the original mixture, and produce less hydrate in the first few minutes. This agrees with other researchers^(17,22).

These results can be attributed to high sand to coarse aggregate ratio, use of superplasticizer and the small particle size of aggregate⁽¹⁷⁾. As the particle size decreases, the surface area of the particles increases. Thus, the particle size influences material properties which depend upon the surface area. The

increase in specific surface area of paste gives an indication of workability and flowability of Self-Compacting Concrete.

The type of filler influenced the workability of the SCC. The results show that the slump-flow of SCC mix with pigment is relatively higher than those containing limestone powder as well as metakaolin by (3, 9) %, and T_{50} cm of SCC mix with pigment is lesser than limestone powder and metakaolin by (20, 24) %. This high workability can be attributed to the dispersion of pigment powder throughout the concrete mix which can be obtained by using superplasticizer^(31,32).

Limestone powder gives higher workability than metakaolin by (7) % for slump-flow and less by (17) % for T_{50} cm. The relatively low value of metakaolin can be attributed to the shape and size of metakaolin particles which are long, hexagonal plates making obstructions in the fresh mix. Relatively, these materials deform by viscous flow, the same manner in which liquid deform; this characteristic property for viscous flow, (viscosity) is a measure of a non-crystalline material resistance to deformation⁽⁹⁹⁾. Also the chemical composition of metakaolin particles consists of two layers of (Si_2O_5) connected together by weak van der Waals forces cause decrease in workability⁽⁹⁹⁾. The higher the slump-flow value is, the greater ability to fill formwork under its own weight, and the shorter flow times of T_{50} cm indicates greater flowability.

ξ-2-2- L-Box Test

The results in Table (ξ-1) show that the blocking ratio (H_2/H_1) is ranged between (0.90-0.95). The L-box results reflected a good flowability and show

that the blocking ratio values for all fillers are greater than 0.8, which is often considered in the ENARC 2002⁽²²⁾ as the critical low limit.

It can be seen from the results that the SCC mix with metakaolin gives relatively less value of blocking ratio than the SCC mixes with pigment and limestone powder by (6, 3) % respectively. This behavior can be attributed to the relatively high viscosity of metakaolin compared to pigment and limestone powder, because the viscosity increased markedly with the increase of SiO₂⁽¹⁰⁰⁾, as shown in the chemical analysis of metakaolin (SiO₂ = 68.8%), also this behavior may be attributed to the shape and the composition of metakaolin particles.

4-2-3- U-Box Test

The test is used to measure the filling ability of Self-Compacting Concrete. The results presented in Table (4-1) show that the SCC used can be described as Self-Compacting due to the fact that after opening the sliding gate, the concrete raised in the other half of the U-box to a height greater than 0.8 of the maximum possible height. (H₁-H₂) must be ranged between (0-3) cm. According to Table (4-1), the results of U-box are ranged between (0-0.4) cm, which is an acceptable limits. This may be attributed to the limit of coarse aggregate content which reduces the potential for the formation of internal stresses leading to blockage of the mix. The results show that the filling ability of the fresh SCC mixes with pigment, limestone powder and metakaolin is (0, 0.1, 0.4) respectively. The less value of filling ability of SCC with metakaolin can be attributed to the shape and composition of metakaolin particle, long hexagonal plates. If concrete flows as freely as water at rest, it will be

horizontal, so when $(H_1 - H_2 = 0)$, better flow and passing ability of the concrete will be achieved⁽²³⁾.

ξ-2-ξ- V-Funnel Test

This test measures the ease of concrete flowing, where shorter flow times indicate to greater flowability. From the results shown in Table (ξ-1) it can be seen that the time of flow is between (6-8) seconds for SCC mixes containing fillers. This gives an indication for the high flowability of the concrete mixes, which is in agreement with the requirements of EFNARC 2002⁽²³⁾, and other researchers Celik and Stephen⁽²³⁾. This behavior can be attributed to the use of fillers and also, use of SP which reduces surface tension (dispersion activity)⁽²³⁾.

It is apparent from Table (ξ-1) that the flow time of SCC mix with metakaolin is slightly higher than SCC mixes with pigment and limestone powder by (33, 13) % respectively. This may be due to the high viscosity of metakaolin compared to pigment and limestone powder because the viscosity increases markedly with the increase of SiO_2 ⁽¹⁰⁰⁾ as shown in the chemical analysis of metakaolin ($\text{SiO}_2 = 78.8\%$). The high flow time can be associated with low deformability due to the higher paste viscosity, and higher interparticle friction⁽²⁴⁾.

ξ-3- Free Shrinkage Test for Beams

By using the steel beam described in chapter three, concrete beam with a gap at its middle was cast to ensure free movement. Free shrinkage strain was measured for all mixes in winter and summer. Shrinkage strain development of concrete beams for different drying periods of normal concrete and Self-

Compacting Concrete are shown in Figures (ξ-1) and (ξ-2) in winter and summer respectively.

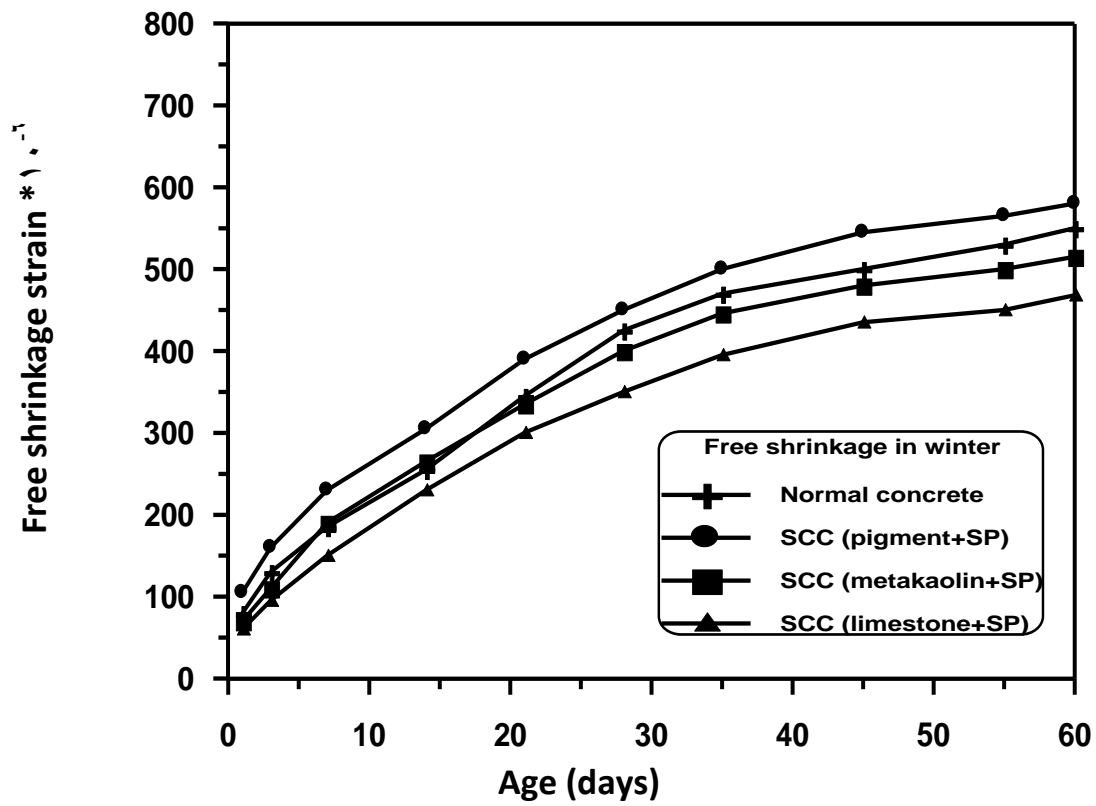


Figure (ξ-1): Free Shrinkage Development With Age for End Restrained

Beam in Winter

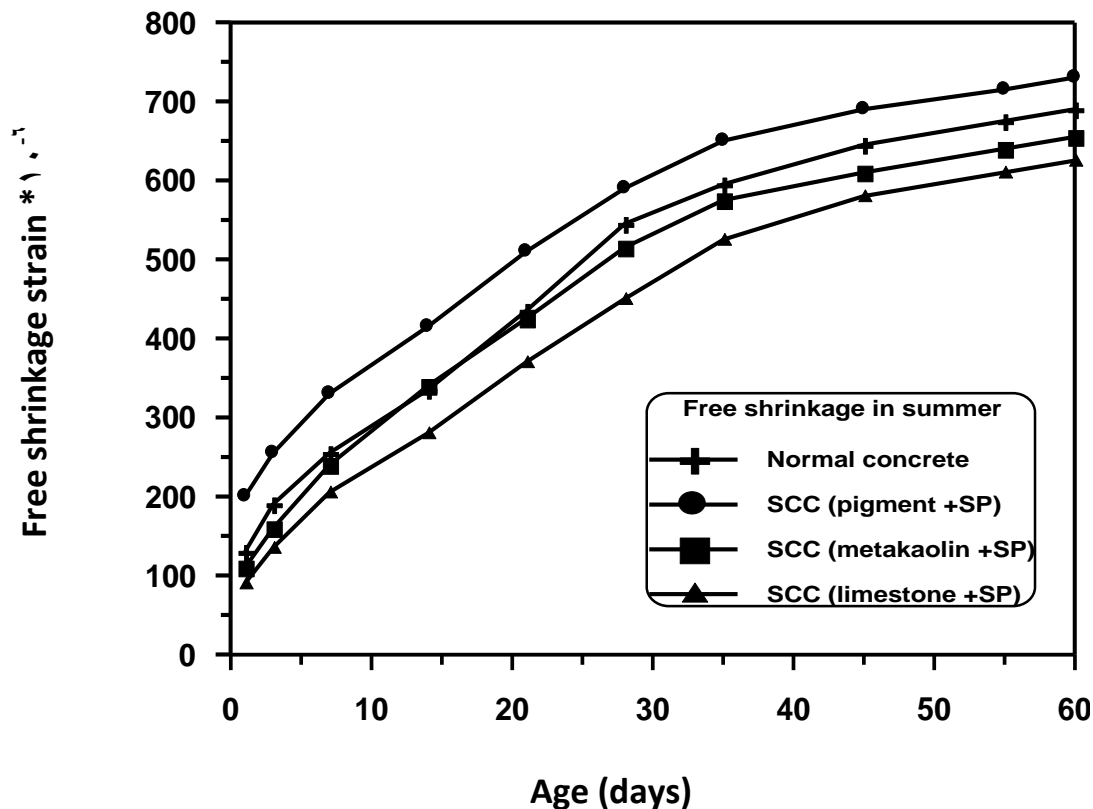


Figure (4-2): Free Shrinkage Development With Age for End Restrained Beam in Summer

The experimental results for normal concrete and Self-Compacting Concrete mixes show that the drying shrinkage of SCC mix with pigment is higher than that the normal concrete mix by (24 % for 1-day and 6 % for 60-days) in winter and by (24 % for 1-day and 6 % for 60-days) in summer. This is may be relating to the effect of volume of paste on drying shrinkage amount and high content of fine materials (powder) which increase drying shrinkage. This is compatible with the study carried out by Johansen and Hammer⁽²⁰⁾

Figures (4-1) and (4-2) show that the free shrinkage of SCC mix with pigment is higher than the SCC mixes with limestone powder and metakaolin by (33, 43 for 1-day and 11, 19 for 60-days) % respectively in winter and by (40, 50 for 1-day and 10, 14 for 60-days) % respectively in summer. This may be attributed

to the large surface area of the pigment which is presented to the reaction with the water and hydration takes place rapidly.

Free shrinkage of SCC mix with metakaolin is relatively higher than the SCC mix with limestone powder in the two seasons (winter and summer) by (1.8, 1.8 for 1-day and 9, 0 for 28-days) % respectively. This may be due to the high content of ($\text{SiO}_2 = 68.8\%$) in metakaolin (as shown in the chemical analysis of metakaolin) that is able to react with calcium hydroxide (produced by the hydration of Portland cement) in the presence of water to form calcium silicates hydrates. This reaction results in a reduction of large crystals of $\text{Ca}(\text{OH})_2$ and consequently produce of shrinkage. The SCC with limestone powder has lower drying shrinkage than SCC mixes with pigment and metakaolin by (7.0, 1.7 for 1-day and 2.8, 1.0 for 28-days) % respectively in winter and by (1.22, 2.2 for 1-day and 1.7, 0 for 28-days) % respectively in summer, because of slow hydration rate and lower evaporation. This is compatible with the study carried out by Holschemacher and Klug⁽⁶⁶⁾ and Rahim⁽⁶⁷⁾.

ξ-ξ- Restrained Shrinkage Test for Beams

ξ-ξ-1- Tensile Strain Capacity

The determination of tensile strain capacity was based on the end restrained shrinkage beam. Table (ξ-2) shows the values of tensile strain capacity obtained in the present work. In general it can be observed from the results that the tensile strain capacity increases with the increase of date of crack. This result is compatible with the study carried out by Hughes and Ghunaim⁽⁶⁸⁾ and Hobbs⁽⁶⁹⁾.

Table (4-2): Properties of End Restrained

Mix notation	Date of crack (day)	Free shrinkage $\times 10^{-3}$	Loss of restraint $\times 10^{-3}$	Tensile strain capacity $\times 10^{-3}$	Elastic tensile strain capacity $\times 10^{-3}$	Creep $\times 10^{-3}$	Width of crack (mm)
Normal concrete mix	28	0.40	8.0	460	161	3.4	0.40
Plain SCC mix (pigment+SP)	7	33.0	6.0	27.0	1.7	163	0.30
Reinforced SCC mix (pigment+SP)	Crack 1	3	200	4.0	210	70	0.2
	Crack 2	14	410	7.0	340	9.0	0.20

Beams

It is clear from Table (4-2) that the tensile strain capacity for normal concrete mix, plain SCC mix and reinforced SCC mix for two cracks (crack 1, crack 2) is (460, 27.0, 210, and 340 $\times 10^{-3}$) respectively. The higher tensile strain capacity of the normal concrete mix can be attributed to the longer time for the occurrence of cracking (28-day) compared with its counterparts of the SCC mix (3, 7, 14-day).

The tensile strain capacity decreased when addition of pigment powder. This may be due to the high early shrinkage and early shrinkage cracking (3, 7, 14-day) for plain and reinforced SCC mixes, and when strength of concrete is in a weak stage and the tensile strength was [1.0 N/mm²] in 1-day and [2.3 N/mm²] in 3-days compared with the tensile strength for normal concrete mix which was [1.0 N/mm²] in 1-day and [2.0 N/mm²] in 3-days.

4-2-2- Elastic Tensile Strain Capacity

Elastic tensile strain capacity of concrete was obtained directly by measuring the immediate movement after cracking of concrete on end restrained beams.

Table (ξ-ϒ) shows that the elastic tensile strain capacity for normal concrete mix, plain SCC mix and reinforced SCC mix for two cracks is (161, 107, 70, and 9.0*10⁻¹) respectively. The reduction in elastic tensile strain capacity for SCC mix can be attributed to the decrease of cracking time.

ξ-ξ-ϒ- Creep

Creep strain of concrete subjected to the restrained shrinkage was calculated as the difference between the tensile strain capacity and the elastic tensile strain capacity. Table (ξ-ϒ) shows that the creep for normal concrete mix, plain SCC mix and reinforced SCC mix for two cracks is (3.4, 163, 140, and 200*10⁻¹) respectively.

It is obvious that the lower creep strain (at cracking) for SCC mixes may be attributed to that SCC mixes hydrate more rapidly and more evaporation which causes early cracks therefore, the given period for creep is lower. The increase in creep for the normal concrete mix is due to the elongation of cracking time and restrained shrinkage stress.

ξ-ξ-ξ- First Crack Time

The first crack time can be used as an index for the liability of concrete to crack⁽¹⁰⁾.

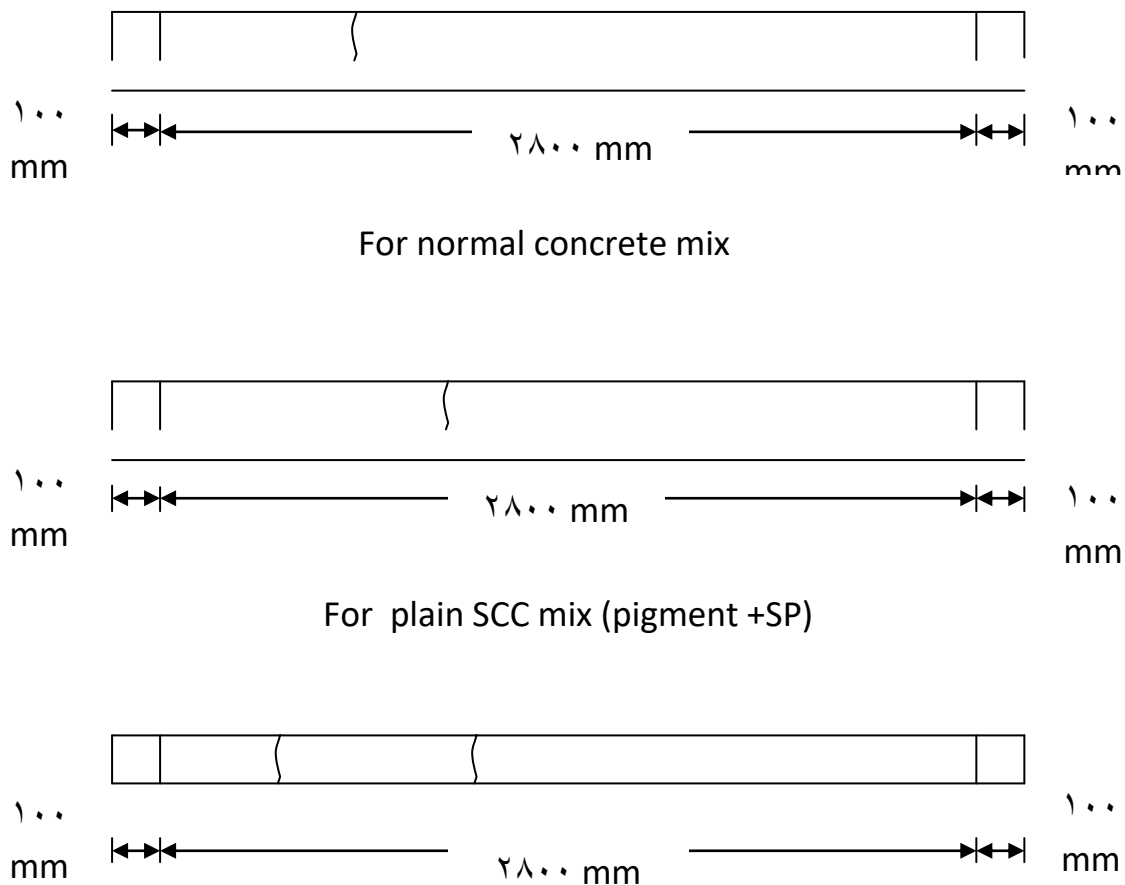
Table (ξ-ϒ) shows that for normal concrete mix, the first cracking time takes place at 28-days. When the pigment and superplasticizer were used, 7-days were required for occurrence of the first crack. For reinforced SCC model, two cracks appeared on the surface of the same beam, one at 7-days and the other

at 14-days. It can be observed that the cracking time decreases with the addition of pigment powder and superplasticizer to the mix. This may be related to the fact that these additions would increase drying shrinkage, thus, the possibility of cracking at early ages will be increased, and the time required for cracking will be lower.

For reinforced SCC mix the cracking time decreased. That means more microcracks, higher internal restraint, higher stresses, which indicate that cracks appear earlier because the strength of concrete is still in a weak stage.

4-4-0- Crack Location

Figure (4-3) shows the location of crack for normal concrete mix and plain as well as reinforced SCC mixes.



For reinforced SCC mix (pigment +SP)

Figure (4-3): Location of Cracks of Concrete Beam Specimens

The results show that the cracks occurred within the middle third of the beam rather than at the side. This means that the restraint shrinkage strain is higher at the middle thirds of the beam than at the sides.

Al-Rawi⁽⁴⁾ attributed this behavior to the generation of a strain gradient at the end part which increases the loss of restraint and reduces the possibility of cracking, while at interior zones, higher restraint would be developed due to the build up of friction forces and the absence of strain gradient, so crack would be expected at the interior zones and away from the ends.

4-4-6- Crack Width

The results of crack width for normal concrete mix and plain as well as reinforced SCC mixes are given in Table (4-3) and plotted in Figure (4-4).

From the figure, it can be seen that the crack width development of plain SCC mix after cracking is higher than its companion of the normal concrete mix. This may be due to the present of fine powder.

It is obvious, that the rate of crack widening is high at early ages and decreases at later ages. This notice is expected as a higher percentage of creep would be consumed for the later age crack, and consequently less crack widening would be experienced in this case, and also the rate of shrinkage reduced at the later ages.

For reinforced SCC, the rate of crack widening for two cracks in the same beam is less compared with plain SCC, because steel reinforcement

redistribute the tensile strain resulting from restrained volume changes for many small cracks rather than single wide crack width.

Table (٤-٣): Crack Width of Beam Specimens of Normal and SCC Mixes

Age (days)	Crack width (mm)			
	Normal mix	Plain SCC mix (pigment +SP)	Reinforced SCC mix (pigment +SP)	
			Crack ١	Crack ٢
٣	---	---	٠.٢٠	---
٧	---	٠.٣٠	٠.٢٤	---
١٤	---	٠.٣٩	٠.٣٠	---
٢١	---	٠.٥٣	٠.٣٧	٠.٢٥
٢٨	٠.٤٥	٠.٦٦	٠.٤١	٠.٣١
٣٥	٠.٥٠	٠.٧٨	٠.٤٥	٠.٣٦
٤٥	٠.٥٨	٠.٨٧	٠.٤٨	٠.٣٩
٥٥	٠.٦٥	٠.٩٢	٠.٥٠	٠.٤١
٦٠	٠.٦٨	٠.٩٥	٠.٥٠	٠.٤٢

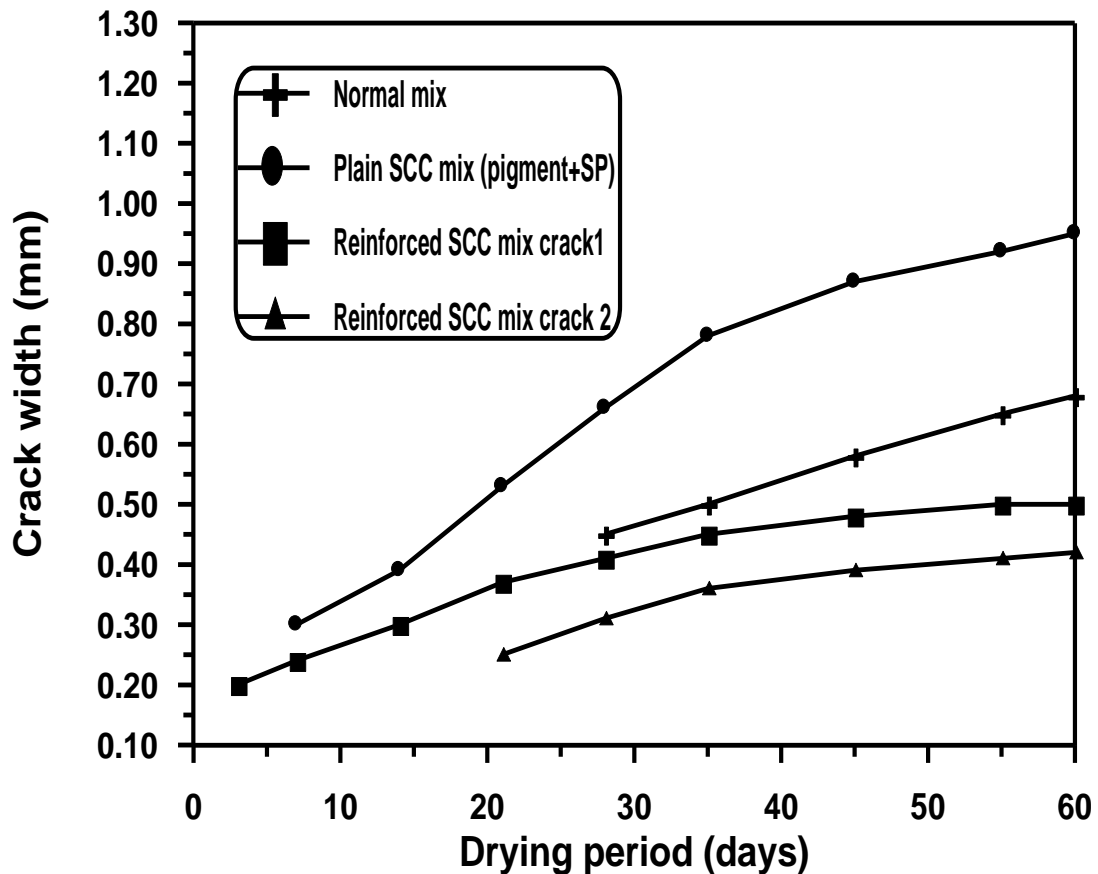


Figure (ξ-ξ): Development of Crack Width With Age of Beams for ates
Normal Mix, Plain SCC Mix and Reinforced SCC

The free shrinkage strain of Self-Compacting Concrete plates was measured under the same indoor exposure conditions of the restrained plates. Figure (ξ-ξ) shows the free shrinkage strain development in the plates with drying period.

In the first day, there was a contraction in the plates due to the drop of the concrete plate temperature from its peak temperature (due to heat of hydration) to its temperature when the first reading was taken, which was carried out early in the morning. The temperature drop observed in the plate was about 1°C. Thus, the amount of free thermal contraction will be

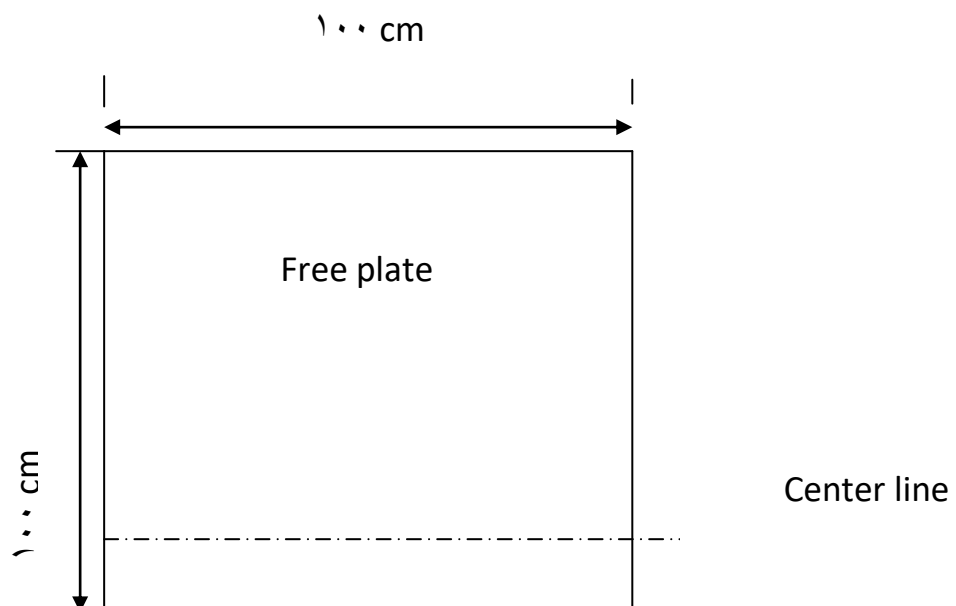
$$e_{th} = C_T * T \quad \dots\dots (ξ-1)$$

C_T : linear coefficient of thermal expansion of concrete which is taken as

$$1.0 \times 10^{-5} / ^\circ\text{C} (^{\wedge}).$$

Therefore, a total contraction strain of 17.0×10^{-5} , due to the effect of temperature drop was recorded.

Because it is difficult to measure the first day shrinkage strain directly from the free plate due to the difficult position of the demec points on the surface of plates since the SCC plates are not yet hardened, it was measured by using the end restrained beam which is cast and measured from (1-July to the 1-September) as shown in Figure (ξ-1). Also, this figure shows the free shrinkage in summer for SCC containing (pigment+SP) and normal concrete cast and measured in (1-March to 1-May) compared with SCC containing (pigment+SP) cast and measured from (1-July to the 1-September).



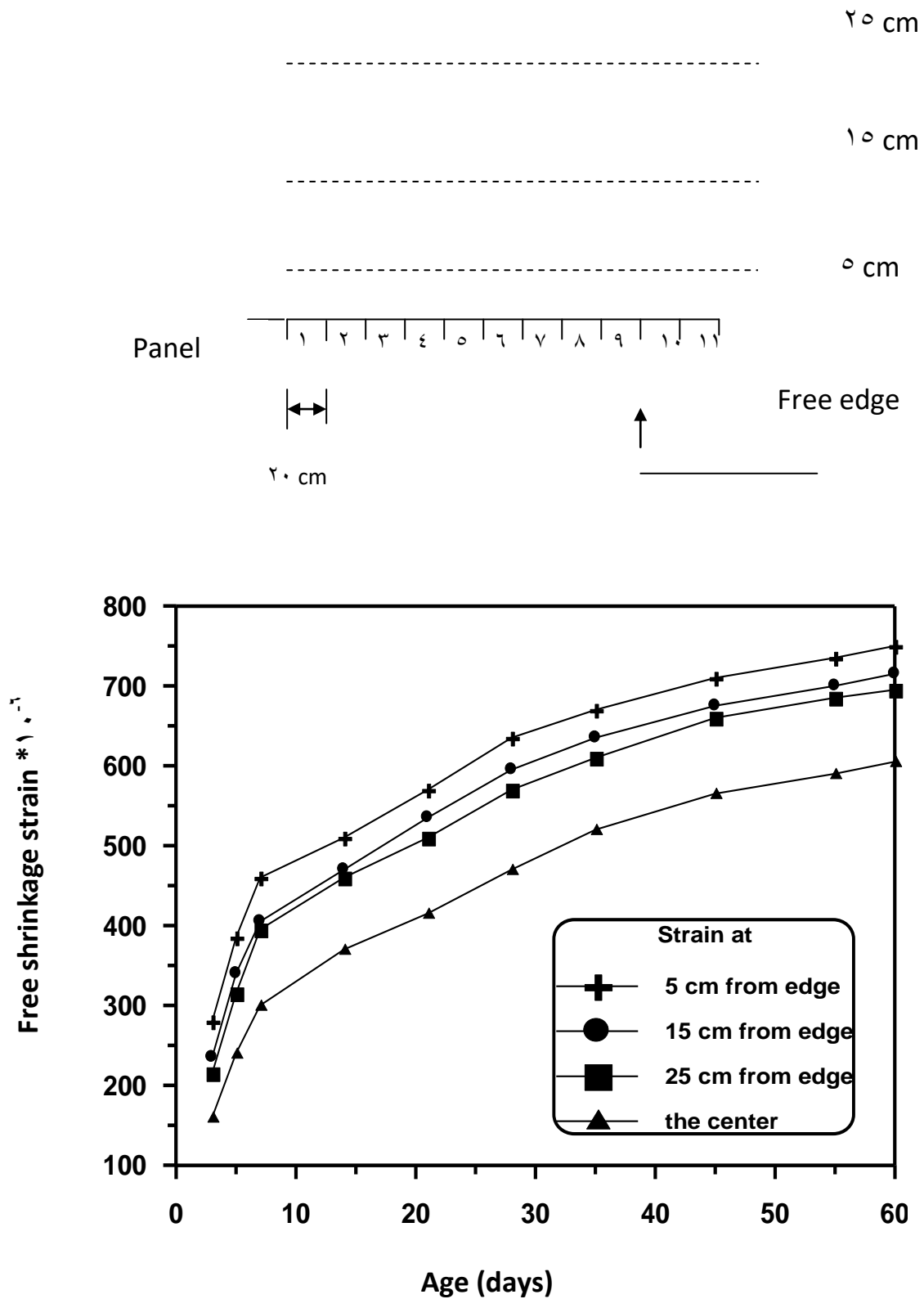


Figure (4-5): Free Shrinkage Development With Age for Plain SCC Free

Plate.

Free shrinkage strain of the plates as illustrated in Figure (4-5) was not uniform with distance from the edge to the center of the plates. In general, the shrinkage strain at 0 cm from the edge was greater than that at the center of plate (20 cm) by (43 % for first 3-days and 19 % for 60-days). The surface area at 0 cm from the edge includes (edge and surface area) which is more subjected to the drying shrinkage than at the center which includes the surface area of plate only.

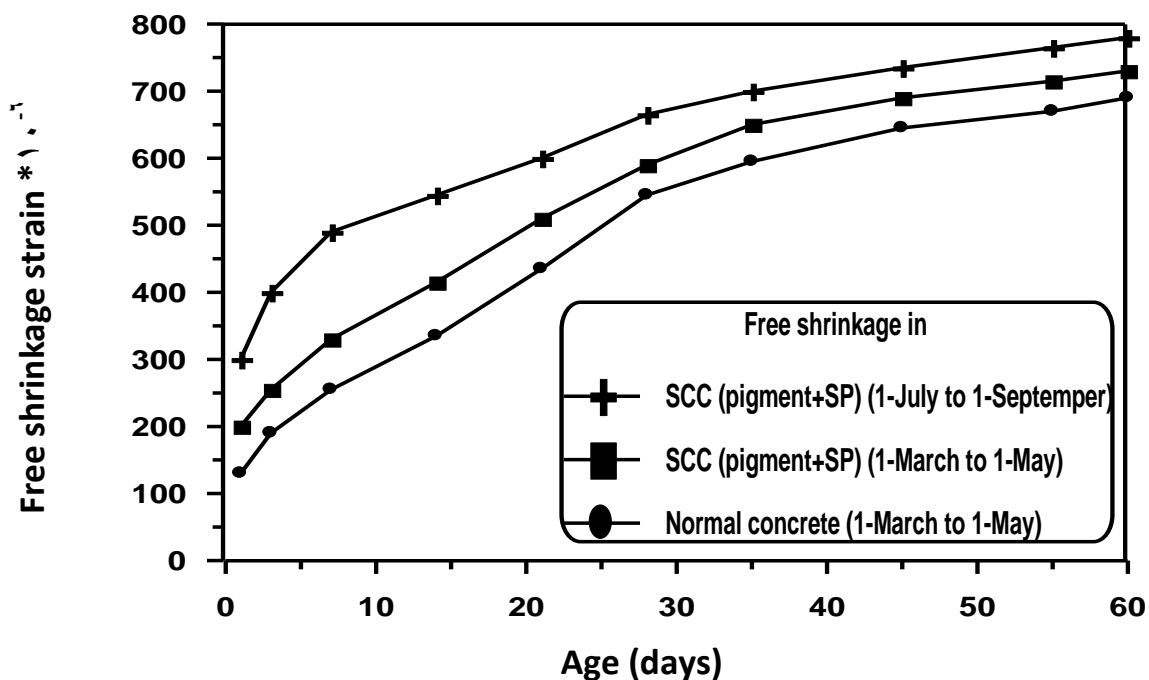


Figure (4-6): Free Shrinkage Development in Summer with Age for Beam Model in Different Cast and Measured of SCC (Pigment+SP) and Normal Concrete.

Figure (4-7) shows the free shrinkage strain development with age for reinforced SCC free plate at three rows (0, 10 cm a part from the edge and at

the center) of the plate. This figure shows that free shrinkage strain of reinforced SCC at 5 cm from the edge was greater than the shrinkage strain at the center of this plate (112.5 cm by 31 % for first 3-days and 13 % for 60-days). The surface area at 5 cm from the edge includes (edge and surface area) which is subjected to the drying shrinkage more than at the center which includes the upper surface area of plate only.

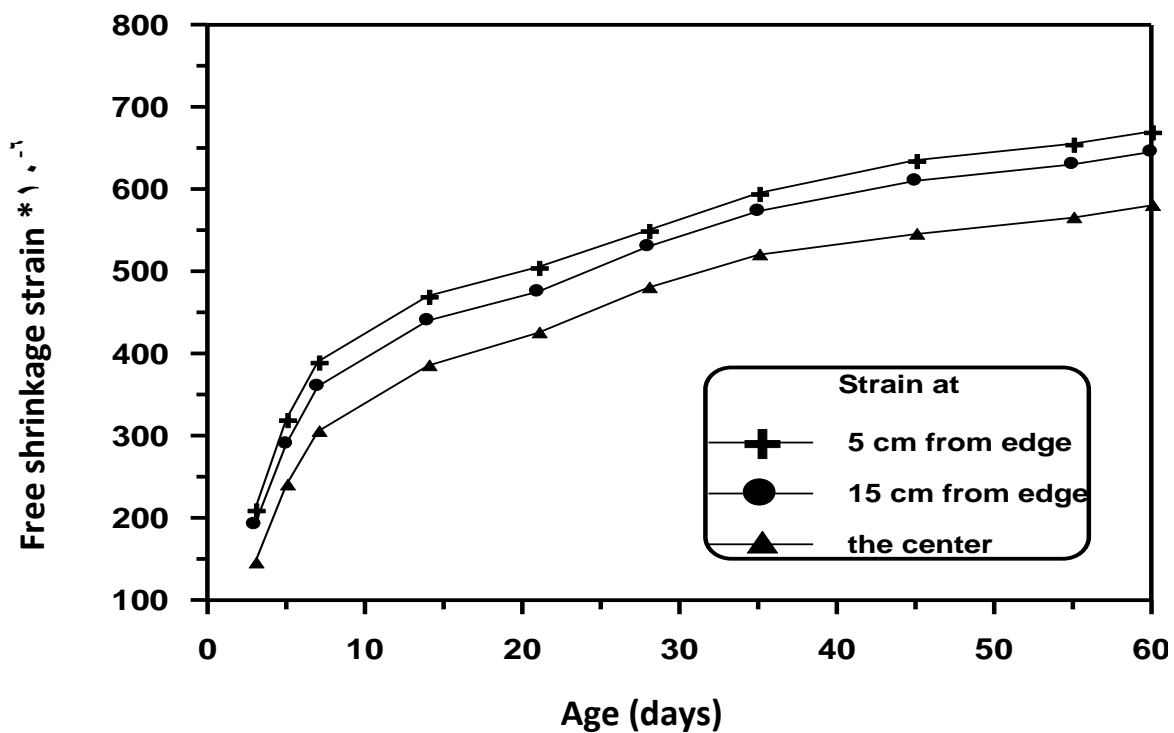


Figure (4-7): Free Shrinkage Development With Age for Reinforced SCC

Free Plate.

From Figure (4-7) also, it is clear that the effect of internal restrained (reinforcement) on SCC free plate at the centerline (112.5 cm for 60-days) gives relatively the same trend compared with plain SCC (without reinforcement) free plate (110 cm for 60-days). While at the edge the effect of internal

restraint (reinforcement) on SCC free plate ($\gamma_{\text{SCC}}^{\text{free}}$ for t -days) is higher compared with plain SCC (without reinforcement) free plate ($\gamma_{\text{SCC}}^{\text{plain}}$ for t -days). This means that the internal restraint affects on the edges of plate and has a lower effect toward the centerline of plate.

3-6- Restrained Movement of the Plates

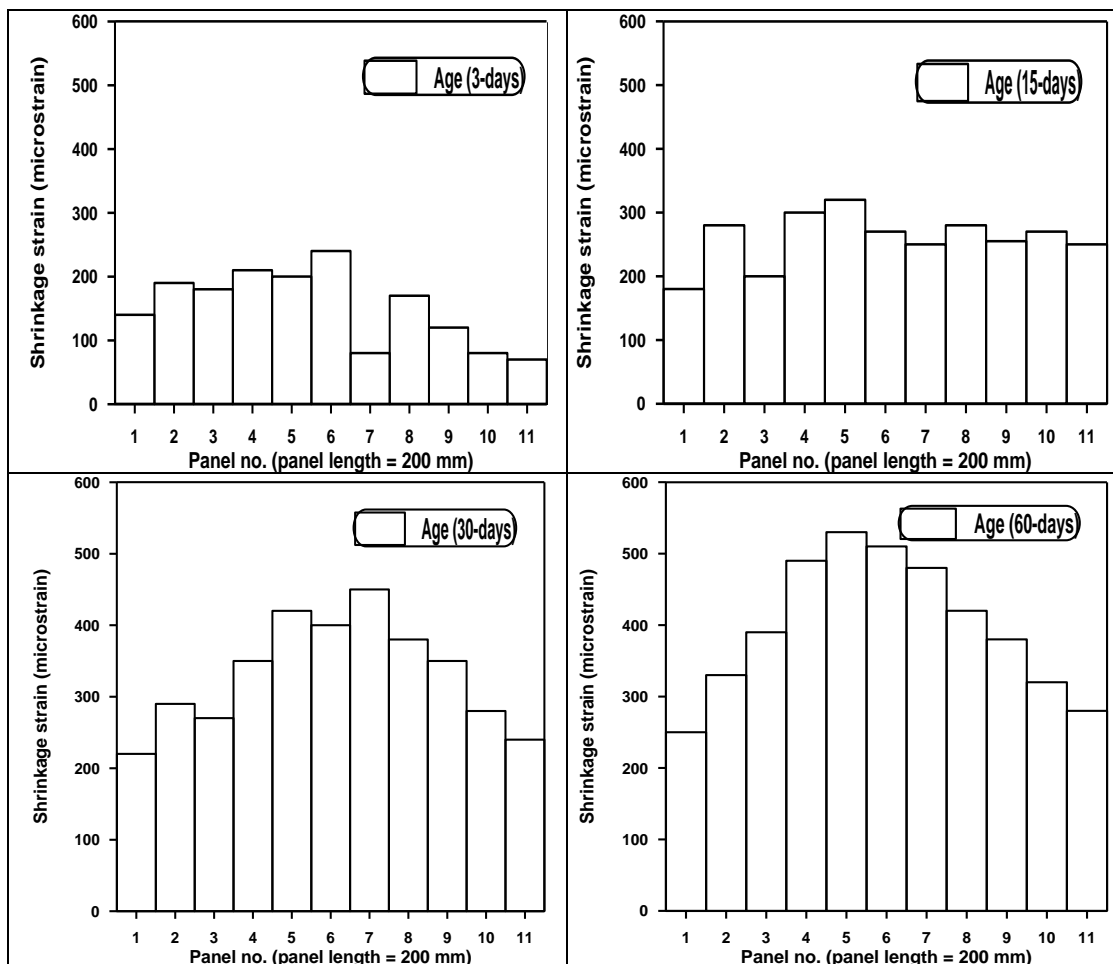
The movements of the plates were measured at three rows (0, 10 cm a part from the edge and at the center) of the plate by using a demec gauge (extensometer) to investigate the effect of base (the roughness or interaction between edge of plate surround slab and the edge of restrained slab) as shown in Figure (3-6)) and end restraint on the cracking behavior (cracking age, cracking sequence, crack spacing, crack width, crack length, and location of maximum crack width). These measurements were conducted for a drying shrinkage period of 2 months (1-July to the 1-September).

For the restrained plates (two, three and four end restrained), the restraining effect of the base decreases towards the centerline of plate, therefore, the movement of the plate will vary with the distance from the restraining base. This is compatible with the study carried out by Al-Mashhedi⁽¹⁴⁾.

Figures (3-7 to 3-13) show the measured movement of the plates studied. From Figures (3-7 to 3-13) it can be observed that movements of the plate increase towards the centerline of the plate from the restrained edge. The main reason of this behavior is the base restrained effects which decrease toward the centerline of the plate from the restrained edges. A gradual reduction in the readings of measured shrinkage strain at any panel would

indicate a crack occurrence at that panel. An abrupt positive change would indicate that cracking had taken place at that panel which is denoted by zero strain in these figures.

In addition to the measurement of the plate movement, the contraction of the slabs (which were used as base in order to provide different restrained cases from the ends to the plate models) was also measured during the same period. The contraction of the slabs was called “Loss of restraint” “L.O.R.”. The average value of loss of restraint for slabs is about $\nabla \cdot$ microstrain.



o cm ||

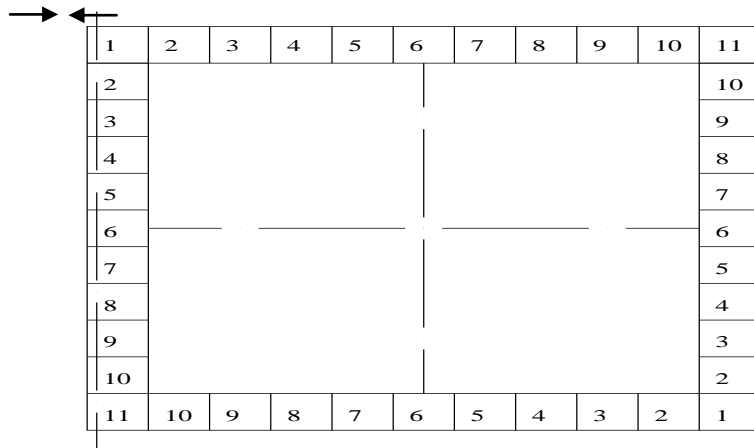
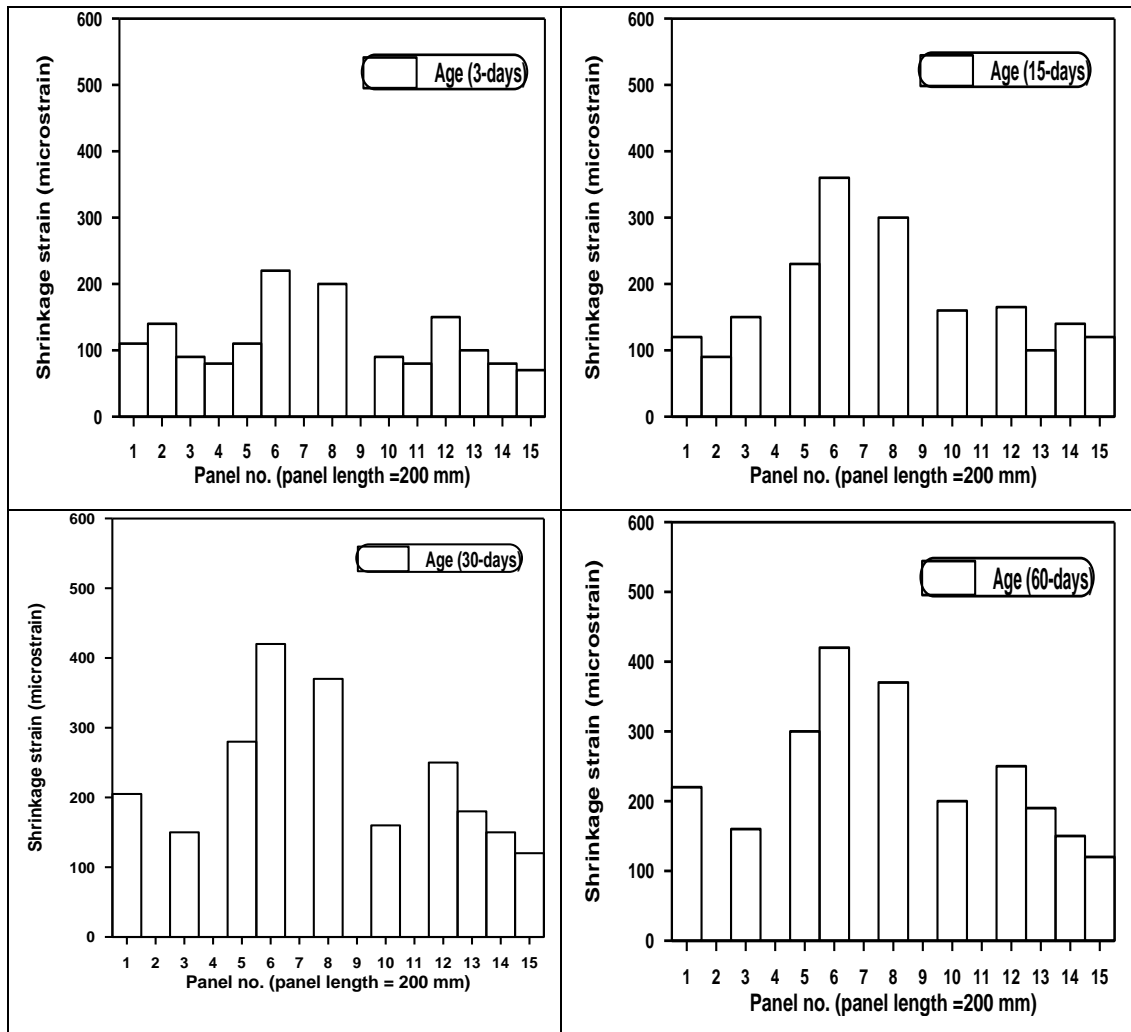


Figure (ξ-λ): Shrinkage Strain Development for Reinforced SCC Free Plate

at 0 cm from the Edge



0 cm ↓
5 cm

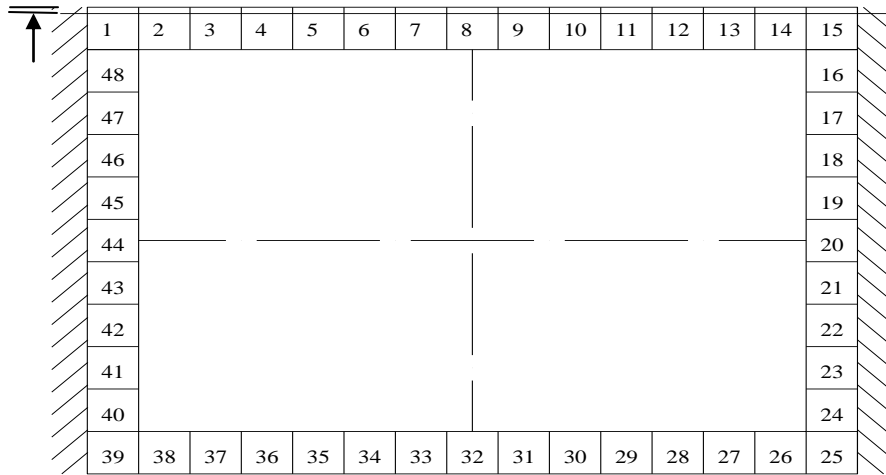
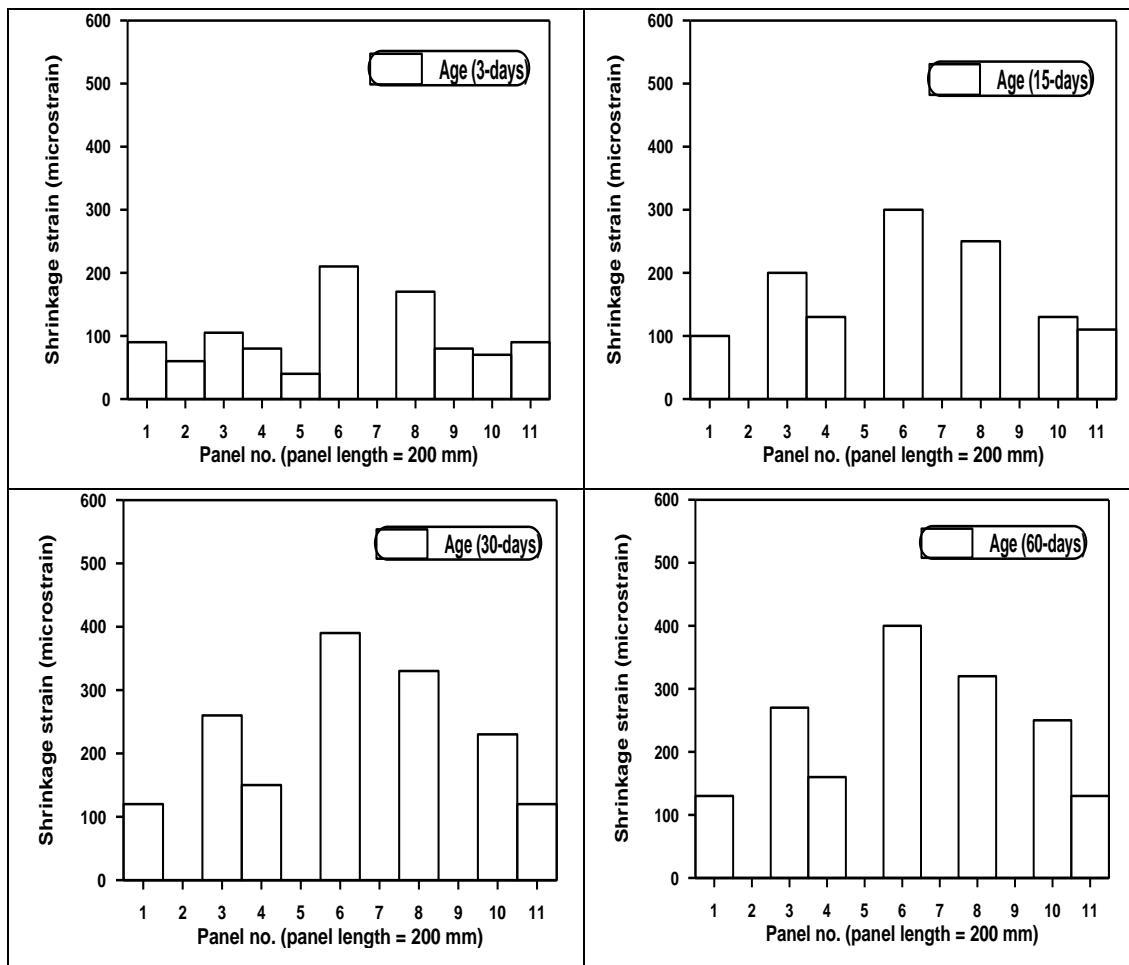


Figure ($\xi-9$): Shrinkage Strain Development of Two End Restrained SCC

Plate at ϕ cm from the Free Edge



ϕ cm

||

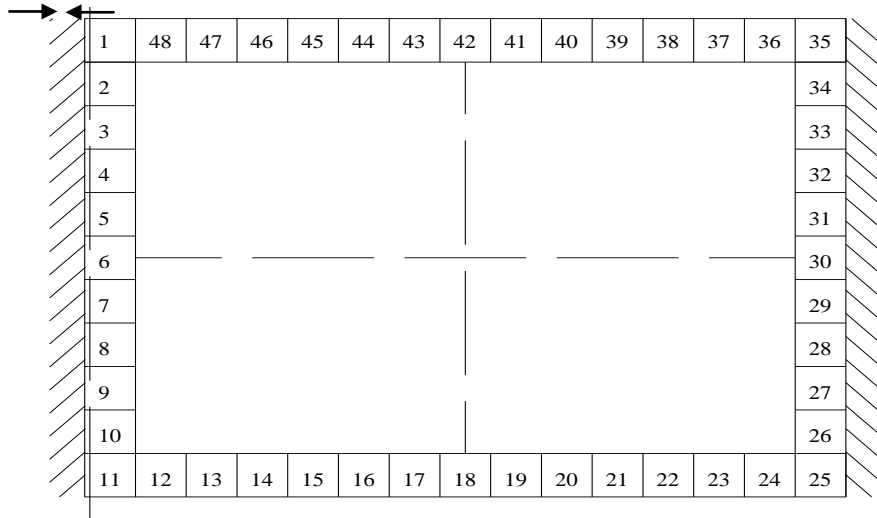
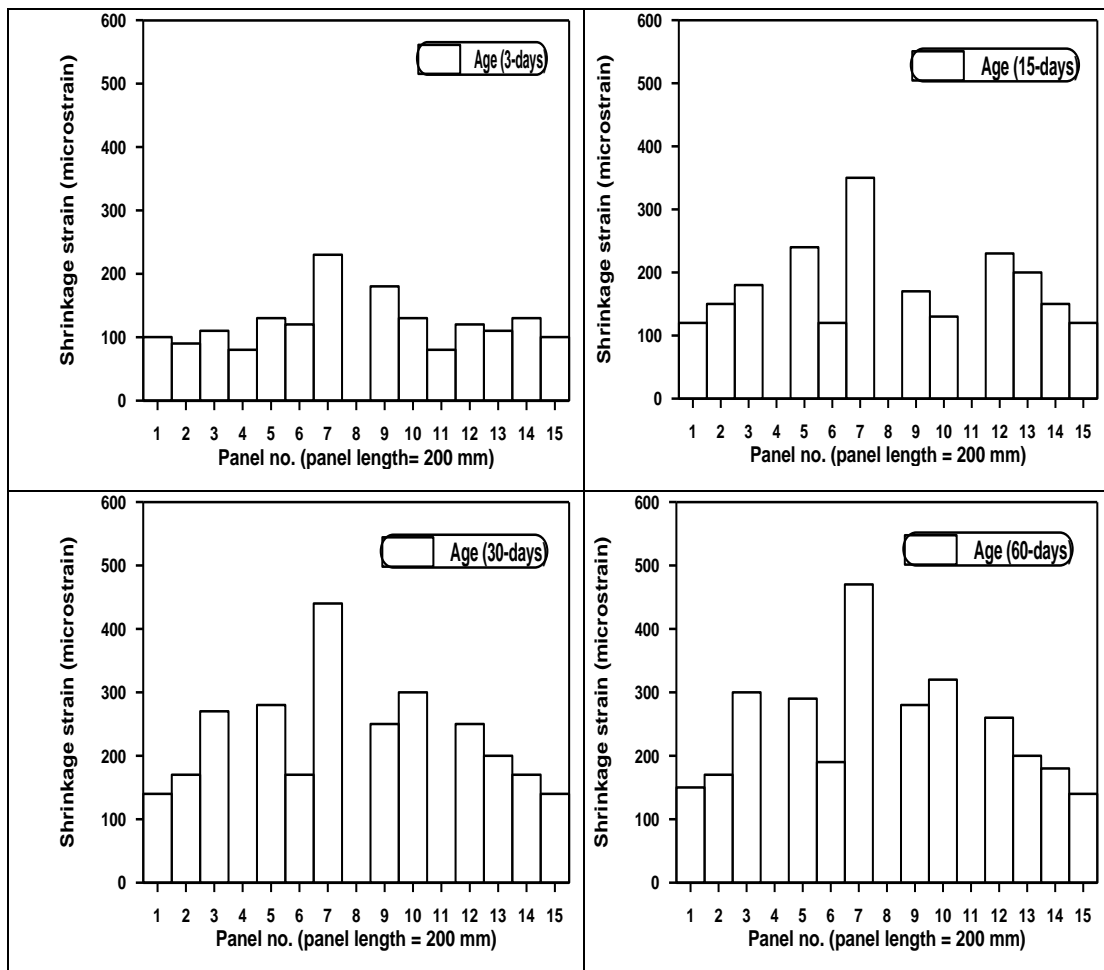


Figure (ξ-1): Shrinkage Strain Development of Two end Restrained SCC

Plate at 0 cm from the Restrained Edge



0 cm ↓

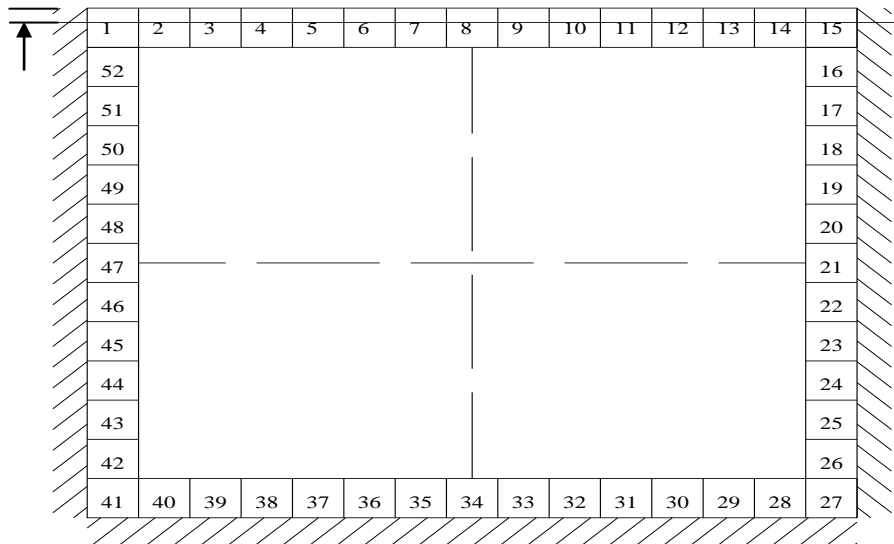
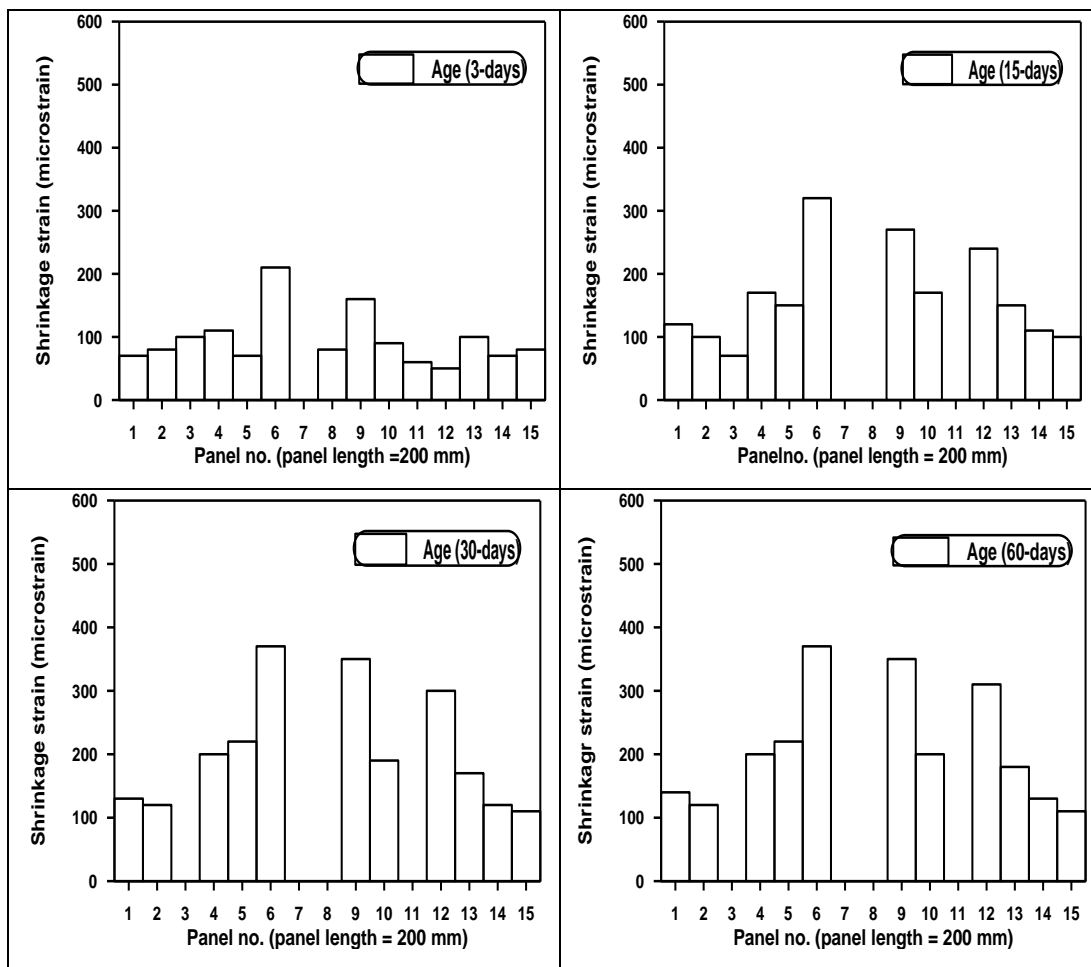


Figure (3-11): Shrinkage Strain Development of Three End Restrained SCC Plate at 20 cm from the Free Edge



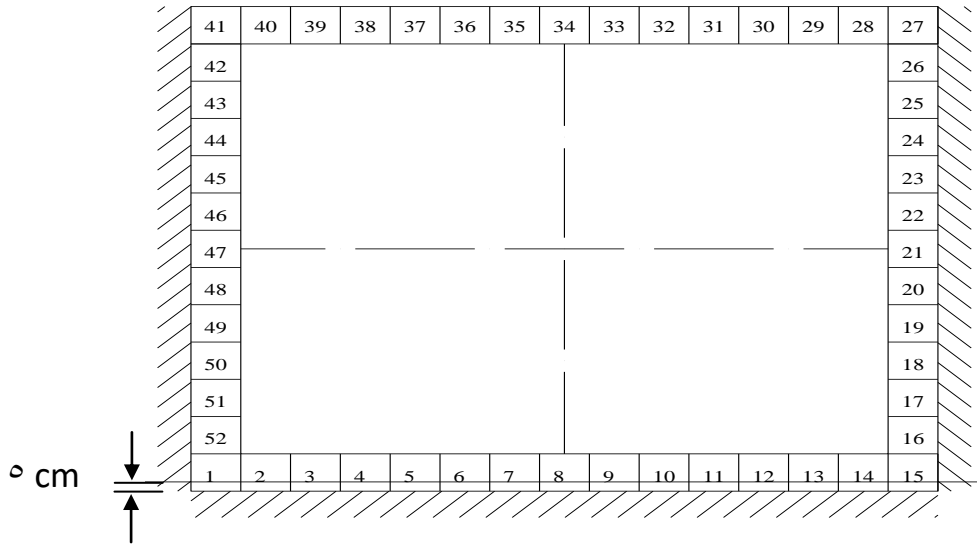
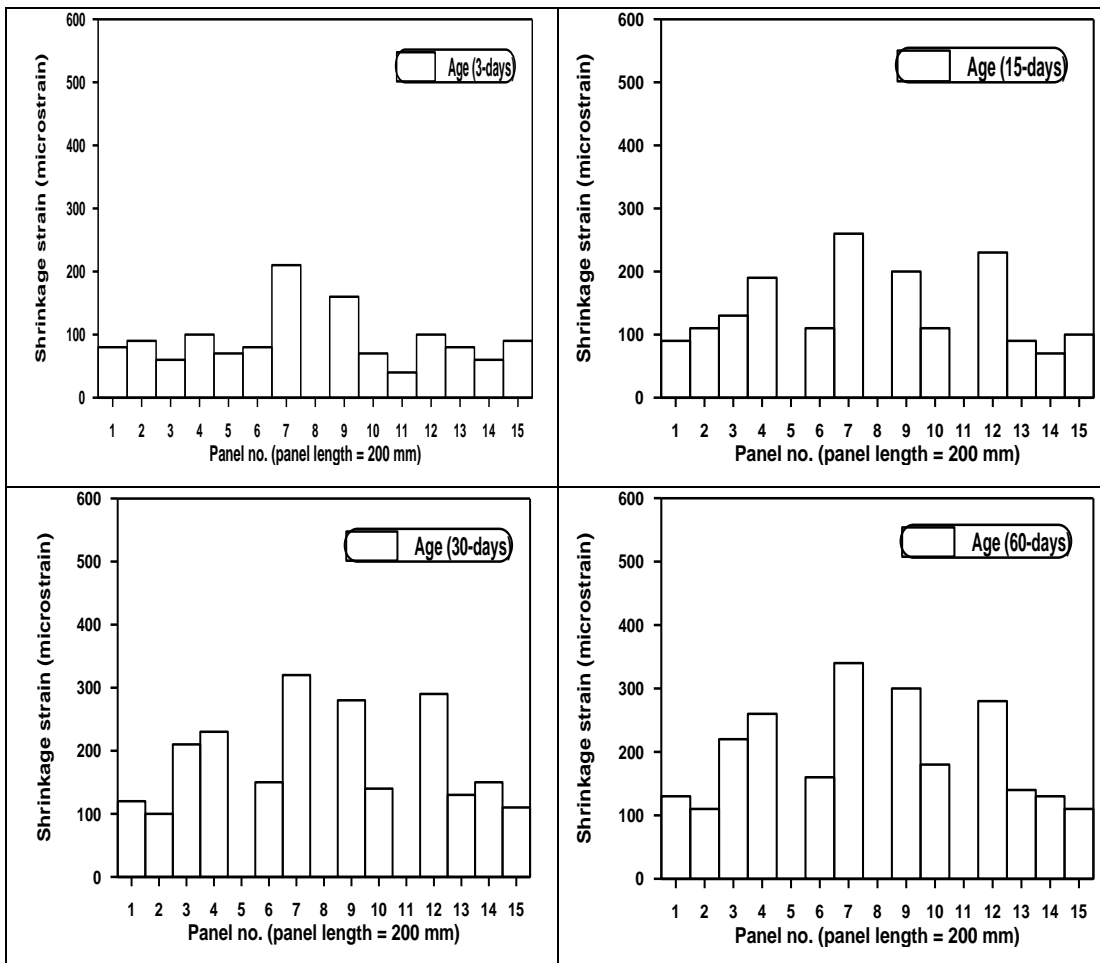


Figure (ξ-١٢): Shrinkage Strain Development of Three End Restrained SCC

Plate at o cm from the Restrained Edge



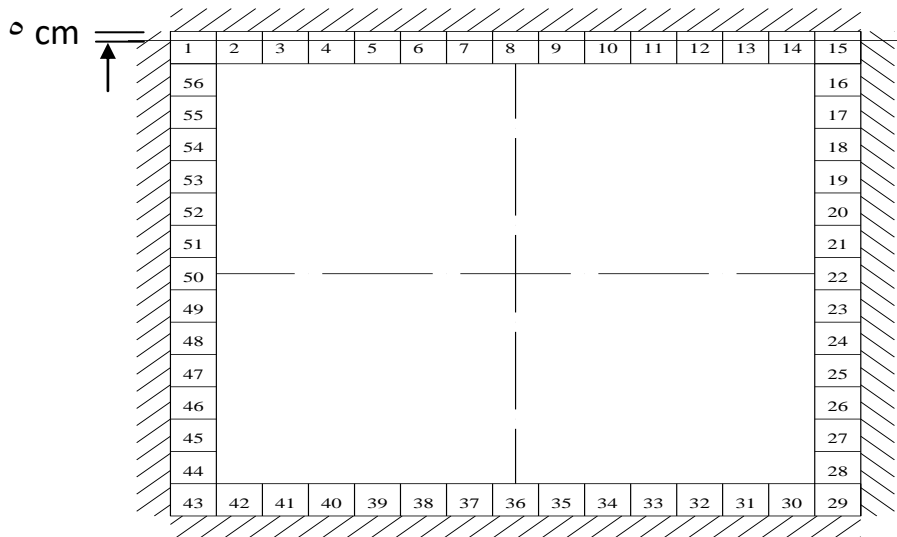


Figure (ξ-١٣): Shrinkage Strain Development of Four End Restrained SCC

Plate at 0 cm from the Restrained Edge

ξ-٧- Elastic Tensile Strain Capacity of Beams

Elastic tensile strain capacity of Self-Compacting Concrete was obtained directly by measuring the immediate movement after cracking of concrete on end restrained beams. The result is about ١٣٠ microstrain.

ξ-٨- Cracking of the Plates

The cracking characteristics of plates (two, three and four end restrained) are shown in Table (ξ-٩) at age of ٦٠ days.

Table (ξ-٩): Cracking Data of Plates

Plates	Number of crack	Maximum Lc (mm)	D-Wmax From edge (mm)	observed crack spacing at edge (mm)	Maximum crack width (mm)

					Min.	Max.	
Two end restrained	At free edge	۱۳	۵۵.	.	۱۵.	۸۸.	۱.۲۲
	At restraint edge	۹	۵۵.	۲۵.	۱۰.	۷۷.	۱.
Three end restrained	At free edge	۳	۵۰.	.	۵۴.	۹۹.	۰.۸۷۵
	At restraint edge	۱۳	۶۵.	۲۷۵	۱۶.	۹۷.	۱.۲۷
Four end restrained		۱۵	۷۰.	۳۰.	۸.	۱۲۴.	۱.۳۵

Lc: Length of crack.

D-Wmax: Distance of maximum crack width from edge

ξ-۹- Cracking Age and Sequence

The cracking age can be used as an index for the tendency to the cracking. Table (ξ-۵) shows the effect of restraint condition variations on the cracking age.

Table (ξ-۵): Cracking Age of Reinforced SCC Plates.

Types of restraint	Cracking age (days)
Two end restrained	۱-۲۸
Three end restrained	۱-۲۰
Four end restrained	۱-۲۵

From this table, it is obvious that all plates of various restraint conditions mentioned above are cracked early at the same period (in the first day after casting). These results deviated from the results obtained by Kadhum^(۸۳), which

concluded other trend in his study that the normal concrete slabs cracked at later ages (16, 18, and 21-days) for (four, three and two end restrained) respectively. This means that the cracking age of SCC is earlier compared with normal concrete. The reason for this behavior may be attributed to the roughness between SCC plate and the edge of restrained slab, and addition of pigment powder and SP.

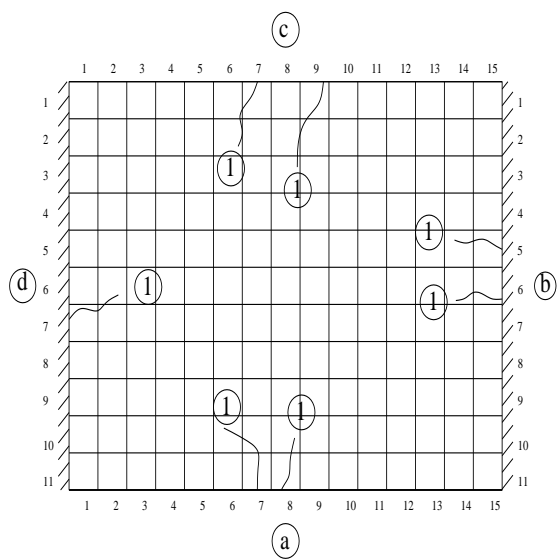
The schematic pattern of crack development when stress is relieved by creep is shown in Figure (2-9). Cracking could occur only when the stress induced by restrained shrinkage strain, reduced by creep, reaches the tensile strength of concrete. Figures (2-12 to 2-16) show the development of crack pattern of plates during 28-days period of observations.

At the restrained edge, the restraint is the highest at the middle third of the edge for two, three and four end restrained plates. This agrees with other researchers^(1,17,18). So, the early first crack occurs at this position for each edge assuming that concrete is homogeneous and other characteristics are the same. This behavior is due to the effect of base restraint (the roughness or interaction between edge of plate surround slab and the edge of restrained slab) on two end restrained plate at restrained edge, and effect of base and end restraints on three and four end restrained at restrained edge. While, at free edge in two end restrained plate the first crack generally occurs at the weakest section of the plate as indicated in Figure (2-12) [a and c edges] due to the effect of end restraint, when the stresses induced due to restrained shrinkage exceeding that provided by the concrete section. This section is either weaker in tension than the rest of the plate or under a higher restraint which tends to increase the cracking force imposed section. This is compatible with the study carried out by Kadhum⁽¹⁷⁾.

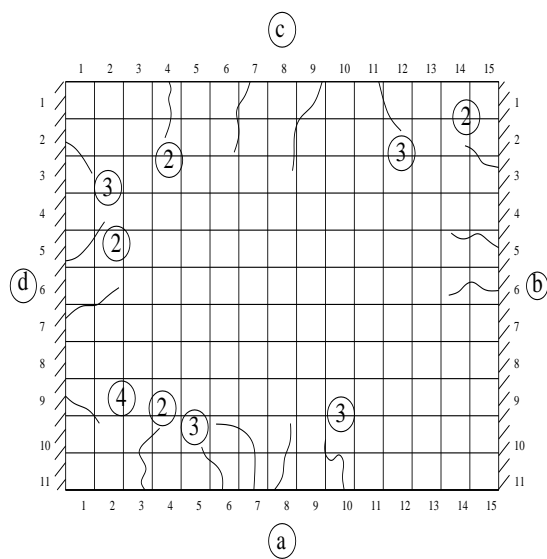
It is known that the degree of base restraint is the highest at the end of the plate and decreases towards the centerline. This agrees with other

researchers^{(^),(^y)}. Thus, cracks should initiate at the end of plates and propagate at different lengths and directions.

After the formation of early first crack in each edge of plates, the formation of further cracks became rather difficult. This is because the tensile strength of concrete plates increases with increasing age and the remaining amount of restrained volume change decreases with age. This is compatible with the study carried out by Mashhedi^(^y). The position of further cracks depends on the new arrangement of degree of restraint along the plate.



Panel No.:(Panel length = 200 mm)
drying period (1-day)



Panel No.:(Panel length = 200 mm)
drying period (5-days)

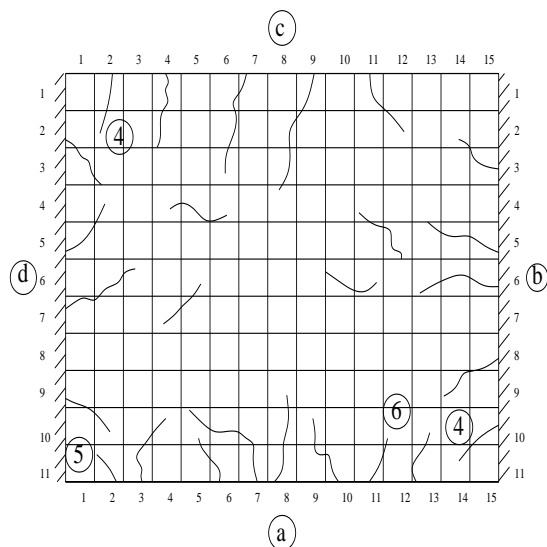
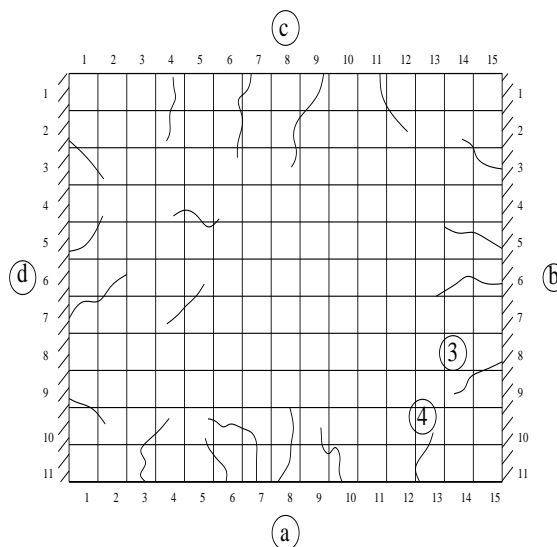


Figure (٤-١٤): Crack Formation Sequence in Two End Restrained SCC Plate.

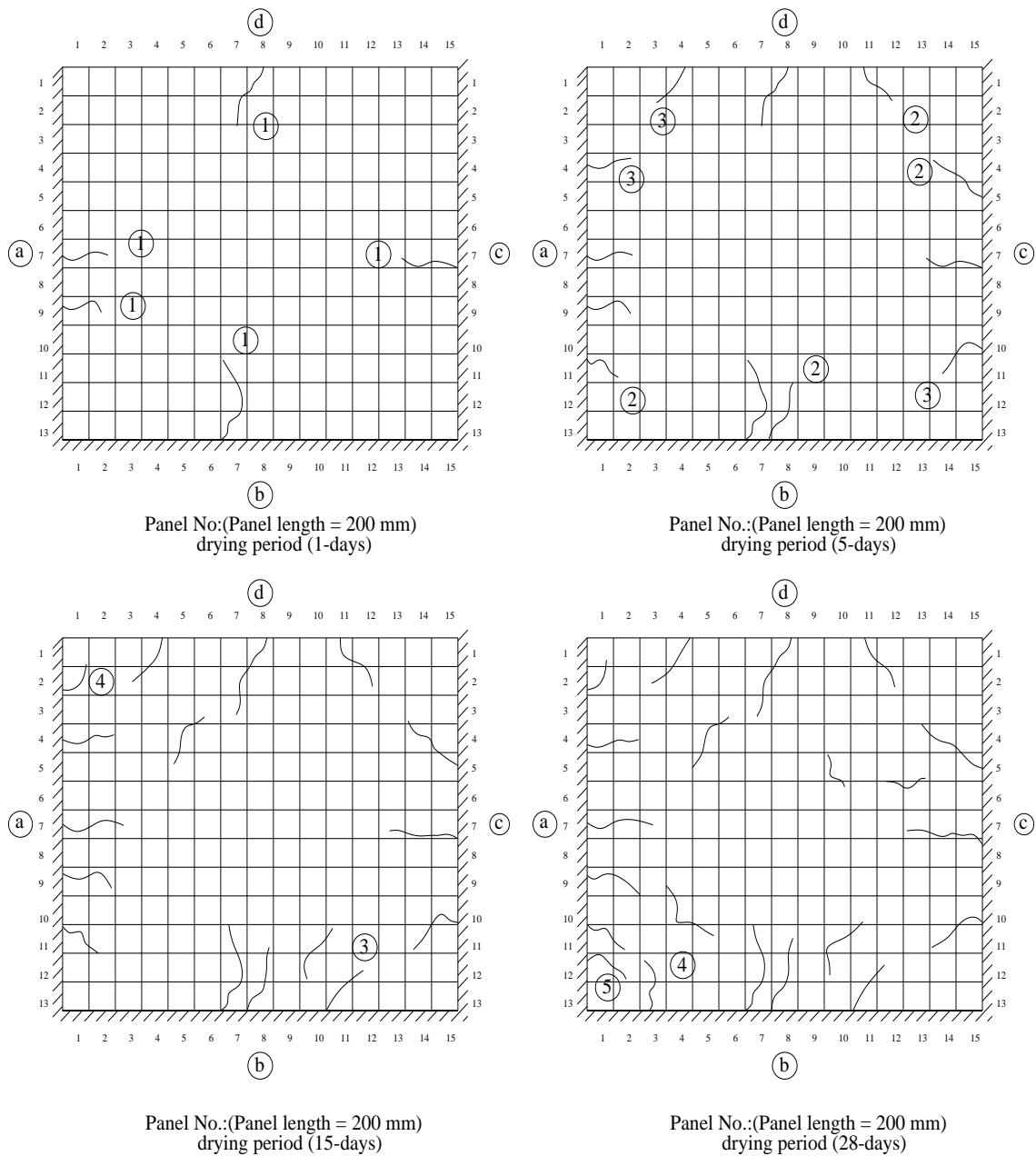


Figure (4-10): Crack Formation Sequence in Three End Restrained SCC Plate.

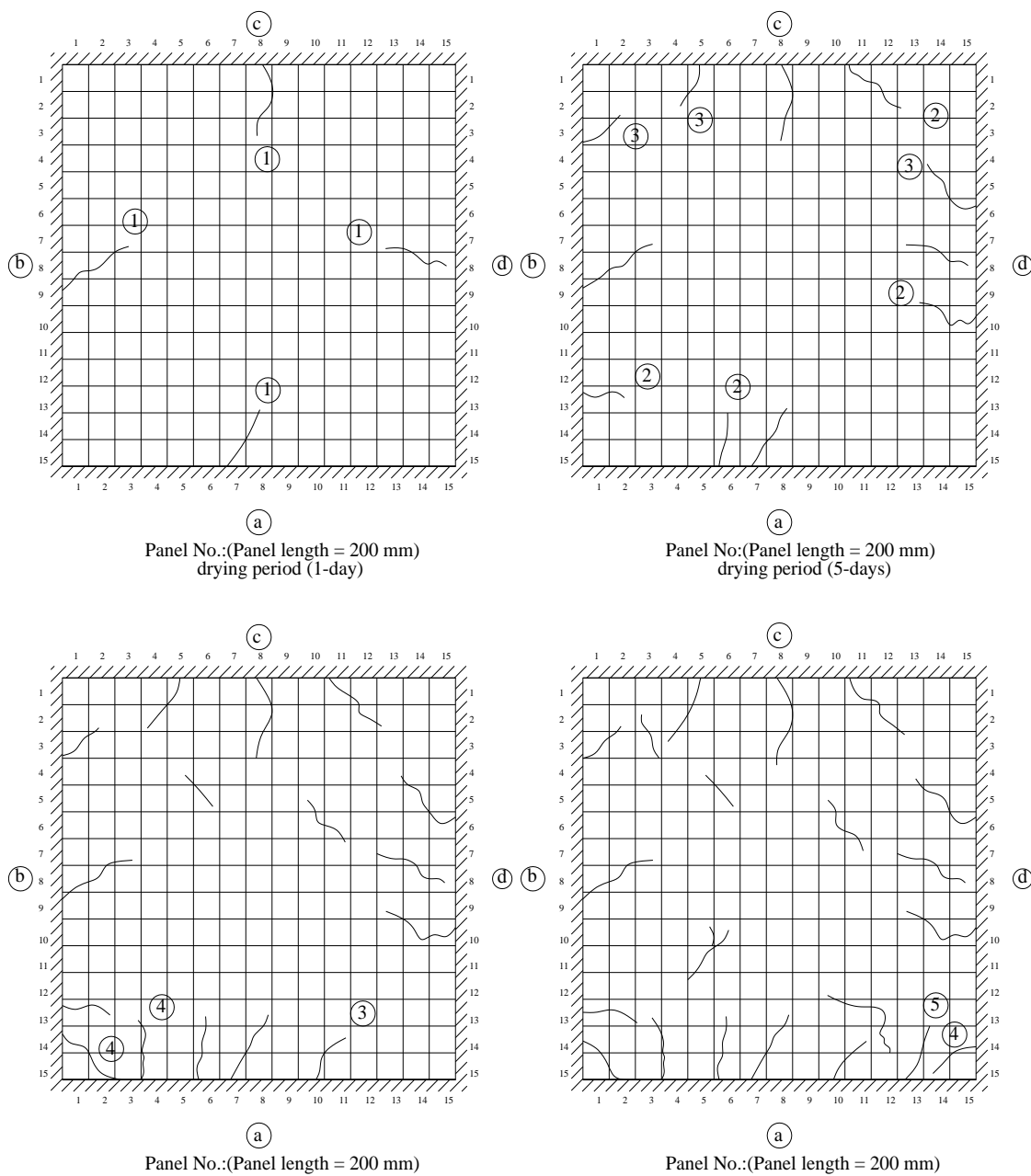


Figure (4-16): Crack Formation Sequence in Four End Restrained SCC Plate.

Indicating to the same figures it can be observed also that the cracks at and near the centerline of plate propagated towards the point of intersection of centerlines of these plates. Whereas, the cracks near edge of plates extended in a direction inclined to the other restrained edge (at the corner) with degree about (45°) for two end restrained edge, (60°) for three end restrained and (90°) for four end restrained.

4-17 - Crack Spacing

In Table (4-4) the observed minimum and maximum crack spacing are summarized. The minimum and maximum crack spacing was based on the observation of crack locations.

Figures (4-17 to 4-19) show the final cracks pattern in the experimentally investigated plates.

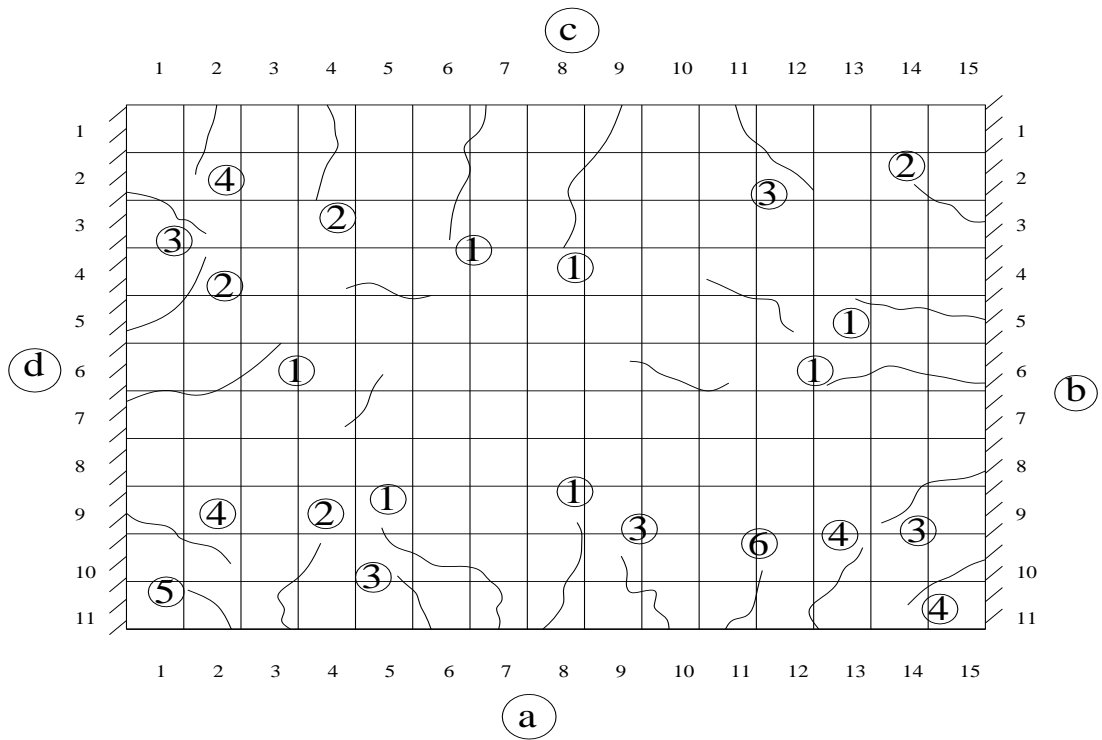


Figure (4-17): Final Cracks Pattern in Two End Restrained of Reinforced

SCC Plate.

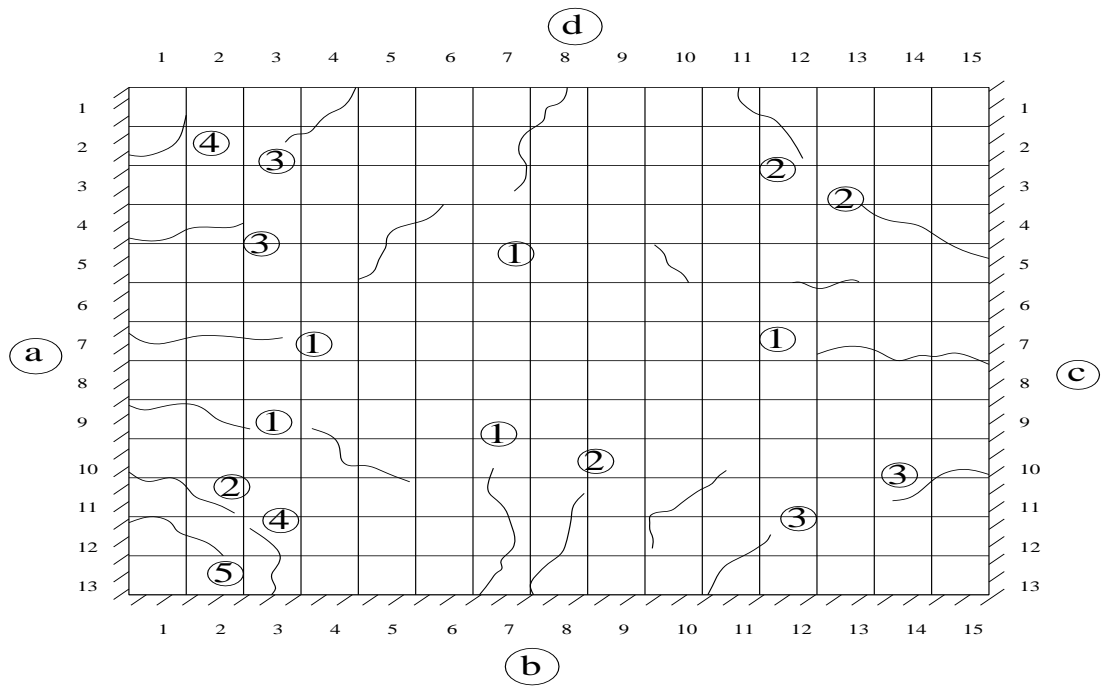


Figure (4-18): Final Cracks Pattern in Three End Restrained of Reinforced

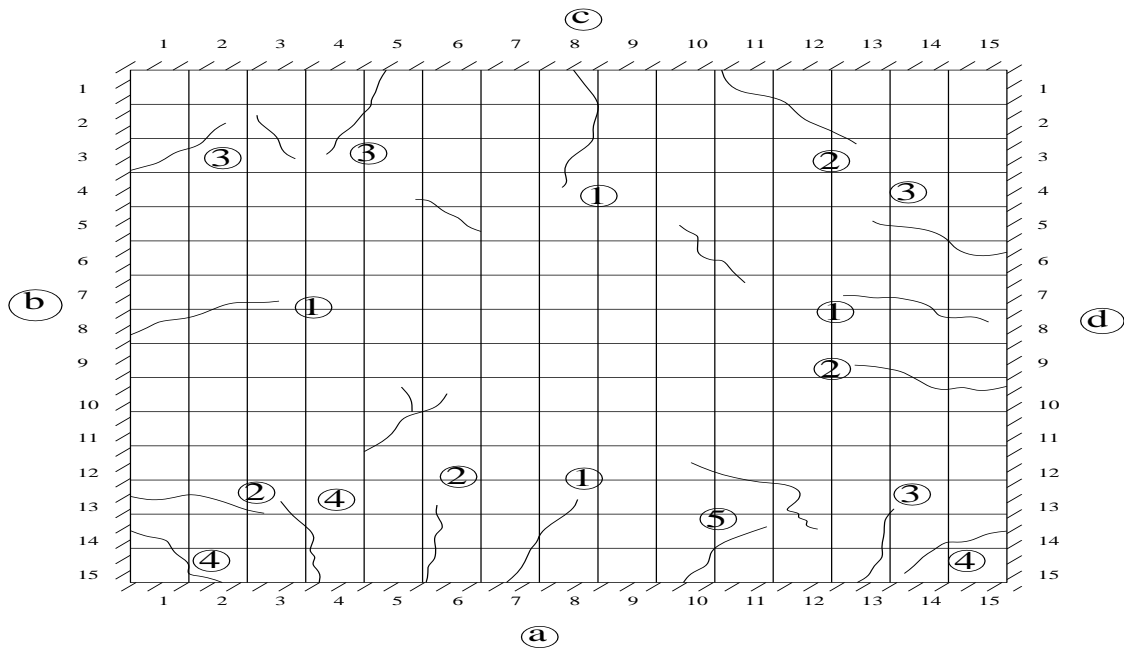


Figure (ξ-19): Final Cracks Pattern in Four End Restrained of Reinforced

From these figures, it appears that the cracks were generally more numerous in the proximity of the edge than at some distance from it. It can be stated that the maximum crack spacing in the plates increases with increasing distance from the edge. The maximum crack spacing was measured experimentally and , it was (770 mm, 970 mm and 1240 mm) for two, three and four end restrained respectively as shown in Table (ξ-ξ) and Figures (ξ-17 to ξ-19).

It is observed also, that the observed crack spacing was affected by the varying restrained conditions investigated, which they play an active part in the distribution of cracks.

Al-Rawi⁽¹⁹⁾ presented the following equation, for the prediction of minimum crack spacing, S_{min} , in the members subjected to end restraint:

$$S_{\min} = 0.85 * K * \left(\frac{d}{\rho}\right) \quad \dots\dots \quad (\xi-2)$$

In the present work the equations used for two, three and four restrained plates which subjected to the base restraint (the roughness or interaction between edge of plate surround slab and the edge of slab restraint) and end restraint were concluded from equations suggested by Al-Rawi⁽¹⁴⁾ and Kadhum⁽¹⁷⁾.

For two and three end restrained plates at free edge the equation used was based on equation by Kadhum⁽¹⁷⁾:

$$S_{\min} = 0.85 * K * \frac{d}{(\rho + \rho_R)} \quad \dots\dots \quad (\xi-3)$$

$$\rho_R = 0.9 - a * \left(\frac{l}{L}\right)^b \quad \dots\dots \quad (\xi-4)$$

a, b: constant were estimated by STATISTICA program version 9.0 from experimental data with coefficient of correlation $R = 0.99$, as follows:

$$a = 1.8, b = 0.8$$

$$\rho_R = 0.9 - 1.8 * \left(\frac{l}{L}\right)^{0.8} \quad \dots\dots \quad (\xi-4)$$

S_{\min} : minimum crack spacing (mm).

S_{\max} : maximum crack spacing (mm).

$$S_{\max} = 2 * S_{\min} \quad \dots\dots \quad (\xi-5)$$

K: constant depending on the type of reinforcement. It can be taken as

0.8 for indented deformed bars and 0.75 for ribbed deformed bars.

d: bar diameter (mm).

ρ : reinforcement steel ratio (%).

ρ_R : effect of end restraint as a ratio.

l: distance from the edge to the position of calculated crack width (mm).

L: plate length (mm).

From the above equation it can be noticed that the effect of end restraint can be expressed in terms (ρ_R). Thus, in reinforced restrained plates, the total steel ratio is equal to the summation of actual steel ratio (ρ) and the calculated ratio (ρ_R).

The equations which can be used for calculating the minimum crack spacing for cracks which appear at restrained edge for three and four end restrained reinforced SCC plate can be written as follows:

For three end restrained at restrained edge the equation used was based on equation by Kadhum⁽¹⁷⁾:

$$S_{min} = 0.85 * K * \frac{d}{(\rho + K_{R1})} \quad \dots\dots \quad (\xi-6)$$

$$K_{R1} = 1 - a * \left(\frac{l}{L}\right)^b \quad \dots\dots \quad (\xi-7)$$

a, b: constant were estimated by STATISTICA program version 9.0 from experimental data with coefficient of correlation R = 0.99, as follows:

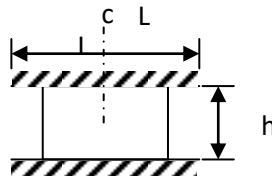
$$a = 2.1, b = 0.9$$

$$K_{R1} = 1 - 2.0 * \left(\frac{l}{L}\right)^{0.9} \quad \dots\dots \quad (\xi-\gamma)$$

For four end restrained the equation used was based on equation by Kadhum^(^*):

$$S_{min} = 0.85 * K * \frac{d}{(\rho + 0.8 * K_R)} \quad \dots\dots \quad (\xi-\lambda)$$

: is taken from Figure (ξ-γ). K_R



Two end restrained plate.

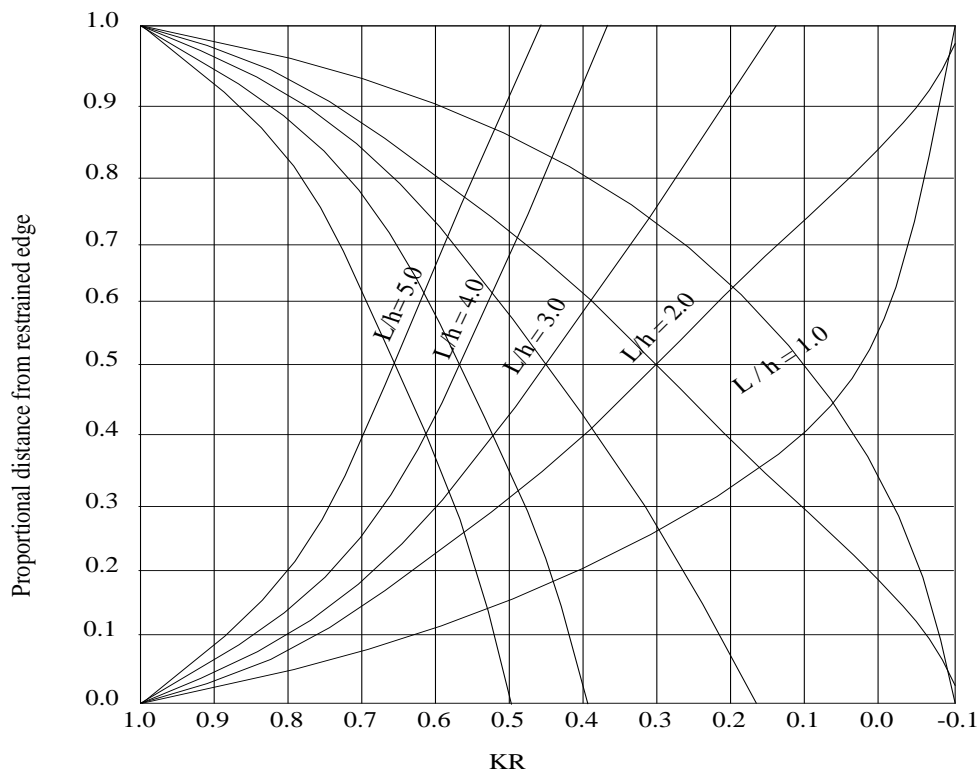


Figure (4-20): Degree of Tensile Restraint at Center Section⁽⁴³⁾.

Based on the information in Figure (3-10) of ACI Committee 209⁽⁴¹⁾ which was used to find the degree of restraint at center section of base restrained walls, a relationship demonstrated in Figure (4-20) is used, adopted and modified by Kadhum⁽⁴³⁾. This relation could be used to estimate the degree of restraint at center section of restrained plates.

4-11 - Crack Length

From Table (4-4), it can be seen that the maximum crack width increases with increasing maximum crack length as can be seen in Figure (4-21) and expressed by the expression below:

For two, three and four end restraint

$$W_{max} = a \times L_{max} - b \quad \dots\dots \quad (4-9)$$

a, b : constant were estimated by STATISTICA program version 9.0 from experimental data with coefficient of correlation $R = 0.99$, as follows:

$$a = 0.02, b = -0.021$$

W_{max} : maximum width of crack (mm).

L_{max} : maximum length of crack (cm)

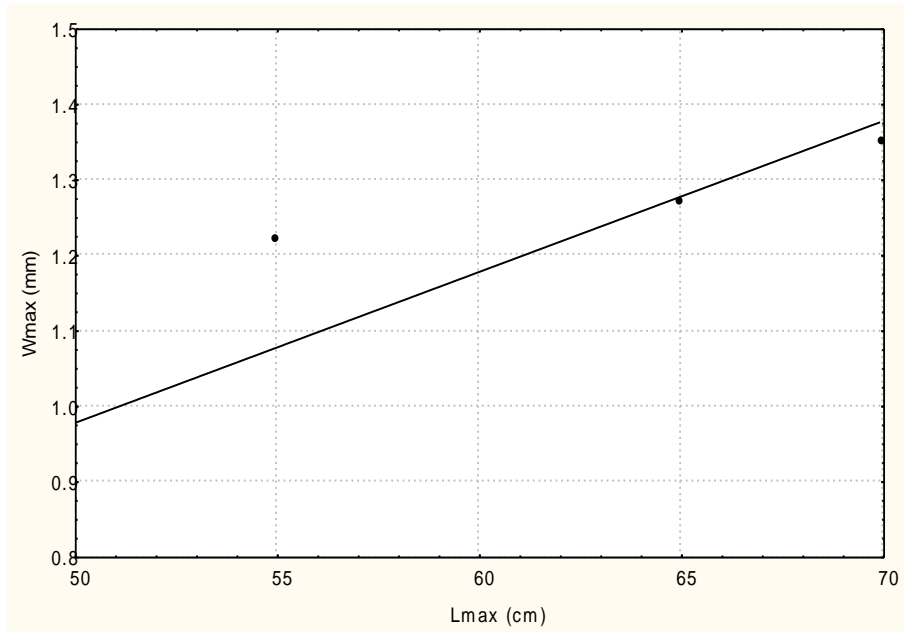


Figure (4-21): Relation Between the Maximum Crack Width and Maximum Crack Length for Plates

From figure above, it is obvious that if the prediction of maximum crack length is satisfactory, an assumption of maximum crack width can be made. Hence, the reduction of the width of cracks which is developed in reinforced concrete plates is associated with the reduction in maximum crack length.

The position of maximum crack width from free and restrained edge plates was denoted as (D-Wmax). It was observed that D-Wmax for each crack at restrained edge was related to its maximum crack length (Lmax) as shown in Figure (4-22). At restrained edge, the equation used to calculate D-Wmax for

two, three and four end restraint is shown below:

$$D-W_{max} = a \times L_{max} - b \quad \dots\dots\dots (4-10)$$

a, b : constant were estimated by STATISTICA program version 9.0 from experimental data with coefficient of correlation $R = 0.99$, as follows:

$$a = 0.0075, b = -0.631$$

D-Wmax: Distance of maximum crack width from edge

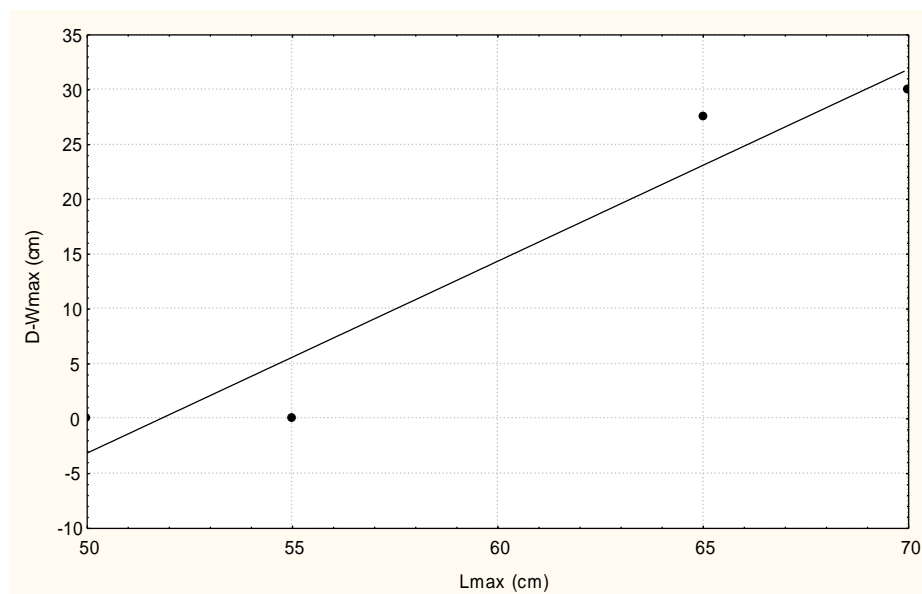


Figure (4-22): Position of Maximum Crack Width From the Restrained Edge Versus Crack Length for the Different Restrained Condition

This behavior is due to the effect of end restraint and base restraint (the roughness or interaction between edge of plate surround slab and the edge of slab restraint) for three and four end restrained plates and effect of base restraint for two end restrained.

At free edge the D-Wmax was equal to zero for two and three end restrained due to the effect of end restrained only.

For two end restrained the D-Wmax at free edges (a edge = 0 and c edge = 0 cm) while, D-Wmax at restrained edges (b edge = 20 and d edge = 20 cm), for three end restrained the D-Wmax at free edge (d edge = 0 cm) while, D-Wmax at restrained edges (a edge = 20, b edge = 27.0 and c edge = 20 cm), and for four

end restrained the D-Wmax for (a edge = 20, b edge = 20, c edge = 30, and d edge = 20 cm).

ξ-12- Crack Location

From cracking Figures (ξ-14 to ξ-16), it can be seen that early cracks of plates initiated mainly within the middle third of the edges rather than at its end. End portions of plate edges showed that the strain values are higher than the middle third of edges. This means that the restrained shrinkage strain is higher at the middle third of edges of the plate than at its end. This leads to suggest that stress concentration in these regions is higher.

Al-Rawi^(A4) attributed this behavior to the generation of a strain gradient at the end parts which increases the loss of restraint and reduces the possibility of cracking. While at middle third of edges, higher restraint would be developed due to the build up of friction forces and the absence of strain gradient, hence, cracks would be expected to appear at the interior zones and away from the ends. This behavior of SCC plates is in the same with normal concreter slabs studied by Kadhum^(A3).

ξ-13- Crack Width

Crack widths were measured at regular distances (every 20 mm from edge to the center of plate) by using portable micrometer- microscope with an accuracy of (20 micron).

Figure (ξ-23) shows the development of the maximum crack width with different ages for the plates investigated. These cracks widened progressively until a certain nearly constant width which occurred in about 70 days. The first

crack in each plate was observed at the age which is indicated by the first point in the corresponding curve.

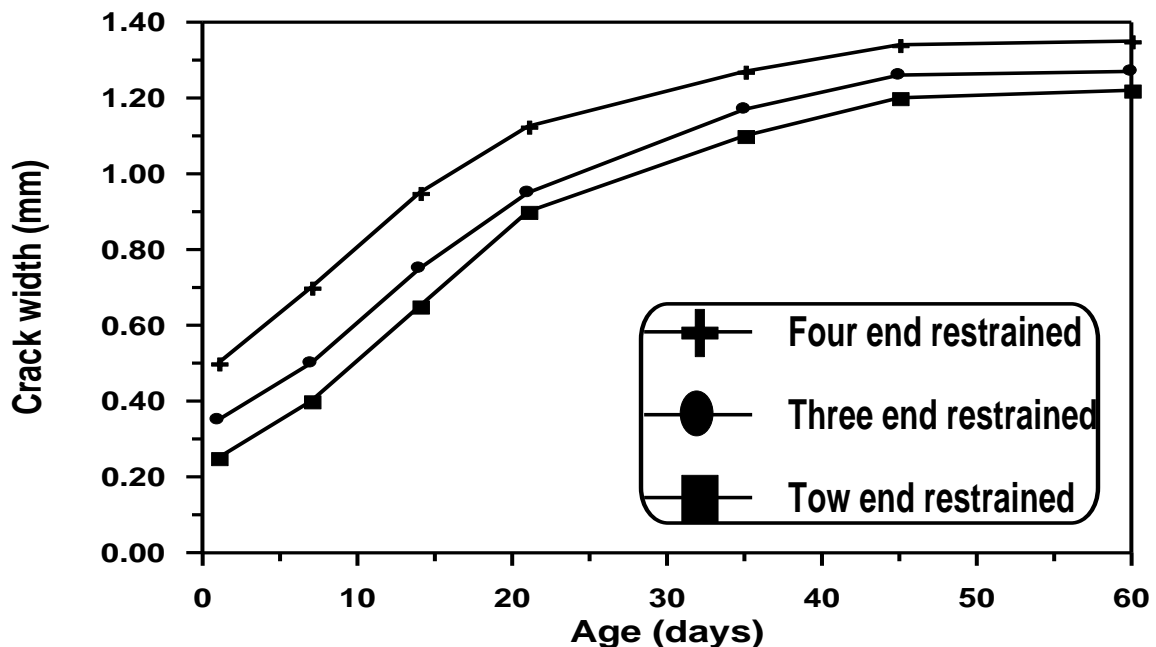
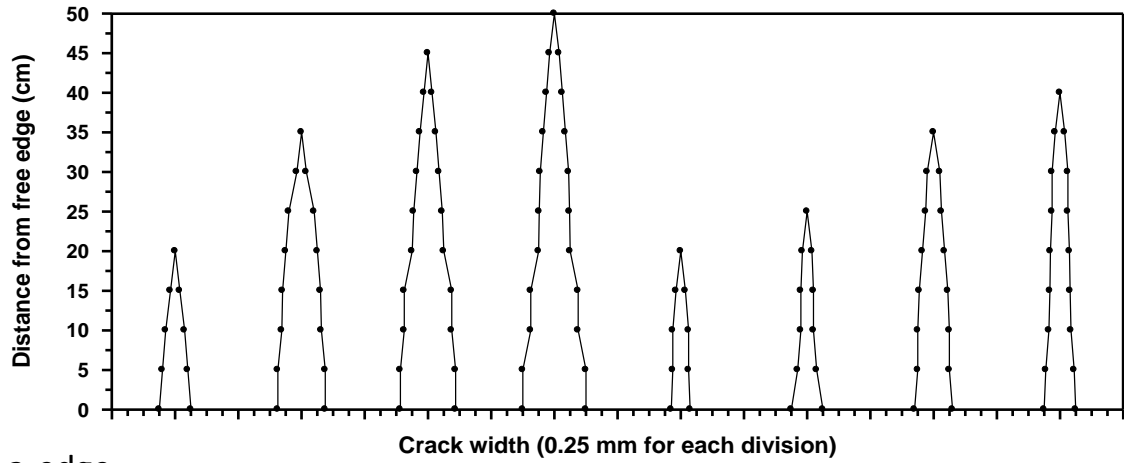


Figure (4-23): Development of Maximum Crack Width With Age of

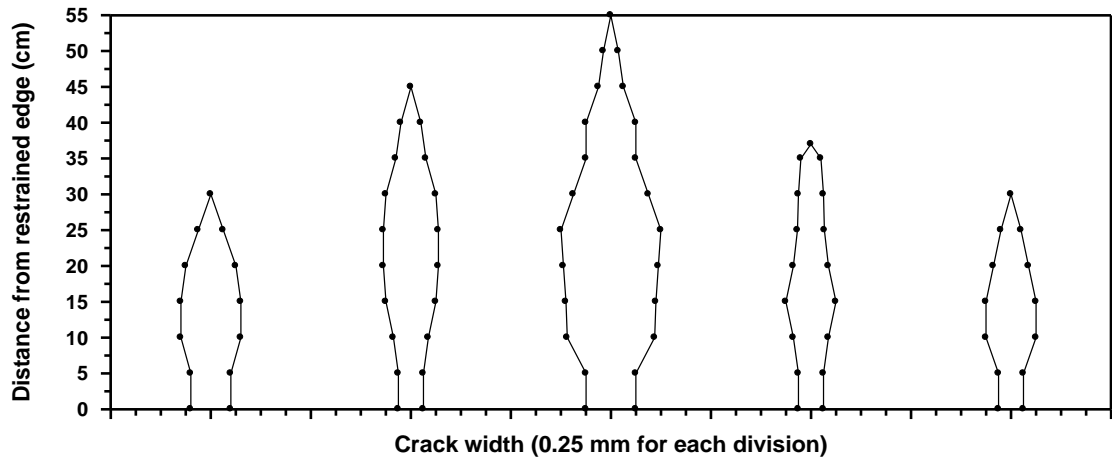
Reinforced SCC Plates for Different Restrained Cases

It can be observed that the occurrence of earlier cracking age of plates may be attributed to the use of the fine powder (pigment) and also to the roughness of the edges of slabs (interaction between the slabs and the edge of plates). Results indicate that the maximum crack width in each plate was that of the earliest crack. The cracks which have been observed for the crack width measurement were plotted in Figures (4-24 to 4-26).



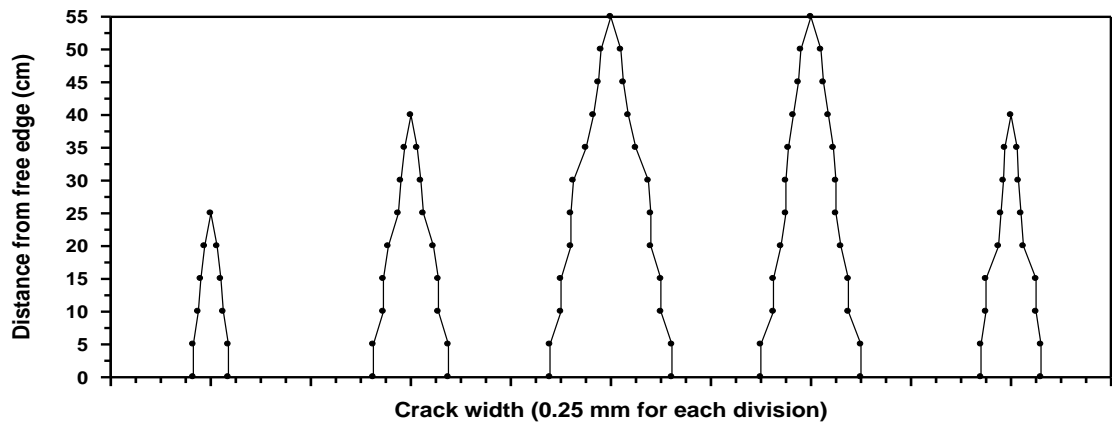
a-edge

6 4 1 3 3 1 2 5



b-edge

1 1 3 4 2



c-edge

1 1 2 4

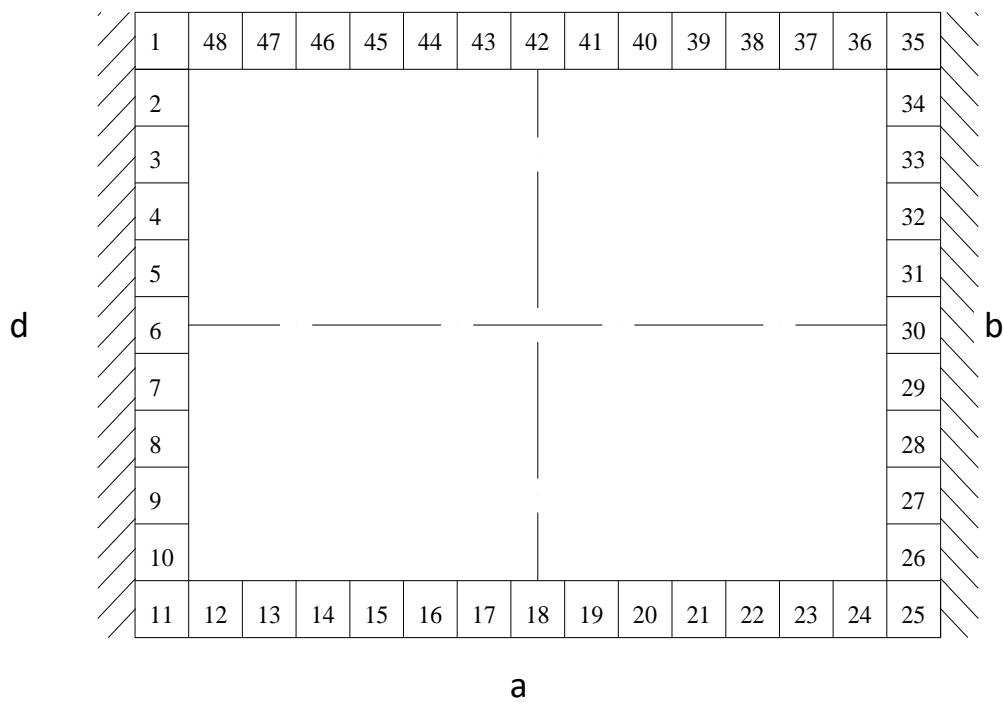
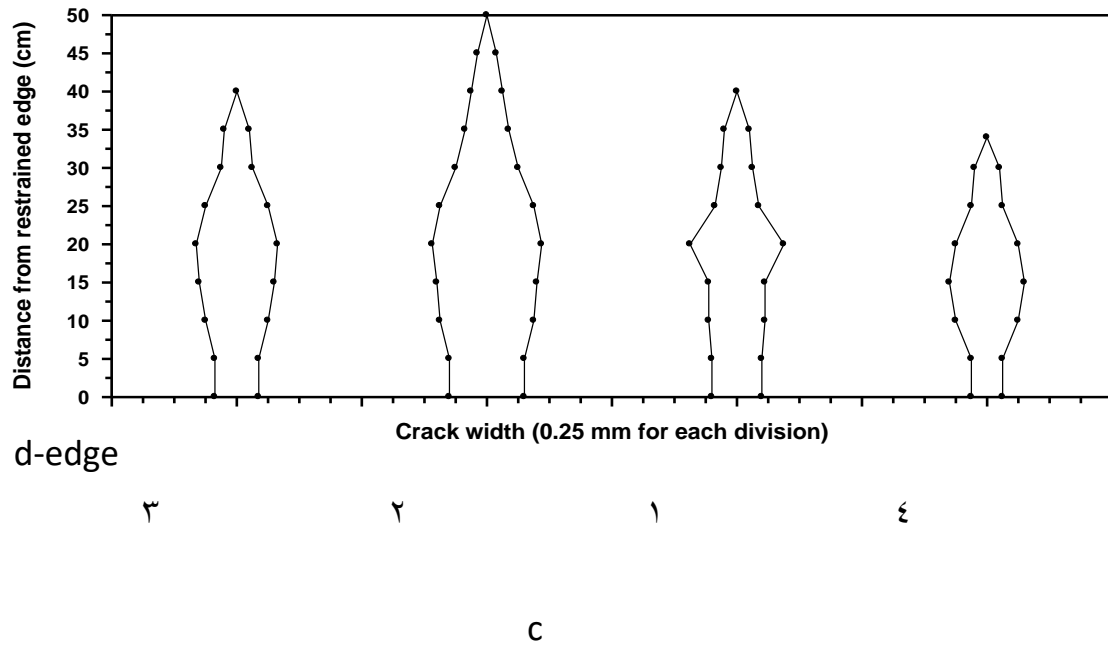
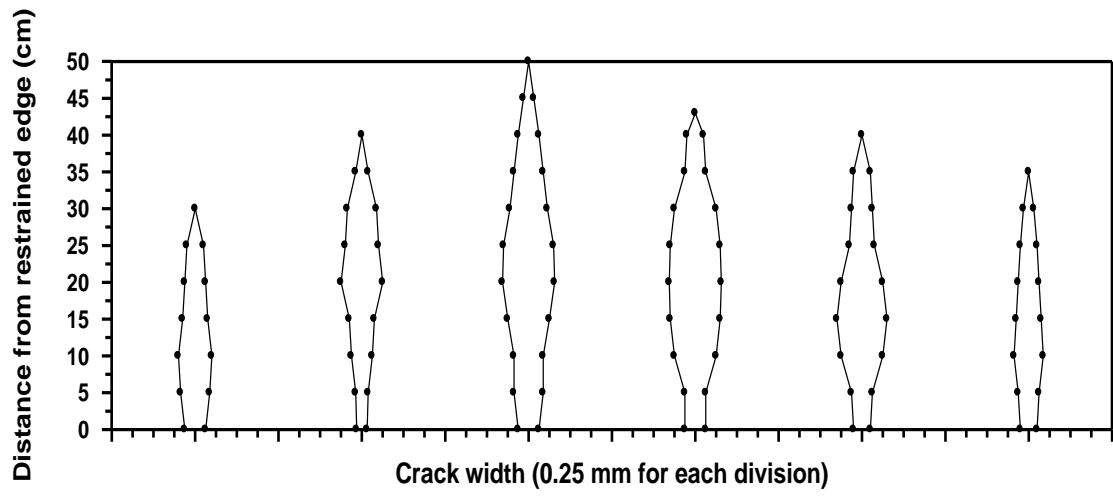


Figure (4-24): Variation of Final Crack Width With Distance for Two End

Restrained SCC Plate.

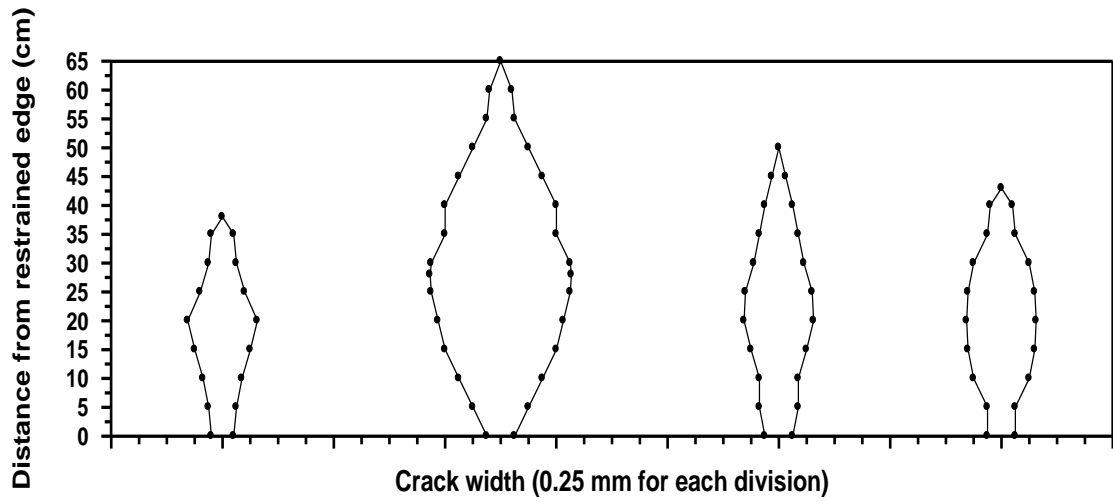
Note:

1, 2, 3, 4, 5, 6: number of cracks according to the formation of them as shown in Figure (ε-17, ε-18 and ε-19).



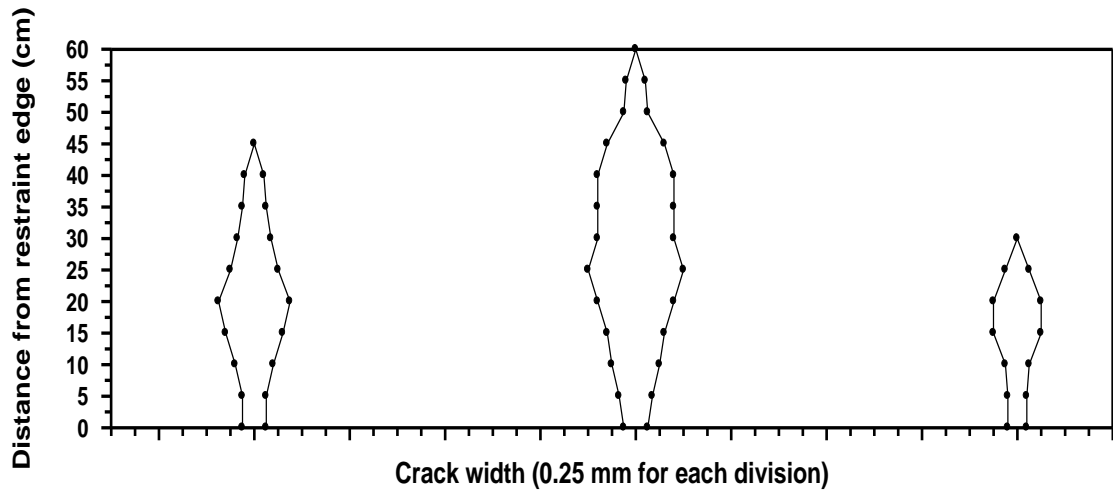
a-edge

2 1 3 1 4



b-edge

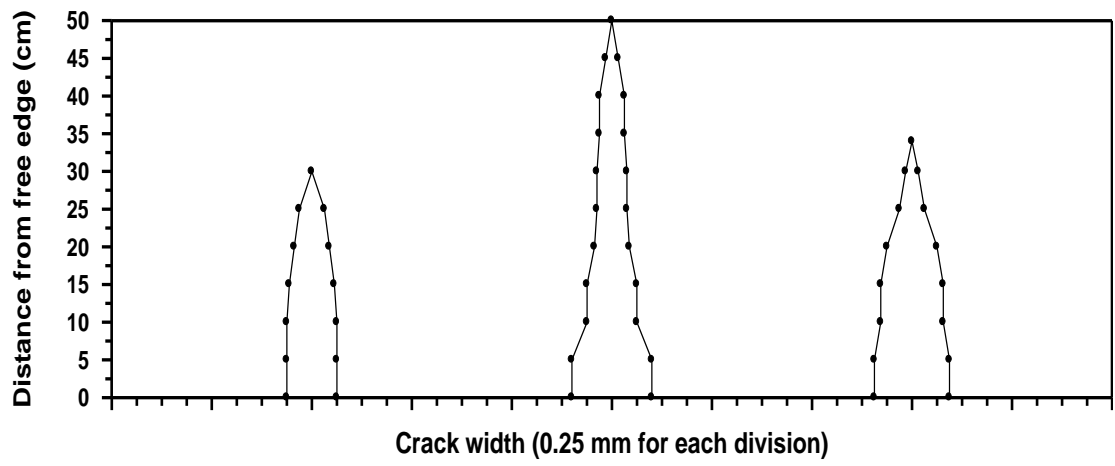
2 3 4 1



c-edge

1

2



d-edge

2

1

3

d

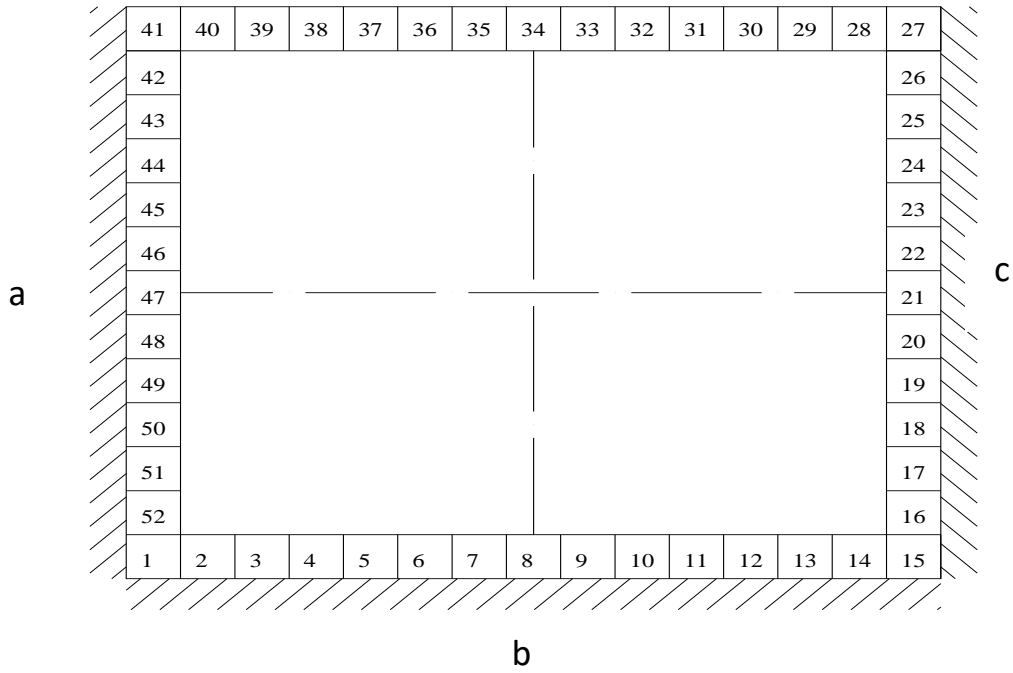
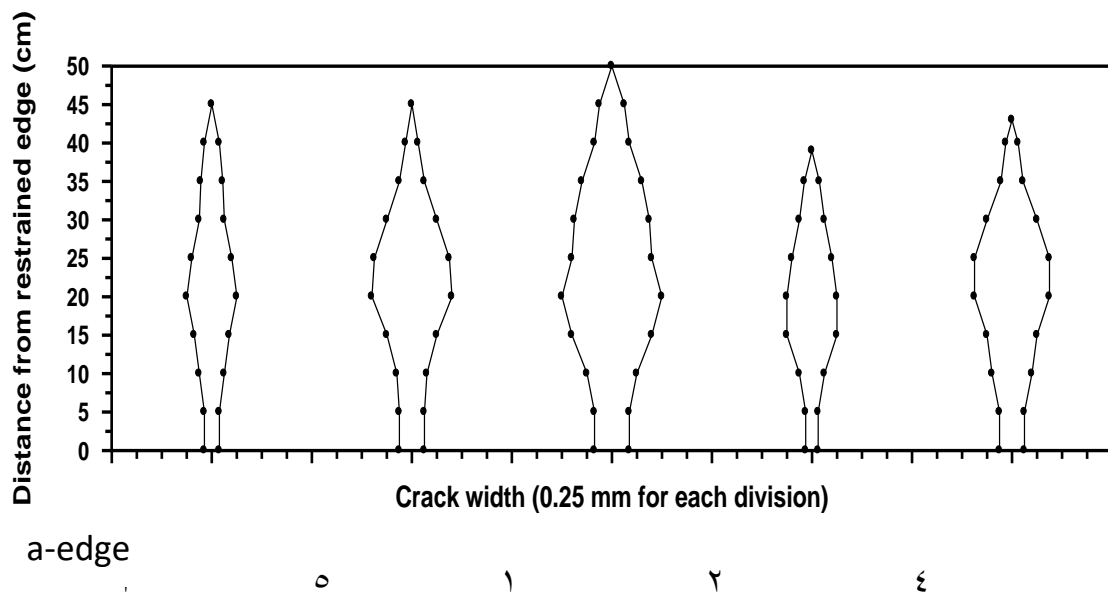
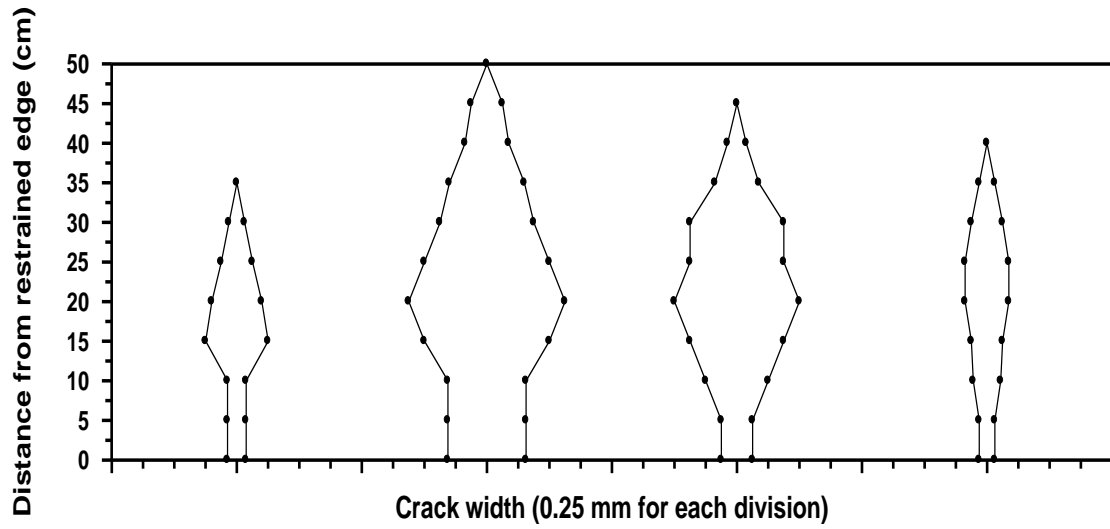


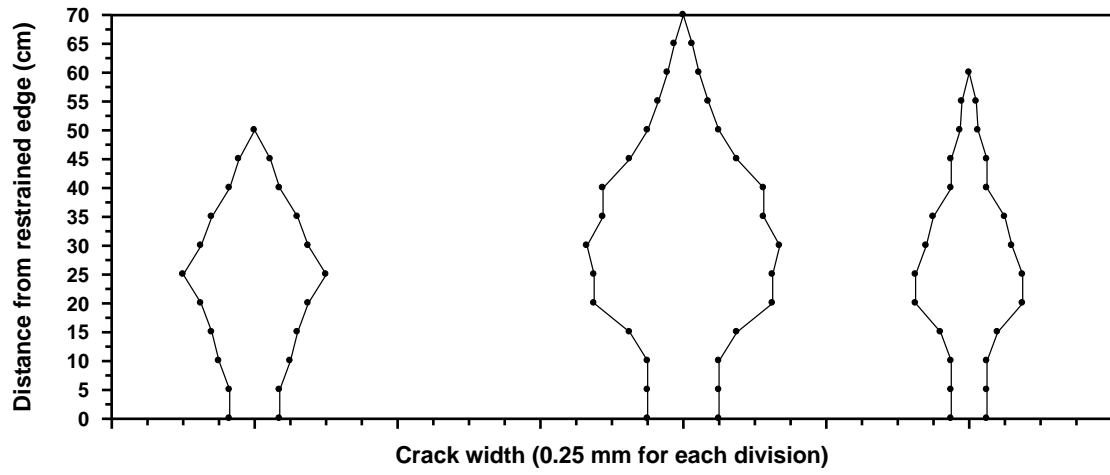
Figure (٤-٢٥): Variation of Final Crack Width With Distance for Three End

Restrained SCC Plate.

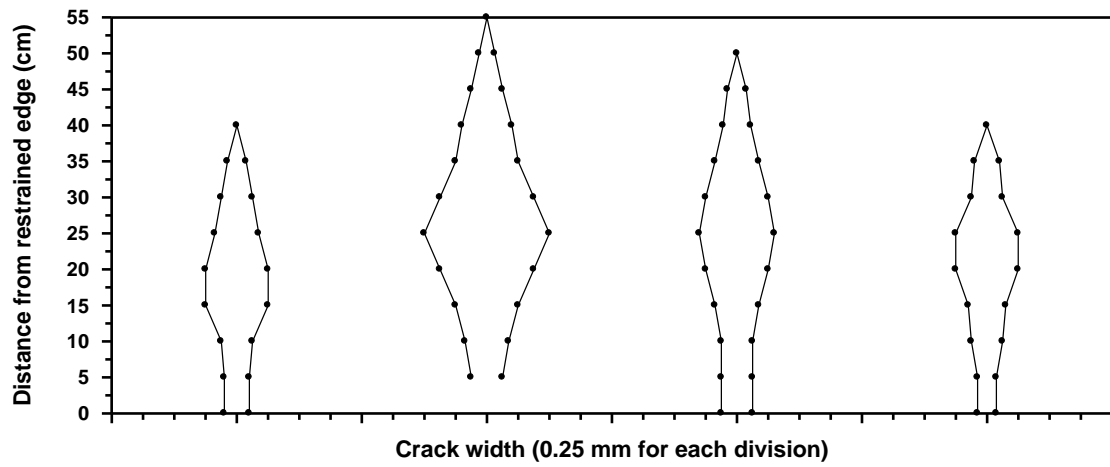




b-edge



c-edge



d-edge

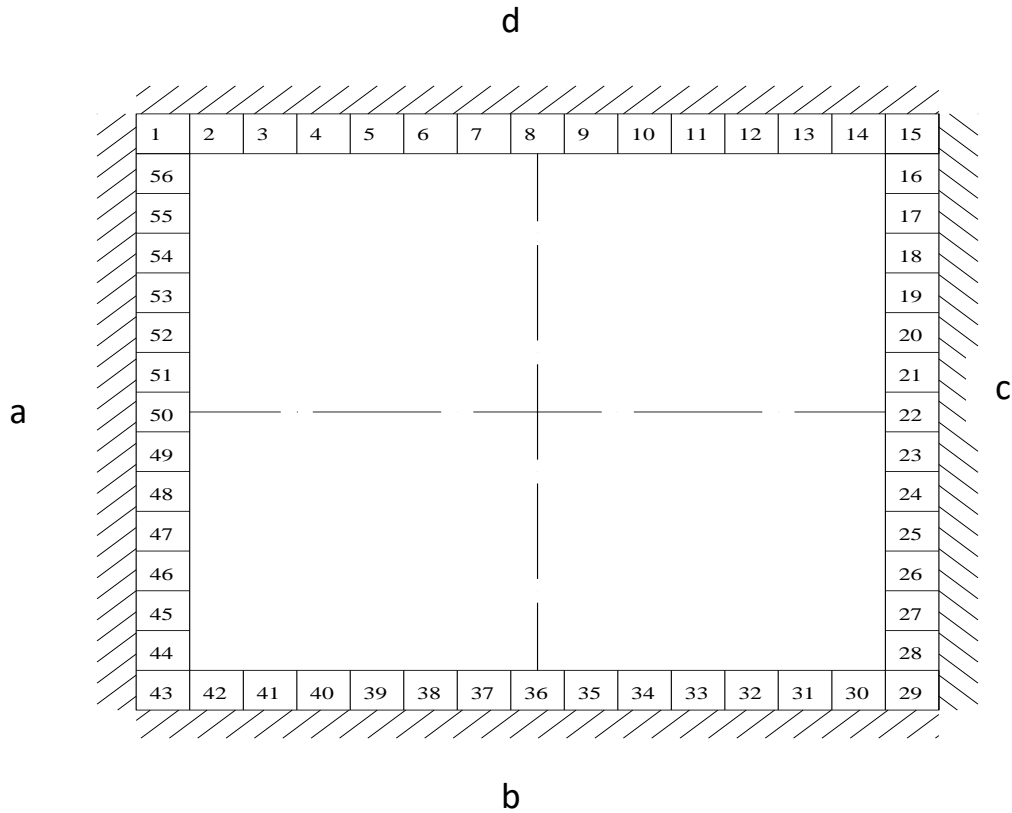


Figure (4-26): Variation of Final Crack Width With Distance for Four End

Restrained SCC Plate.

From these figures it is seen that the crack width initiated at a certain value at the restrained edge (\cdot cm) and, then, increased towards the center of the plate up to a certain level (γ° cm at b-edge and γ^{\cdot} cm at d-edge) for two end restrained, (γ^{\cdot} cm at a-edge, $\gamma^{\gamma^{\circ}}$ cm at b-edge and γ° cm at c-edge) for three end restrained and (γ^{\cdot} cm at a-edge, γ^{\cdot} cm at b-edge, γ^{\cdot} cm at c-edge and γ° cm at d-edge) for four end restrained, beyond which it decreased to zero at the top of the crack.

At the free edge, the crack width was the maximum at (\cdot cm) for two end restrained at (a-edge and c-edge) and for three end restrained at (d-edge), and

gradually decreases towards the center of the plate, and diminishes at the end of crack. The same trend was also observed in walls by Al-Mashhed⁽¹⁷⁾ and for slabs by Kadhum⁽¹⁸⁾.

The equation used to calculate crack width developed by Kadhum⁽¹⁸⁾ was adopted by considering the strain distribution in Figure (2-11) and using non-linear estimation analysis. The equation used to calculate crack width for two and three end restrained for cracks which appear at the free edge at any level of the plate, is as follows:

For two and three end restrained at free edge the equation used was based on equation by Kadhum⁽¹⁸⁾:

$$Wc_{max} = S \max \left[e_{shn} - C_f - \frac{e_{ult}}{2} \right] \quad (2-11)$$

$$C_f = K * e_{shn} \quad (2-12)$$

The equation can be adopted and modified as follows:

$$Wc_{max} = S \max \left[a * e_{shn} (1 - K) - b * \frac{e_{ult}}{2} \right] \quad (2-13)$$

a, b : constants (estimated statistically)

For two end restrained:

$$a = 29.12, b = 98.71$$

Coefficient of correlation (R=0.99).

For three end restrained:

$$a = 33.68, b = 124.01$$

Coefficient of correlation (R=0.98).

The notations of the model referred to are as follows:

- S_{max} : maximum crack spacing, (mm).
- e_{shn} : net shrinkage stain, ($e_{shn} = e_{sh} - L.O.R$).

- e_{sh} : shrinkage strain plus strain due to decrease in temperature.
- L.O.R : loss of restraint due to ends contraction before cracking.
- e_{ult} : elastic tensile strain capacity.
- C_f : final creep strain.

It was assumed that the value of the final creep strain of the SCC to be constant (K) of the net shrinkage strain where K equals to 0.7 and 0.70 for reinforced and plain concrete walls respectively^(AV).

The equation which is used to calculated crack width for three and four end restrained plates for cracks which appear at the restrained edge at any level of the plate by considering the strain distribution as shown in the Figure (2-11) can be written as follows:

For three and four end restrained at the restrained edge the equation used was based on equation by Kadhum^(AV):

$$Wc \max = S \max \left[e_{sh}(Rb - 0.8Ra) - C_f - \frac{e_{ult}}{2} \right] \dots\dots\dots (2-14)$$

$$C_f = K * e_{shn} \dots\dots\dots (2-15)$$

The equation can be adopted and modified as follows:

$$Wc \max = S \max \left[a * e_{shn}((Rb - 0.8Ra) - K) - b * \frac{e_{ult}}{2} \right] \dots\dots\dots (2-16)$$

a, b = constants (estimated statistically)

For three end restrained:

$$a = 73.32, b = 40.09$$

Coefficient of correlation (R=0.99)

For four end restrained:

$$a = 77.12, b = 40.03$$

Coefficient of correlation (R=0.99)

The notations of the model referred to are as follows:

S_{max} : Maximum calculated crack spacing, (mm)

R_b : Degree of restraint before cracking (at plate center)

For three end restrained:

$$R_b = 1 - 2.0 * \left(\frac{l}{L}\right)^{0.9}$$

For four end restrained:

R_b = from Figure (ε-۲۶).

R_a : Degree of restraint after cracking,

$$R_a = 1 - \frac{e_{sr}}{e_{sf}}$$

e_{sr} : restrained strain in the plate.

e_{sf} : free strain in the plate after cracking, ($e_{sf} = e_{shn} (1 - R_b)$).

Using the previous Equations (ε-۱۳ and ε-۱۵), with the experimentally measured values for e_{sh} , e_{ult} and L.O.R, the crack width for experimental plates at three different levels are calculated.

Tables (ε-۶ to ε-۹) summarize the required parameters to calculate maximum crack widths by using Equation (ε-۱۳) for two end and three end restrained at the free edge and by using Equation (ε-۱۵) for three end and four end restrained at the restrained edge.

The maximum crack widths calculated (W_c) at the three levels using Equations (ε-۱۳ and ε-۱۵) are summarized in the mentioned tables together with the maximum crack widths that are measured experimentally (W_o) at ۶۰-days.

Table (ε-۶): Maximum Crack Width Calculations for Two End Restrained

Plate at Free Edge Equ. (ε-۱۳).

Level (cm)	S_{max} (mm)	e_{sh} (*۱۰ ^{-۶})	L.O.R. (*۱۰ ^{-۶})	e_{shn} . (*۱۰ ^{-۶})	K	e_{ult} (*۱۰ ^{-۶})	W_c (mm)	W_o (mm)
۵	۸۲۰	۷۵۰	۷۰	۶۸۰	۰.۶	۱۳۰	۱.۲۳۴	۱.۲۲۰
۱۵	۸۸۰	۷۱۵	۷۰	۶۴۵	۰.۶	۱۳۰	۰.۹۶۵	۱.۰۰۰
۲۵	۹۵۰	۶۹۵	۷۰	۶۲۵	۰.۶	۱۳۰	۰.۸۲۱	۰.۸۰۰

Table (ε-۷): Maximum Crack Width Calculations for Three End

Restrained Plate at Free Edge Equ. (ε-13).

Level (cm)	S _{max} (mm)	e _{sh} (*10 ⁻¹)	L.O.R. (*10 ⁻¹)	e _{shn} (*10 ⁻¹)	K	e _{ult} (*10 ⁻¹)	W _c (mm)	W _o (mm)
0	82.	70.	7.	78.	0.7	13.	0.902	0.870
10	88.	710	7.	740	0.7	13.	0.003	0.720
20	90.	790	7.	720	0.7	13.	0.340	0.300

Table (ε-8): Maximum Crack Width Calculations for Three End Restrained Plate at Restrained Edge Equ. (ε-10).

Level (cm)	S _{max} (mm)	e _{sh} (*10 ⁻¹)	L.O.R. (*10 ⁻¹)	e _{shn} (*10 ⁻¹)	K	e _{ult} (*10 ⁻¹)	R _b	R _a	W _c (mm)	W _o (mm)
0	70.	70.	7.	78.	0.7	13.	0.940	0.330	0.494	0.000
10	80.	710	7.	740	0.7	13.	0.800	0.200	1.070	1.000
20	86.	790	7.	720	0.7	13.	0.760	0.082	0.199	1.200

Table (ε-9): Maximum Crack Width Calculations for Four End Restrained Plate at Restrained Edge Equ. (ε-10).

Level (cm)	S _{max} (mm)	e _{sh} (*10 ⁻¹)	L.O.R. (*10 ⁻¹)	e _{shn} (*10 ⁻¹)	K	e _{ult} (*10 ⁻¹)	R _b	R _a	W _c (mm)	W _o (mm)
0	91.	70.	7.	78.	0.7	13.	0.87	0.20	0.729	0.720
10	97.	710	7.	740	0.7	13.	0.76	0.07	0.989	1.000
20	102.	790	7.	720	0.7	13.	0.78	-0.00	1.207	1.200

Tables (ε-10 to ε-13) give a comparison between values of crack width at different levels of plates, using different procedures reviewed in the literature with both calculated and observed crack width.

Table (ε-10): Comparison Between Values of Calculated Maximum Crack Width Using Different Methods for Two End Restrained of the Experimental Reinforced SCC Plate at the Free Edge.

Calculated crack width in mm.

Distance from the edge (cm)	Kadhum ^(٨٣)	BS : ٥٣٣٧ ^(٨٦)	Evans and Hughes ^(٨٥)	W _c	W _o
٥	٠.٧٢	٠.٦٣	٠.٥٦	١.٢٣٤	١.٢٢٠
١٥	٠.٥٩	٠.٦٥	٠.٥٧	٠.٩٦٥	١.٠٠٠
٢٥	٠.٥٢	٠.٦٨	٠.٥٩	٠.٨٢١	٠.٨٠٠

Table (٤-١١): Comparison Between Values of Calculated Maximum Crack Width Using Different Methods for Three End Restrained of the Experimental Reinforced SCC Plate at the Free Edge.

Distance from the edge (cm)	Calculated crack width in (mm).				
	Kadhum ^(٨٣)	BS : ٥٣٣٧ ^(٨٦)	Evans and Hughes ^(٨٥)	W _c	W _o
٥	٠.٧٢	٠.٦٣	٠.٥٦	٠.٩٠٢	٠.٨٧٥
١٥	٠.٥٩	٠.٦٥	٠.٥٧	٠.٥٥٣	٠.٦٢٥
٢٥	٠.٥٢	٠.٦٨	٠.٥٩	٠.٣٤٠	٠.٣٠٠

$$\text{for Kadhum}^{(٨٣)} \quad W_c = S_{\max} \left[-10.06 \times e_{sh} + 26.92 \times c_f - 50.22 \times \frac{1}{2} \times e_{ult} \right]$$

$$\text{for BS: } ٥٣٣٧^{(٨٦)} \quad W_{\max} = S_{\max} \left[e_{th} / 2 + e_{sh} - e_{ult} / 2 \right]$$

$$W_{\max} = S_{\max} \left(e_{sh} - \frac{e_{ult}}{2} \right)$$

for Evans and Hughes^(٨٥)

W_c = Calculated crack width from equation (mm) (٤-١٣)

W_o = Observed crack width (mm)

Table (٤-١٢): Comparison Between Values of Calculated Maximum Crack Width Using Different Methods for Three End Restrained of the Experimental Reinforced SCC Plate at the Retrained Edge.

Distance from the edge (cm)	Calculated crack width in mm.				
	Al-Rawi ^(٨٧)	Kadhum ^(٨٣)	Harrison ^(٨٨)	W _c	W _o

0	0.178	0.348	0.276	0.494	0.500
10	0.180	0.292	0.249	1.060	1.000
20	0.193	0.209	0.227	1.199	1.200

Table (4-13): Comparison Between Values of Calculated Maximum Crack Width Using Different Methods for Four End Restrained of the Experimental Reinforced SCC Plate at the Retrained Edge.

Distance from the edge (cm)	Calculated crack width in (mm).				
	Al-Rawi ^(AV)	Kadhum ^(AR)	Harrison ^(AA)	W _c	W _o
0	0.228	0.430	0.301	0.629	0.620
10	0.233	0.308	0.263	0.989	1.000
20	0.240	0.317	0.234	1.207	1.200

$$\text{for Al-Rawi}^{(AV)} \quad W_{\max} = S_{\max} [K(R_b - 0.8R_a)e_{sh} - e_{ult} / 2]$$

$$\text{for Kadhum}^{(AR)} \quad W_c = S_{\max} [0.83 \times (R_b - 0.7R_a)e_{sh} + 3.9 \times c_f - 23.46 \times \frac{1}{2} \times e_{ult}]$$

$$\text{for Harrison}^{(AA)} \quad W_{\max} = S_{\max} [0.5R_b(e_{th} + e_{sh}) - e_{ult} / 2]$$

W_c = Calculated crack width from equation (mm) (4-10)

W_o = Observed crack width (mm)

The results of calculated maximum crack widths, using the methods proposed by various researchers, together with the observed maximum crack widths for experimental plates were compared with the present theoretically predicted values. This comparison is shown in Figures (4-28 to 4-31). It is clear that there is a very close agreement between the observed maximum crack widths and the calculated maximum crack widths using the present

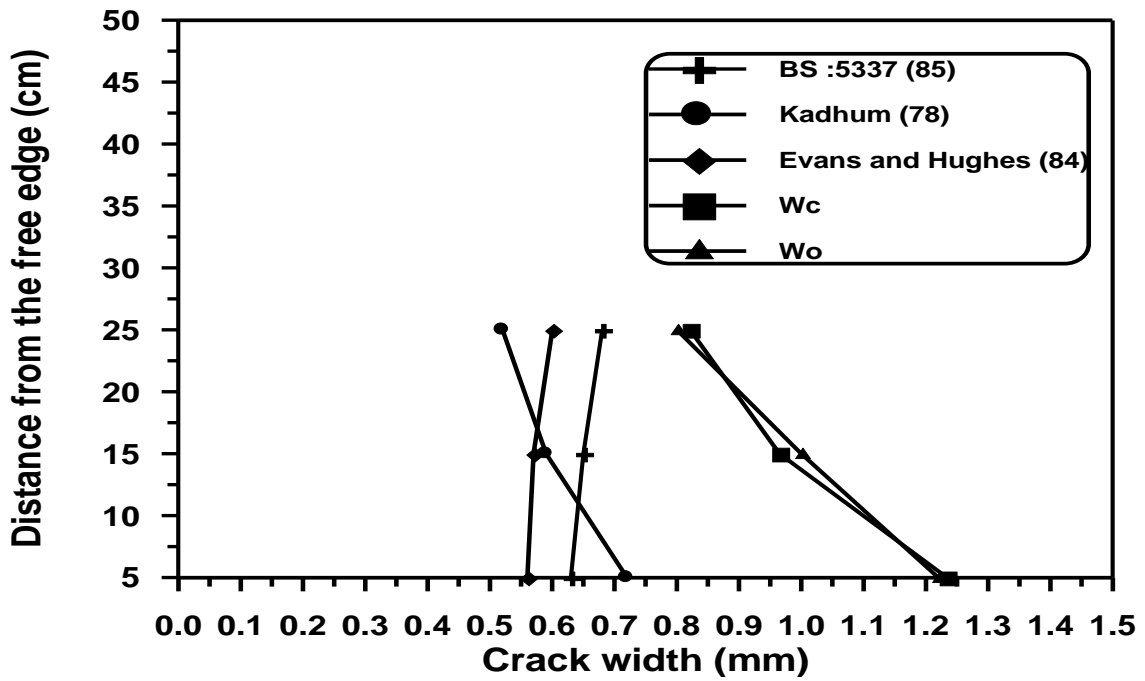


Figure (4-27): Comparison Between the Observed and Calculated Maximum Crack Width at Different Levels for Two End Restrained Reinforced SCC Plate at Free Edge.

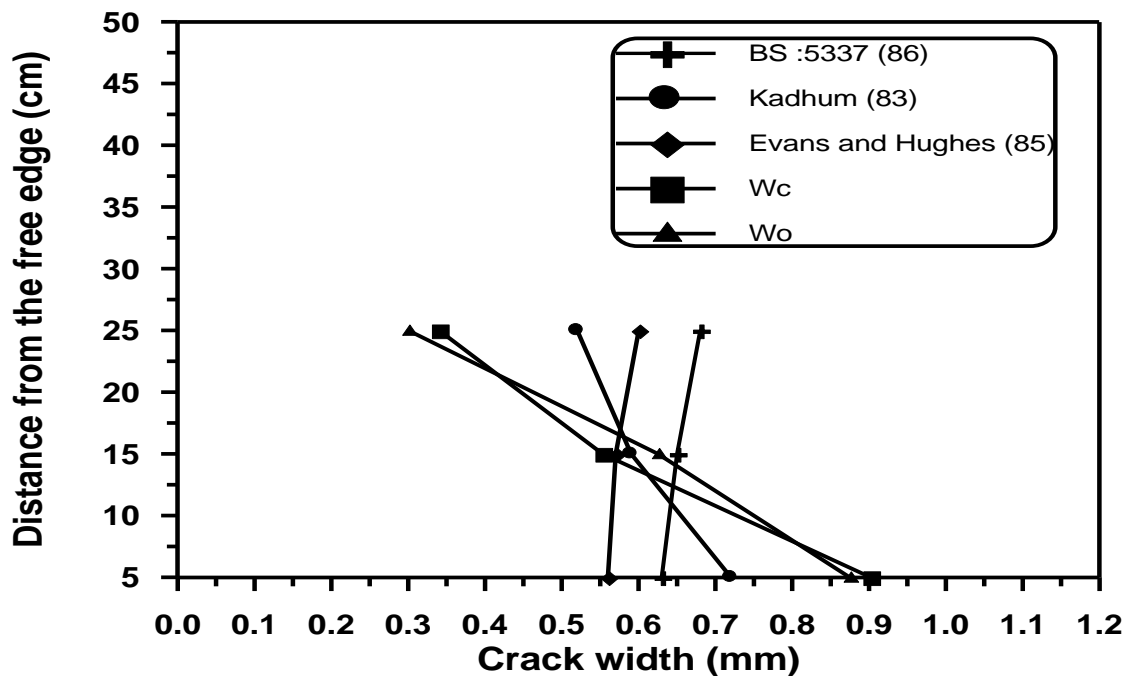


Figure (٤-٢٨): Comparison Between the Observed and Calculated Maximum Crack Width at Different Levels for Three End Restrained Reinforced SCC Plate at Free Edge.

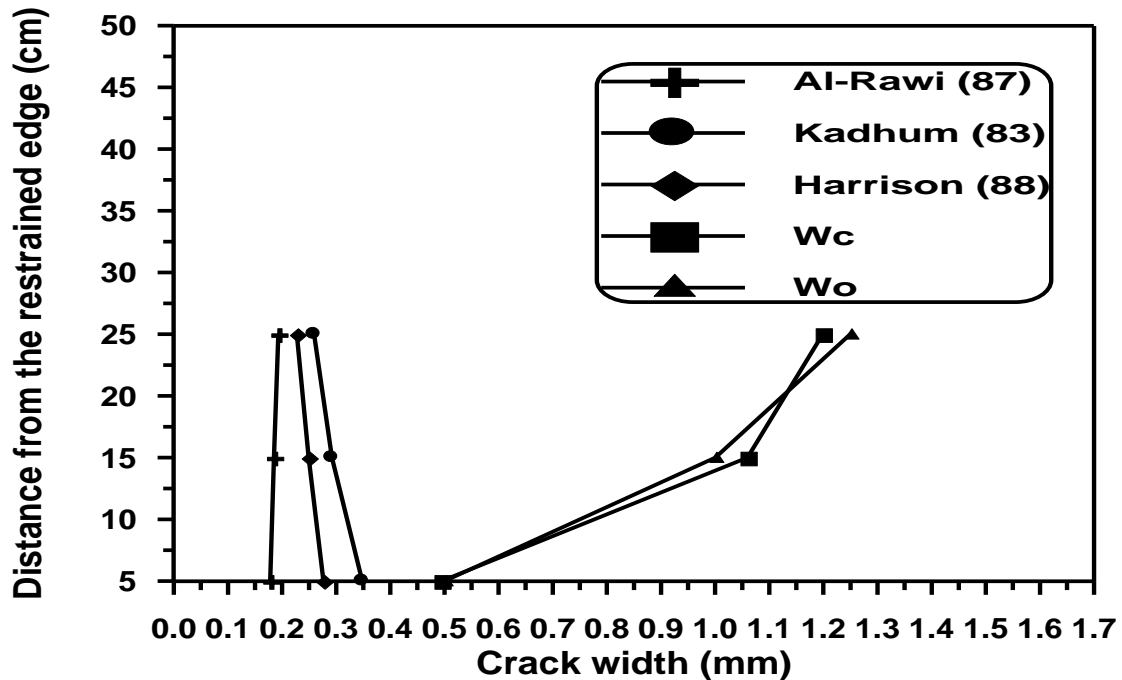


Figure (٤-٢٩): Comparison Between the Observed and Calculated Maximum Crack Width at Different Levels for Three End Restrained Plate at Restrained Edge.

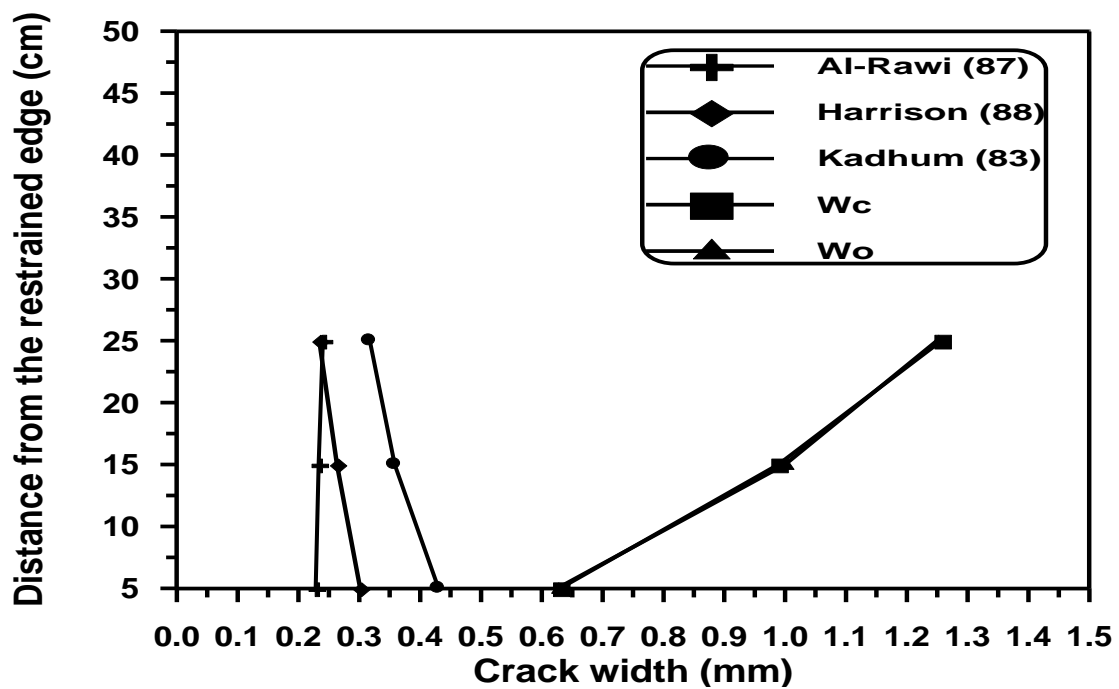


Figure (4-30): Comparison Between the Observed and Calculated Maximum Crack Width at Different Levels for Four End Restrained Plate.

CHAPTER FIVE

CONCLUSIONS AND RECOMMENDATIONS

5-1 - Conclusions

Based on the experimental results presented in the preceding chapters and on the basis of the observations made in the present work, the following conclusions were found:

1. SCC can be produced with locally available materials (pigment, limestone powder and metakaolin) by careful proportioning and mixing.
2. The values of slump-flow and T_{50} cm for SCC range between (680-700) mm and between (2.0-3.0) sec respectively, the results show that SCC mix with pigment is more than SCC mixes with limestone powder and metakaolin by (3, 9) % for slump flow and less by (20, 40) % for T_{50} cm respectively.
3. The values of blocking ratio (H_2/H_1) range between (0.90-0.95). The SCC mix with metakaolin relatively gives less value of blocking ratio than SCC mixes with pigment and limestone powder by (6, 3) % respectively.
4. The filling height values of U-box range between (0-0.4) cm.
5. The time of flow of SCC mixes is between (6-8) sec. The SCC mix with metakaolin is higher than SCC mixes with pigment and limestone powder by (33, 13) % respectively.

٦. The drying shrinkage of beams cast with SCC mix with pigment is higher than the normal mix by (٢٤% for ١-day and ٥% for ٦٠-days) in winter and by (٥٤% for ١-day and ٦% for ٦٠-days) in summer.
٧. The free shrinkage of beams cast with SCC mix with pigment is higher than the SCC mixes with limestone powder and metakaolin by (٣٣, ٤٣ for ١-day and ١١, ١٩ for ٦٠-days) % respectively in winter and by (٤٥, ٥٥ for ١-day and ١٠, ١٤ for ٦٠-days) % respectively in summer.
٨. The cracking time in the end restrained beams for SCC mix containing pigment powder and Superplasticizer occurs earlier through (٣-١٤ days), while the normal mix without addition the cracking time is (٢٨-days).
٩. The cracks in the end restrained beams occurred within the middle third of the beam rather than at the side.
١٠. The crack width development of plain SCC mix after cracking is higher than its counterpart in normal concrete mix.
١١. For plain and reinforced SCC free plates, the shrinkage strain at ٥ cm from the edge was greater than that at the center of free plates by (١٩, ١٣) % for ٦٠-days respectively.
١٢. The cracking age results show that all plates (two, three and four end restrained) casting with SCC are cracked early at the same period (in the first day after casting).
١٣. The interaction between the plate and the edge of restrained slab (base restraint) decreases the cracking time.
١٤. Addition of pigment powder to the SCC mix decreases the cracking time.

15. For reinforced SCC plates, the first crack occurs at the middle third of the restrained edge, while, at free edge the first crack occurs at the weakest section of the plate.
16. The cracks of SCC plates at and near the centerline propagated towards the point of intersection of centerline of these plates, whereas, the cracks near edge of plate extended in a direction inclined to the other restrained edge with degree about (45°) for two end restrained edge, (30°) for three end restrained and (45°) for four end restrained.
17. The cracks in the end restrained plates are more numerous in the proximity of the edge and decrease away from the edge. It appears that the minimum crack spacing for cracks decreases linearly with the distance from the edge.
18. The crack width in the end restrained plates is variable with its length, and its variation depends on the degree of restraint.
19. The reduction of the maximum width of cracks in reinforced SCC plates is associated with the reduction in maximum crack length.
20. The position of maximum crack width ($D-W_{max}$) at the restrained edge was equal to $(0.75 L_{max} - 9.63)$, while at free edge it was equal zero.
21. The crack width at the restrained edge initiated at a certain value (at edge), as the distance from the restrained edge increases, the crack width increases up to $(20-60\%)$ of crack length, than the width decreases to zero at the top of crack. While, at the free edge the crack width was the maximum at (the edge) and decreases to zero towards the center of the plates.

٢٢. Formulas for calculating width of crack at any level from edge are adopted and modified. The maximum crack width (W_{max}) can be calculated from the following equation.

For two and three end restrained plates from free edge.

$$W_{c \max} = S \max \left[a * e_{sh} \langle 1 - K \rangle - b * \frac{e_{ult}}{2} \right]$$

For three and four end restrained from restrained edge.

$$W_{c \max} = S \max \left[a * e_{sh} \langle \langle Rb - 0.8Ra \rangle - K \rangle - b * \frac{e_{ult}}{2} \right]$$

٢٣. The predicted values of maximum crack width using the present method and those proposed by various previous researchers were compared with experimental reinforced SCC plates. This comparison shows that the present method gives the closest results to the observed crack width experimental plates.

٥-٢- Recommendations for the Works

١. Studying the effect of maximum size and grading of coarse aggregate on SCC shrinkage cracking.
٢. Use of supplementary cementitious materials such as sand, fly ash, silica fume and rice husks ash to produce SCC and studying their effect on shrinkage cracking of SCC.
٣. Using fibers in SCC mix such as steel fiber, polypropylene, nylon and cellulose to increase early tensile strength and crack resistance.
٤. Suggestion a test method to assess the early age shrinkage (shrinkage occurring immediately after mixing the concrete and continuing for the first ٢٤-hours) of SCC.

- . Studying the effect of admixtures quantity and their types on the behavior of SCC shrinkage cracking.

REFERENCES

١. Ravindrarajah R. S., Farrokhzadi F., and Lahond A., “**Properties of Flowing Concrete and Self-Compacting Concrete With High-Performance Superplasticizer**” Center for Built Infrastructure Research, University of Technology, Sydney, Australia.
٢. Al-Nassar, W.A.A., “**Effect of Some Admixtures on the Shrinkage of Concrete**”, M.Sc. Thesis, University of Baghdad, College of Engineering, November. ٢٠٠٢.
٣. Collepardi M., “**Rheoplastic Concrete**”, Cement and Concrete Research, pp. ١٩٥-٢٠٤, (٢٠٠٠).
٤. Collepardi M., “**Assessment of the Rheoplasticity of Concretes**”, Cement and Concrete Research, pp. ٤٠١-٤٠٨, (٢٠٠٢).
٥. Wallevik O., Nielsson I., “**Self-Compacting Concrete-Rheological Approach**”, Proceedings of International Workshop on Self-Compacting Concrete, Kochi University, Japan, (August ١٩٩٨).
٦. The Concrete Promotional Group, “**Self-Consolidating Concrete**”, Vol.٢, Issue ٤, (٢٠٠٠).
٧. Tviksts L.G., “**Guideline for SCC**”, Brite Euram, Task ٩ End Product, Swedish Cement and Concrete Research, No.١٠, ١٣/٧/٢٠٠٠, pp.(١٠-٢٠).

8. Ralf A.B., and Sika A.G., **“Self-Compacting Concrete, Modern Concrete & Admixture Technology”** RCMA-Coference, Kuala Lumpur, (May 2000).
9. Bartos J.M., **“Measurement of Key Properties of Fresh Self-Compacting Concrete”**, CENPNR Workshop, Paris (2000).
10. Colleparidi M., **“A Very Close Precursor of Self-Compacting Concrete”**, Symposium on Sustainable Development and Concrete Technology, Supp^l. Vol., pp. 431-450, San Francisco (USA), (2001).
11. Okamura H., **“Self-Compacting High-Performance Concrete”**, Concrete International, pp. 50-54 (1997).
12. Ozawa K., **“Development of High Performance Concrete Based on the Durability Design of Concrete Structure”**, ENSEC-2, Vol. 1, pp. 440-450 (1989).
13. Kosmatka S.H., Kerkhoff B., and Panarese W.C., **“Design and Control of Concrete Mixture”**, 14th Edition, Portland Cement Association (2002).
14. Okamura H., and Ouchi M., **“Self-Compacting Concrete”**, Journal of Advanced Concrete Technology, Vol.1, No.1, Japan, (April 2003).
15. Kennedy C.T., **“The Design of Concrete Mixes”**, Proceedings of the American Concrete Institute, Vol.36 pp.373-400.
16. Fakulta S., **“Development in Design and Technology of Concrete Structures”**. Czech Technical University in Prague Faculty of Civil Engineering. Doc. Ing. Jan Vitek, CSc..
17. Abed M.K., **“Influence of Filler Type on Workability and Mechanical Properties of Self-Compacting Concrete”**, MSc. Thesis, University of Al-Mustansiriya, College of Engineering, 2000.

18. Bentz D.P., **“Drying/ Hydration in Cement Pastes During Curing”**, Materials and Structures, Vol.34, No.243, pp.557-565 (2001).
19. Atkins H.N., **“Highway Materials, Soils, and Concretes”**. 4th Edition, Prentice Hall. Pp.277-330 (2003).
20. Jin- Keun Kim, Sang Hun HAN, Yon Dong Park and Jae Ho Noth, **“Material Properties of Self-Flowing Concrete”**, Journal of Material in Civil Engineering, (November 1998).
21. Tam Chat Tim, A.M.M. Sheinn and D.Ho.W.S., **“Some Major Issues of Self-Compacting Concrete”**, Materials Technology, National University of Singapore, (2001).
22. Domone P.L., Jin J., and Chai H.W., **“Optimum Mix Proportioning of Self-Compacting Concrete”**, Innovation in Concrete Structures: Design and Construction, Proceedings of Creating with Concrete, University of Dundee, (1999).
23. EFNARC: European federation dedicated to specialist construction chemicals and concrete system, **“Specification and Guidelines for Self-Compacting Concrete”**, (2002).
24. David H., and Sheinn M., **“Some Major Issues of SCC”**, National University of Singapore, (2001), pp.(74-80).
25. Newman J., and Choo B.S., **“Advanced Concrete Technology”**, Processes, London and Edinburgh, 2003.
26. Gagne R., Boisvert A., and Pigeon M., **“Effect of Superplasticizer on Mechanical Properties of High-Strength Concretes With and Without Silica Fume”**, ACI Materials Journal, Vol.93, No.2, pp.111-120 (1996).

27. Whiting D., **“Effects of High-Range Water Reducers on Some Properties of Fresh and Hardened Concrete”**, Portland Cement Association, R&D Bulletin 061-01T (1979).
28. Bouzoubaa N., Lechemi M., **“Self-Compacting Concrete Incorporating High Volumes of Class F Fly Ash”**, Cement and Concrete Research, Vol.31, No.3, March 2001, p.413-420.
29. Ayano, Toshiki, Bana, Masanori, Kawanaka, Ryouichi, Oh, Ryou and Sakata Kenji, **“Effect of Particle Size Characteristics of Limestone Powder on Flowability of Self-Compacting High Performance Concrete”**, Zairyo/ Journal of the society of materials science, Japan, Vol.51, No.10, Oct. 2002, p.1099-1104.
30. BSEN 206-1 and BS 8000 specify concrete, **“Addition”** August, 2002.
31. BS 1014: 1970 **“Specification for Pigments for Portland Cement and Portland Cement Products”**.
32. Neville A.M., **“Properties of Concrete”** Fourth and Final Edition, Wiley, New York and Longman, London, 1990.
33. Newman J., and Choo B.S., **“Advanced Concrete Technology”**, Elsevier Ltd., (2003).
34. Nawa T., Izumi T., and Edamatsu Y., **“State-of-the-Art report Materials and Design of Self-Compacting Concrete”**. Proceedings of International Workshop on Self Compacting Concrete Kochi University, Japan. August (1998).
35. EFNARC: **“The European Guidelines for Self-Compacting Concrete Specification, Production and Use”**, May 2000.

36. HODWS, Sheinn AMM, Ngcc, lim W, B, and Tam CT.: “**Self-Compaction Concrete for Singapore**”, Concrete in our World in Concrete and Structures, 2001.
37. Emborg M., “**Mixing and Transport**”, Final Version of Task 1, 2006-2007 p 1-64.
38. Okamura H., and Ozawa K., (1990). “**Mix-Design for Self-Compacting Concrete.**” Concrete Library of JSCE, 20, 107-120.
39. Hayakawa M., Matsuoka Y., and Shindoh T., “**Development & Application of Super Workable Concrete.**” RILEM International Workshop on Special Concretes: Workability and Mixing (1993).
40. Ouchi M., “**Testing and Mix Design of Self-Compacting Concrete**”, Kochi University of Technology, Japan, (2003).
41. Sonebi M., Bartos P.J.M., Zhu W., Gibbs J., and Tammi A., “**Properties of Hardened Concrete**” Task 4, Partner: Advanced Concrete Masonry Center, University of Paisley, Scotland, United Kingdom, 26-0-2007, Page 48-73.
42. Tattersall G.H. and Banfill P.F.G., “**The Rheology of Fresh Concrete**”, Pitman Books Limited, London, (1983).
43. Celik O., and Stephen L., “**Evaluation of Self-Consolidation Concrete**”, VTRC 03-R13, Final Report, (June 2003).
44. Chiara F., Ferraris, Lynn B., Celik O., and Joseph D., “**Workability of Self-Compacting Concrete**”, National Institute of Standards and Technology, Orlando, Florida, sep. 2000, p.20-27.
45. Petersson O., “**Workability**”, Swedish Cement and Concrete Research Institute, Final Report of Task 2, 26-9-1999, p.1-06.

੪੬. Ozawa K., Sakata N., and Okamura H., “**Evaluating of Self-Compactibility of Fresh Concrete Using the Funnel Test**”, Concrete Library of JSCE, No.੨੦, pp.੦੧-੧੦, (੧੯੯੦).
੪੭. Victor C.Li., Kong H.J., and Chan Y.W., “**Development of Self-Compacting Engineered Cementitious Composites**”, Department of Civil and Environmental Engineering, University of Michigan, USA, (੨੦੦੩).
੪੮. Ferrais C.F., Brower L., Daczko J., and Ozyldirim C., “**Workability of the Self-Compaction Concrete**”, Journal of Research of NIST, Vol.੧੦੪, No.੦, pp. ੪੬੧-੪੭੮ (੧੯੯੯).
੪੯. Dietz J., and Ma, J., “**Preliminary Examinations for the Production of Self-Compacting Concrete Using Lignite Fly Ash**”, LACER No.੦, pp.੧੨੦-੧੩੯ (੨੦੦੦).
੫੦. Petersson O., Billberg P., and Van B., “**A Model for SCC**”, Proceedings of the International RILEM Conference on Production methods and workability of Concrete, Paisely, ੧੯੯੬, pp.(੪੮੩-੪੯੦).
੫੧. Ouchi M., and Hibino M., “**Development, Applications and Investigations of Self-Compacting Concrete**”, International Workshop, Kochi, Japan (੨੦੦੦).
੫੨. Lars M., and Tuiksta G., “**Guidelines**” Task ੧, End Product. No.੧੦, Swedish Cement and Concrete Research, ੧੩-੧-੨੦੦੦ p.੧-੨੮.
੫੩. Shetty M.S., “**Concrete Technology: Theory and Practice**”, College of Military Engineering, Published by S. Chand and Company Ltd., Ram Nagar, India, New Delhi, (੧੯੮੨).
੫੪. Holt E., and Schodet O., “**Self-Compacting Concrete: Early Age Shrinkage**”, Technical Research Center of Finland, (April ੨੦੦੨).

٥٥. Johansen K., and Hammer T.A., **“Drying Shrinkage of 'Norwegian' Self-Compacting Concrete”**, MSC Eng., Research Engineer, SINTEF Civil and Environmental Engineering, ٧٤٦٥ Trondheim Norway.
٥٦. Holschemacher K., and Klug Y., **“A Data Base for the Evaluation of Hardened Properties of SCC”**, LACER No.٧, Leipzig University, (٢٠٠٢).
٥٧. Rahim J.O., **“The Influence of Volume Ratio and Size of Coarse Aggregate on the Properties of Self-Compacting Concrete”**, MSc. Thesis, University of Al-Mustansiriya, College of Engineering, August, ٢٠٠٥.
٥٨. Neville A.M., and Brooks, J.J. **“Concrete Technology”**, John- Wiley and Sons., Revised Reprint ١٩٩٠. Printed in Singapore.
٥٩. Powers T.C., and Brownyard T.L., **“Studies of the Physical Properties of Hardened Portland Cement Paste”**, Proceeding of the ACI, V.٤٣, October-December, ١٩٤٦.
٦٠. Mehta P.K., and Monteiro P.J.M., **“Concrete Structures, Properties and Materials”**, Second Edition, Prentice Hall, Englewood Cliffs, New Jersey, ١٩٩٣.
٦١. Holt. E.E, **“Early Age Autogeneous Shrinkage of Concrete”**, VTT Building and Transport, Technical Research Center of Finland Espoo ٢٠٠١.
٦٢. Holt E., and Janssen D., **“Influence of Early Age Volume Changes on Long Term Concrete Shrinkage”**, Transportation Research Board, Washington, D.C., ١٩٩٨.
٦٣. Houk I.E., Borge O.E., and Houghion D.L., **“Studies of Autogenous Volume Change in Concrete of Dworshak Dam”**, J. Amer. Concr. Inst., ٦٦, (July ١٩٦٩). pp.٥٦٠.

٦٤. Tazawa E., and Miyazawa S., **“Autogenous Shrinkage of Concrete and its Importance in Concrete, in Creep and Shrinkage in Concrete”**, Eds Z P. Bazant and I, Carol, Proc ٥th International RILEM Symposium, (E and FN Spon, London. ١٩٩٣), pp.٦٨-١٥٩.
٦٥. Delarrard F., Acker P., and Leroy R., **“Shrinkage and Thermal Properties”**, ١٩٩٤.
٦٦. Troxell G.E., Davis H.E., and Kelly J.W., **“Composition and Properties of Concrete”**, Mc Graw Hill, Second Edition, ١٩٦٨.
٦٧. ACI Committee ٢٢٤, **“Control of Cracking in Concrete Structure”**, concrete international, V.٢, No.١٠, Oct. ١٩٨٠.
٦٨. Lerch, W., **“The Influence of Gypsum on the Hydration and Properties of Portland Cement Pastes”**, ASTM proc, V. ٤٦, ١٩٤٦
٦٩. Carlson R.W., **“Drying Shrinkage of Concrete as Affected by Many Factors”** Proceedings ASTM, V.٣٥, part ١١, ١٩٣٥, pp.٣٥٠.
٧٠. Carlson R.W., Houghton D.L., and Polivka M., **“Causes and Control of Cracking in Unreinforced Mass Concrete”**, ACI Journal, V.٧٦, No.٧, July. ١٩٧٩.
٧١. Georage, L. E., **“Method of Estimating Creep and Shrinkage Strain in Concrete from Properties of Constituents Materials”**, Journal ACI, ٦٢, (Nov. ١٩٦٥).
٧٢. Brooks, J. J., **“Influence of Mix Proportions, Plasticizers and Superplasticizers on Creep and Drying Shrinkage of Concrete”**, Magazine of Concrete Research, Vol. ٤١, No. ١٤٨, September (١٩٨٩), PP ١٤٥-١٥٣.
٧٣. Rixom M.R., **“Concrete Admixture: Use and Application”**, The construction Press Ltd., Lancaster, England ١٩٧٧.

٧٤. Shah S.P., Karaguler M.E., and Sarigaphuti M., **“Effects of Shrinkage-Reducing Admixtures on Restrained Shrinkage Cracking of Concrete”**, ACI Materials Journal, Vol. ٨٩, No.٣, May-June ١٩٩٢. Pp.٢٨٩-٢٩٥.
٧٥. Lane S., Final Report **“Evaluation of Self-Consolidating Concrete”**. Virginia Transportation Research Council (A Cooperative Organization Sponsored Jointly by the Virginia Department of Transportation and the University of Virginia). June ٢٠٠٣. VTRC ٠٣-R١٣.
٧٦. ASTM C٤٩٤-٩٢ **“Specification for Chemical Admixtures for Concrete”**.
٧٧. Babaei K., and Fouladgar., **“Solutions to Concrete Bridge Deck Cracking”**, Concrete International, Vol.١٩, No.٧, ١٩٩٧, pp.٣٤-٣٧.
٧٨. Mindess S., and Young F., **“Concrete”**, Prentice Hall, Englewood Cliffs, New Jersey, ١٩٨١.
٧٩. Al-Rawi R.S., **“Determination of Tensile Strain Capacity and Related Properties of Concrete Subjected to Restrained Shrinkage”**, ACI Symp. Singapore, Aug. ١٩٨٥, Our world in Concrete and Structure, ١٨.pp.
٨٠. PCA (Portland Cement Association)-**“Cement and Concrete Technology”** ٤/٢٦/٢٠٠٥, Page ١-٣.
٨١. ACI Committee ٢٠٧, **“Effect of Restraint, Volume Change and Reinforcement on Cracking of Massive Concrete”**, ACI ٢٠٧. ٢R-٧٣, ACI Manual of Concrete Practice, ١٩٨٥, Part ١.
٨٢. Al-Mashhdi S.A., **“Control of Secondary Shrinkage Cracks in Reinforced Concrete Walls”**, M.Sc Thesis, University of Baghdad, College of Engineering, Sep. ١٩٨٩.

٨٣. Kadhum M.M., **“Drying Shrinkage of Concrete Slabs Subjected to Fire”**, MSc. Thesis, University of Babylon, College of Engineering, July ٢٠٠٣.
٨٤. Al-Rawi R.S., **“Laboratory Tests on Small Beams to Study Shrinkage Cracking in Continuously Reinforced Concrete Pavement”**, Transportation Research Board, Annual Meeting, Washington, D.C., U.S.A. January ١٩٨٦, ٢٤pp.
٨٥. Evans E.P., and Hughes B.P., **“Shrinkage and Thermal Cracking in a Reinforced Concrete Retaining Wall”**, Proceedings The Institution of Civil Engineers (London), V.٣٩, Jan., ١٩٦٨, pp.١١١-١٢٥.
٨٦. B.S. Code ٥٣٣٧ ١٩٨٢ (Amendment ٢).
٨٧. Al-Aawi R.S., and Kheder G.F., **“Control of Cracking due to Volume Change in Base-Restrained Concrete Members”**, ACI Structural, July-August ١٩٩٠, pp.٣٩٧-٤٠٥.
٨٨. Harrison T.A., **“Early Age Thermal Crack Control in Concrete”**, CIRIA Report No.٩١, Construction Industry Research and Information Association, London, ١٩٨١, ٤٨pp.
٨٩. Hughes B.P., and Ghunaim F., **“An Experimental Study of Early Thermal Cracking in Concrete”**, Magazine of Concrete Research, V.٣٤, No.١١٨, England, March ١٩٨٢, pp.١٨-٢٤.
٩٠. Hobbs, D.W., **“Influence of Aggregate Restraint on the Shrinkage of Concrete”**, ACI Journal, Title No.٧١-٣٠, September ١٩٧٤.
٩١. Mann, **“Designing for Effects of Creep, Shrinkage and Temperature in Concrete Structures”**, ACI Publication SP.٢٧, American Concrete Institute, ١٩٧١.
٩٢. Iraqi Organization of Standards, IOS ٥: ١٩٨٤, for Portland Cement.
٩٣. Iraqi Organization of Standards, IOS ٤٥: ١٩٨٤; for Aggregate.

٩٤. AL-AZRAK Company for Industrial Services Amman Industrial City,
p. O. Box ٣٠, ١١٥١٢ Jordan-Telefax ٤٠٢٦٥٦٥.
٩٥. BS ١٨٨١:١١٦:١٩٨٣ **“Method for Determination of Compressive Strength of Concrete Cubes”**.
٩٦. BS ١٨٨١:١١٨:٨٣ **“Method for Determination of Flexural Strength”**.
٩٧. Hassan J.J., **“Effect of Sulphates in Fine Aggregate on Drying Shrinkage Cracking in End Restrained Concrete Members”**, MSc. Thesis, University of Babylon, College of Engineering, December, ٢٠٠٥.
٩٨. ACI Committee ٣١٨, **“Building Code Requirement for Structural Concrete (٣١٨-٩٩)”**, American Concrete Institute, Michigan, pp. ٦٣.
٩٩. William D., **“Materials Science and Engineering: An Introduction”**, the University of Utah, ٥th Edition, ١٩٩٩, pp. (٣٨١-٤٤٣).
١٠٠. Lea F.M., **“The Chemistry of Cement and Concrete”**, ٣rd. Edition Edward Arnold Ltd..